Discovery of protein biomarker predictive for the response to FOLFOX therapy in colorectal cancer

DISSERTATION

A dissertation submitted in partial fulfillment of the requirements for the degree of Doctor of Natural Science at the Hamburg University.

by

Florian T. Unger

Hamburg 2012

The present work was done between October 2008 and July 2012 at the Indivumed GmbH, in correspondence with the Department of Biochemistry and Molecular Biology, University of Hamburg, Germany.

Thesis Committee:

1. Prof. Dr. R. Bredehorst

2. PD Dr. Kerstin David

Date of Disputation: 13.07.2012

Table of contents

Abbreviations

%	Volume
µg	Microgram
µl	Microliter
µM	Micro molar
5-FU	5-Fluorouracil
ACN	Acetonitrile
AGO 1	Argonaute protein 1
AKT (Gene name)	Akt (*RAC-alpha serine/threonine-protein kinase 1-3*)
ATP	Adenosin-5'-triphosphat
ATPIF1	ATPase inhibitor, mitochondrial
BCA	Bicinchoninic acid
BSA	Bovine serum albumin
Cap	Capillary
COSMIC	Catalogue of Somatic Mutations
Da	Dalton
kDa	Kilo Dalton
D-MEM	Dulbecco’s MEM
DMSO	Dimethylsulfoxid
DNA	Desoxyribonucleic acid
D-PBS	Dulbecco’s phosphate buffered saline
EDTA	Ethylene diamine triacetic acid
EGF	Epidermal growth factor
EGFR	Epidermal growth factor receptor
ELISA	Enzyme-linked immunosorbent assay
ERCC1	Excision repair cross-complementing
ERK 1/2	Extracellular-signal regulated kinase ½
FA	Formic acid

F12	Nutrient mixture F-12
FCS	Fetal calf serum
FOLFOX	Combination chemotherapy, consisting of 5-Fluorouracil, Leucovorine and Oxaliplatin
GAPDH	Glycerinaldehyd-3-phosphatdehydrogenase
GSK-3β	Glycogen synthase kinase 3
h	Hour
HE	Hematoxylin eosin staining
HRP	Horseradish peroxidase
HSC70	Heat shock protein cognate 1
IHC	Immunohistochemistry
IRB	Institutional review board
LC	Liquid chromatography
LCM	Laser capture micro dissection
LV	Leucovorine
MALDI	Matrix-assisted laser desorption/ionization
MAPK	Mitogen-activated protein kinase
MEK 1/2	MAPK-kinase/ERK-kinase 1/2
MEM	Modified eagle medium
min	Minute
MK	Mixed culture
mM	Milli molar
MMR	Mismatch repair
MS	Mass spectrometry
MSD	Meso scale discovery
MSI	Microsatellite instability
mRNA	Messenger ribonucleic acid
mTOR	mammalian target of rapamycin

m/z	Mass-to-charge ratio
Oxa	Oxaliplatin
p…	phosphorylated version of a protein (e.g. pAkt)
P70s6K	ribosomal protein-S6-kinase
PCA	Principal Component analysis
PCR	Polymerase chain reaction
Pen/Strep	Penicillin / Streptomycin
pI	Isoelectric point
ppm	Parts per million
RAS	Rat sarcoma
rel.	Relative
RLU	Relative light unit
RNA	Ribonucleic acid
ROS	Reactive oxygen species
RP-HPLC	Reverse phase high-performance liquid chromatography
RT	Room temperature
Ru(bpy)3	Ruthenium(II)-tris-bipyridin-(4-methylsulfonat)-NHS-ester („SULFO-TAG™“)
SDS	Sodium dodecyl sulfate
SDS-PAGE	Sodium dodecyl sulfate polyacrylamide gel electrophoresis
SOD 1	Superoxide dismutase [Cu/Zn]
SOP	Standard operating procedure
TNM	Classification of Malignant Tumors
TP53 (Gene name)	p53
TS	Thymidylate synthase
UBA52	Ubiquitin-60S ribosomal protein L40
UBXN	UBX domain containing protein 1
vs.	versus

1 Introduction

Colorectal cancer is worldwide the third most commonly diagnosed cancer in males and the second in females, with over 1.2 million new cancer cases and 608,700 cancer related deaths in 2008 [1]. A surgical removal of the tumor, if appropriate and additional adjuvant chemotherapy of the tumor stages II and III are the main therapeutic strategies [2]. At the time of diagnosis, the pathological stage remains the most important prognostic indicator in colorectal cancer [3]. Therefore, the tumor-node-metastasis (TNM) system of the American Joint Committee on Cancer is the most commonly used system for staging colorectal cancer and serves as a benchmark for predicting the likelihood of five-year survival [4]. The earlier a colorectal cancer is diagnosed, the more likely is a complete cure of disease. Despite the advances being made in early detection of colorectal cancer, approximately half of all patients develop metastatic disease [5]. The prognosis for these patients is poor, although prospective studies have shown that, chemotherapy can prolong the survival and enhance quality of life in comparison to palliative care alone [6; 7-10]. A meta-analysis of 13 trials revealed that chemotherapy led to an improvement in 1-year survival from 34 percent to 50 percent and improved the median survival by 3.7 months [11]. Based on results from several phase III trials, combination regimes of infusional 5-Fluorouracil (5-FU) with Leucovorin (LV) and Oxaliplatin (Oxa) have emerged as a standard of care in palliative and adjuvant treatment of colorectal cancer, but the response rates are still low [12; 13; 14]. This combination regime called FOLFOX treatment, consisting of compounds with different modes of action [15], has been shown to be superior to other combination treatments [16; 17]. Oxaliplatin and 5-Fluorouracil were shown to be highly synergistic, not only in preclinical models [18], but also in subsequent clinical trials [19]. One component of the FOLFOX treatment regime for colorectal cancer is fluorouracil, a fluorinated

pyrimidine, which is thought to act primarily by inhibiting the thymidylate synthase, the rate limiting enzyme in pyrimidine nucleotide synthesis [20]. The mechanism of cytotoxicity of 5-FU has also been ascribed to the misincorporation of fluoronucleotides into RNA and DNA [21; 22]. Fluorouracil is administered with leucovorin, a reduced folate, which stabilizes the binding of 5-FU to thymidylate synthase, thereby enhancing the inhibition of DNA synthesis [23]. The other component of FOLFOX is Oxaliplatin, which is a third generation platinum compound. It shares similar mechanisms with cisplatin and carboplatin, by causing mono-adducts and intra-strand or inter-strand cross-links in the double DNA helix, that block DNA and mRNA synthesis [24; 25]. Platinum compounds are also known to generate Reactive Oxygen Species (ROS), which potentially induce single and double strand breaks, during the crosslinking reaction with DNA [26]. Several anticancer drugs, including 5-Fluorouracil and Oxaliplatin, have been shown to increase the intracellular concentration of ROS, the inhibition of the drug induced increase in ROS concentrations partly reversed their cytotoxicity [27-35]. However, chemoresistance of cancer cells is a main obstacle in chemotherapy to a successful outcome. It has been hypothesized that selection pressure resulting from the tumor internal evolution can lead to subpopulations of cells carrying certain cellular mechanism that can be summarized under the term “chemoresistance”. Cellular mechanisms of chemoresistance are mainly characterized by the fact that they lead to increased tolerance of cancer cells to chemotherapeutics. Therefore these cells are most likely to survive chemotherapy and arise as recurrence disease. In order to overcome these problems, the therapy of colorectal cancer has to be patient tailored to be maximal effective. However, the prediction of individual response to therapy is still challenging because molecular determinants of chemoresistance to chemotherapeutic agents are still lacking [36]. Compelling clinical data, combined

with distinct molecular targets, mechanisms of action, and purported mechanisms of chemoresistance for all three agents, set the stage for the development of biomarkers for the prediction of response to FOLFOX chemotherapy [37].

Several protein and genetic markers have been described in an attempt to predict the benefit derived from chemotherapy. Remarkably, none of these markers is in routine clinical use [38]. For example, the determination of microsatellite instability (MSI) status and the DNA mismatch repair (MMR) for the prediction of benefit from single-agent 5-FU are being investigated. Although, the results are not mature and even conflicting [39; 40]. *In vitro* studies have demonstrated that MMR deficiency increases resistance to cisplatin but not Oxaliplatin *in vitro* [41; 42]. The DACH complex in the chemical structure of Oxaliplatin prevents the MMR machinery from recognizing corresponding DNA-platinum adducts. For this reason, Oxaliplatin is not dependent on the MSI/MMR phenotype for activity. The primary mechanisms of platinum derivatives are resulting in damages that interfere with DNA replication and require the activity of DNA repair enzymes to avoid cell death. Several polymorphisms in different DNA repair enzymes have been shown to correlate with function [43]; however, association studies with outcome seem to be regimen and cancer type specific. Among six commonly studied functional polymorphisms in four DNA repair genes (ERCC1, ERCC2, XRCC1 and XRCC3) only ERCC1 Asn118Asn and ERCC2 lys751Gln mutations were associated with overall survival in colorectal cancer in one report [44], but not in another study [45]. Furthermore, the possible roles of RAS mutations, implicated in EGFR related cellular signaling, as predictive markers for response or resistance to therapy have also been studied in colorectal cancer [46; 47]. Present data indicate no use for mutations in RAS oncogenes as predictors of response to chemotherapy [48]. The p53 tumor suppressor gene that encodes a nuclear phosphoprotein involved in the cellular response to DNA damage [49] has

been controversially discussed regarding its predictive value for the response to chemotherapy [50-52]. Nevertheless, there is no proof for a predictive value of the TP53 status. Another potential indicator of chemoresistance to 5-FU therapy is the thymidylate synthase (TS), a key enzyme for pyrimidine biosynthesis and an essential component of the DNA synthesis pathway. TS protein activity is inhibited by 5-FU (a pyrimidine analog), leading to cell cycle arrest and apoptosis [53]. *In vitro* data indicated that the TS expression is a determinant of 5-FU sensitivity, suggesting that the expression of this gene may also determine tumor sensitivity *in vivo* [54, 55]. However, conflicting data make the role of this enzyme as a predictive marker in the adjuvant setting controversial. In the year 2006, the American Society of Clinical Oncology gave an update of recommendations for the use of tumor markers in gastrointestinal cancer and pointed out, that none of the above mentioned biomarkers is recommended for the prediction of response to chemotherapy in the clinical situation [38].

Potentially, there are a multitude of reasons, why none of these biomarkers has finally reached the integration in the clinical situation. First of all, the success of biomarker discovery and validation studies is initially based on the quality and selection of the right biological patient material [56]. It is widely accepted that many factors are suspected to affect the quality of biospecimen, such as drug applications to patients, surgical procedures such the duration of artery legation until tumor resection and the cold ischemia time, before final fixation of the tissue. Especially in large-scale screening studies these external factors can lead to serious misinterpretation of results or analytical artifacts. Furthermore, the heterogeneity in individual tumor architecture complicates the comparability of biospecimen, in regard to the individual tumor content and distribution of different cell types.

Another reason for the lack of robust predictive biomarker might be the need for molecular techniques and preclinical models that enable a robust discovery, validation and integration of predictive biomarker into the clinical situation. In the past decades, research in the field of molecular profiling of cancer was strongly affected by the rapid development of technologies. Progress in all fields of cancer research, ranging from the optimization of cellular models and chemosensitivity assays over proteomics to genomics is revealing more and more facets of determinants of individual chemosensitivity. Besides studies in patients and xenograft models of tumors, *in vitro* cell cultures are the most commonly used systems for the analysis of cellular responses to drug treatment. A whole spectrum of cellular models ranging from secondary cell lines and primary mixed cultures over multicellular spheroids to organoid cultures are being used in cancer research. These models are being constantly optimized to mimic the origin tumor and its tumor microenvironment as close as possible. In order to investigate molecular details of individual drug responses, the newest genomic and proteomic methods were applied in cancer research. These technologies enable comprehensive investigation of multifactorial mechanisms underlying individual drug response by simultaneous analysis of thousands of genes or proteins. High throughput technologies for the analysis of DNA repair, mutation status, gene expression, methylation status, gene copy number and genome stability used in the field of genomics to understand the individual response to chemotherapy. Proteomics mainly describes the study of the wide complement of cellular proteins, their subcellular localization, expression, turnover and interaction with other proteins [57-59]. In contrast to the genome, the proteome is at a constant flux due to diverse environmental influences. Therefore, the proteome is significantly more challenging to map, compared to the genome [60]. In summary all these constantly evolving techniques enable a more and more detailed analysis of

cancer cells, but most importantly the assays have to be proven adequate in terms of sensitivity, specificity and reproducibility for the discovery or detection of a biomarker. Therefore, it is important that studies are not driven primarily by the availability of superior technologies. Ultimately, the end product of a translational study must be a clinically relevant biomarker that can be easily assayed in the clinical setting, producing a direct benefit for the individual patient [61]. The significance of a clinical study is further dependent on elaborate study design and statistical evaluation. The huge amount of data generated by these technologies and the interconnection of all fields of research can ultimately create a complex picture of molecular networks and will significantly contribute to the understanding of the diversity in individual drug response [62].

Since major cellular and tissue regulations are dominated by expression differences on the protein and posttranslational level, proteomic techniques are believed to be valuable tools for biomarker discovery and validation. Given that the proteome of a cell is responsible for key biologic processes and also makes up the bulk of pharmaceutical targets the determination of significant associations between protein expression patterns and *in vitro* chemosensitivity of cancer cells is promising approach. Especially, since gene expression often does not correlate with the corresponding protein expression or the functionality of the encoded protein [63; 64]. Alterations within the proteome also have a potentially higher functional impact than modifications in the genome, because they are more likely to contribute to a drug-resistant phenotype [65].

Having all these issues in mind, this thesis aimed at the discovery of predictive biomarker candidates based on a preclinical model represented by a heterogeneous panel of colorectal cell cultures. The search for these biomarker candidates was conducted by analyzing the expression patterns of the low and high molecular weight

proteome of cell cultures in regard to their individual chemosensitivity. Subsequently, an initial validation of these biomarker candidates will be conducted to reveal the applicability of the workflows and the validity of the biomarker candidates.

2 Material and methods

2.1 Material

2.1.1 Clinical specimen and cell cultures

The Indivumed GmbH is a high quality biobank within a network of several clinics in Hamburg. The stock of approx. 15,000 tumor specimens is constantly expanded by the collection of biospecimens, according to Standard Operating Procedures (SOP). Furthermore, the establishment of primary cell cultures and preclinical models is a part of Indivumeds` cancer research activities. All patients, from whom tumor material was used, gave written consent and IRB approval was obtained by the responsible IRB of the physicians association in Hamburg, Germany. Follow up data of the patients were also collected. Protection of patients' data was warranted according to the international ethical recommended practice and legitimate regulations such as the German Data Protection Act. As mentioned above, primary cell cultures were established from colorectal cancer patients` tumors according to Indivumeds` standard operating procedures. These cell cultures consisted of a mixture of different epithelial cancer cells with a minimum of 10% fibroblasts, these mixed cell cultures are further on labeled with the addition MK. Furthermore, clonal epithelial cancer cell lines were established from these mixed cell cultures, further on labeled with the addition of the clone number. The clinical data of patients matched to established primary cell cultures are summarized in table 1. Secondary cell lines were purchased from CLS-Cell Line Service (Germany) and the ATCC-American Type Culture Collection (USA). The primary cell cultures were grown in supplemented DMEM/F12 cell culture media. Secondary cell lines were grown in supplemented RPMI cell culture media. Basic data of the secondary cell lines are included in table 1. Primary mixed cell cultures and primary clonal cell lines were tested for identification

verification via genetic profiling in reference to corresponding fresh frozen material of the patient. All used cell cultures were tested negative for mycoplasma and bacterial contaminations.

Table 1: Basic data of primary cell cultures and secondary cell lines.

Patients` acronym	Cell culture name	Gender	Age (years)	Tumor-localisation	TNM-classification	Grade
A845	**A845MK**	male	64	Colorectal adenocarcinoma	T2 N2 M0	Dukes' type C
A609	**A609MK**	female	86	Colorectal adenocarcinoma	T3 N1 M1	Dukes' type D
B352	**B352clone3** **B352MK**	male	47	Colorectal, metastatsis peritoneum	M1	Dukes' type D
B429	**B429clone8** **B429MK**	male	44	Colorectal adenocarcinoma	T3 N0 M0	Dukes' type B
A806	**A806clone1** **A806MK**	female	65	Colorectal adenocarcinoma	T4 N2 M0	Dukes' type C
A413	**A413clone11/60** **A413MK**	male	81	Colorectal adenocarcinoma	T4 N2 M1	Dukes' type D
Secondary cell line	**HT-29**	female	44	Colorectal adenocarcinoma	-	-
Secondary cell line	**SW480**	male	51	Colorectal adenocarcinoma	-	Dukes' type B
Secondary cell line	**LS174T**	female	58	Colorectal adenocarcinoma	-	Dukes' type B
Secondary cell line	**LS513**	male	63	Colorectal carcinoma	-	Dukes' type C
Secondary cell line	**HCT-15**	male		Colorectal adenocarcinoma	-	Dukes` type C
Secondary cell line	**HCT-8**	male	67	Colorectal adenocarcinoma	-	-
Secondary cell line	**Colo320**	female	55	Colorectal adenocarcinoma	-	Dukes' type C
Secondary cell line	**Colo678**	male	69	Colorectal, metastatsis lymph node	-	-
Secondary cell line	**Caco-2**	male	72	Colorectal adenocarcinoma	-	-
Secondary cell line	**Lovo**	male	56	Colorectal, metastatic site	-	Dukes' type C,

2.1.2 Chemicals

Chemicals used were supplied by Sigma (Steinheim, Germany), Invitrogen (Karlsruhe, Germany), Roth (Karlsruhe, Germany), Roche (Mannheim, Germany), Qiagen (Hilden, Germany), PAA (Cölbe, Germany), Dako (Hamburg, Germany), Biozol (Eching, Germany) and Proteinsimple (Santa Clara, California).

2.1.3 Anticancer drugs

Anticancer drugs or other substances used are summarized in table 2.

Table 2: Anticancer drugs used for drug treatments of cell cultures.

Substance	Abbreviation	Mode of action	Supplier
Oxaliplatin (Eloxatin®)	Oxa	Alkylating and crosslinking platinum compound	Sigma (Steinheim)
5-Fluorouracil	5-FU	Antimetabolite	Sigma (Steinheim)
Leucovorin	LV	Antimetabolite (Folic acid)	Sigma (Steinheim)

FOLFOX combination treatment, consisting of 5-Fluorouracil, Oxaliplatin and Leucovorin was administered in fold dilutions. One fold FOLFOX combination corresponds to 0.5 mM 5-Fluorouracil, 20 µM Oxaliplatin and 100 µM Leucovorin. The concentration range was selected in reference to peak serum concentrations of the drugs measured in patients.

2.1.4 Antibodies

The following antibodies were used for Western blotting and NanoPro1000 analysis of protein expression.

Table 3: Antibodies.

Antibody	Supplier	Species
anti-Ago1	Abcam	Rabbit, polyclonal
anti-UBXN6	Abcam	Mouse, polyclonal
anti-HSC70	StressMarq	Mouse, polyclonal
anti-Cu/Zn SOD	Millipore	Rabbit, polyclonal
anti-UBA52	Abcam	Rabbit, polyclonal
anti-ATPIF1	Santa Cruz	Mouse, polyclonal
anti-GAPDH	Ambion, Applied biosystems	Mouse, polyclonal
anti-Rabbit	Pierce	HRP-conjugated
anti-Mouse	Pierce	HRP-conjugated

2.1.5 Enzymes

The following enzymes were used for indicated purposes:

- Isolation of primary cells and subcultivation: Collagenase NB6 (Serva; Heidelberg) and Trypsin-EDTA (PAA; Cölbe)
- Tryptic digestion of cell lysates and in-gel digestion: Trypsin (porcine pancreas), proteomics grade (Sigma, Steinheim); Chymotrypsin, proteomics grade, (Sigma, Steinheim).

2.1.6 Kits

Following commercially available kits were used for experiments:

Table 4: Kits used for Western blotting, cell viability assays, MSD analysis and NanoPro1000 experiments.

Kit	Supplier
SuperSignal® West Dura Trial Kit	Pierce (Waltham, MA, USA)
SuperSignal® West Femto Trial Kit	Pierce (Waltham, MA, USA)
EasyLyse Reagenz	Pierce (Waltham, MA, USA)
ATPliteTM Luminescence Kit	Perkin Elmer (Boston, MA)
MS6000 Akt Signaling Whole Cell Lysate Kit [pAkt (Ser473), pp70S6K (Thr421/Ser424), pGSK-3beta (Ser9)]	Meso Scale Discovery (Gaithersburg, MA, USA)
MS6000 Akt Signaling (Total Protein) Panel Whole Cell Lysate Kit [Akt, p70S6K, GSK-3beta]	Meso Scale Discovery (Gaithersburg, MA, USA)
MS6000 Phospho (Y1173) / Total EGFR Whole Cell Lysate Kit	Meso Scale Discovery (Gaithersburg, MA, USA)
MS6000 Phospho (Thr 202 / Tyr 204, Thr 185 / Tyr 187) / Total ERK Whole Cell Lysate Kit	Meso Scale Discovery (Gaithersburg, MA, USA)
MS6000 Phospho (Ser 217 / 221) / Total MEK1/2 Whole Cell Lysate Kit	Meso Scale Discovery (Gaithersburg, MA, USA)
MS6000 ERK-STAT3 Cascade Whole Cell Lysate Kit [pSTAT3 (Tyr 705), pERK 1/2 (Thr 202 / Tyr 204, Thr 185 / Tyr 187), pMEK 1/2 (Ser 217 / 221)]	Meso Scale Discovery (Gaithersburg, MA, USA)
DAB MapTM Kit	Roche (Mannheim)
Superoxide Dismutase Assay Kit	IBL International GmbH (Hamburg, Germany)
NanoPro1000 Master Kit	Proteinsimple (California, USA)
Secondary antibody HUX kit	Proteinsimple (California, USA)
Premix G2, pH 5–8 (nested) gradient kit	Proteinsimple (California, USA)
Premix G2, pH 3–10 gradient kit	Proteinsimple (California, USA)

2.1.7 Instrumentation

All experiments were performed using the equipment listed below.

Table 5: Instrumentation.

Equipment	Supplier
CO^2- Incubator Hera Cell 150	Thermo Life Science (Frankfurt, Germany)
Cryostat HM 500 O	Microm (Walldorf, Germany)
IHC staining unit Discovery® XT	Ventana (Tucson, AZ, USA)
Analytical balance	A&D Engineering (Milpitas, CA, USA)
Special accuracy weighing machine	Sartorius (Göttingen, Germany)
Optical reader FLUOstar Optima	BMG Labtech GmbH (Offenburg, Germany)
Heating Block Thermomixer comfort	Eppendorf (Hamburg, Germany)
Heating mixer MR 3001 K	Heidolph (Schwalbach, Germany)
Cabinet dryer ED 53	Binder GmbH (Tuttlingen, Germany)
Transmitted light microscope and camera Axiovert 25 & AxioCam ICc 1	Carl Zeiss Jena AG (Jena, Germany)
Fluorescence microscope and LCM system P.A.L.M. MicroBeam (MB04022); Microscope Axio Observer.Z1 & AxioCam MRc Rev.3	Carl Zeiss Jena AG (Jena, Germany)
Scanner Mirax Scan	Carl Zeiss Jena AG (Jena, Germany)
Geldocumentation ®Raytest, Diana II Camera	Isotopen Messgeräte GmbH (Straubenhardt, Germany)
Digital Graphics Printer UP-D895	Sony (Berlin, Germany)
Centrifuge 5415 D	Eppendorf (Hamburg, Germany)
Centrifuge Universal 32 R	Hettich (Tuttlingen, Germany)
Cooling centrifuge 5415 R	Eppendorf (Hamburg, Germany)
Multi-functional ELISA-Instrument MS6000	Meso Scale Discovery (Gaithersburg, MA, USA)
pH-Meter SevenEasy	MettlerToledo (Greifensee, Schwitzerland)
Rotation microtome HM 340E	Microm (Walldorf, Germany)
Mixer MicroMix 5	DPC-Biermann (Bad Nauheim)
Sterile work bench HERAsafe KS	Thermo Scientific (Thermo Fisher Scientific) (Waltham, MA, USA)
Nitrogen kipple KGW Isotherm	Roth (Karlsruhe, Germany)
Nitrogen kipple Arpege 170	Air Liquide Kryotechnik GmbH (Düsseldorf, Germany)
Vortexer REAXtop	Heidolph (Schwalbach, Germany)
Waterbath GFL® 1083	GFL (Burgwedel, Germany)
Ultraflex III MALDI-TOF/TOF	Bruker (Bremen, Germany)
RP-HPLC	Agilent (Waldbronn, Germany)
Cap-HPLC	Agilent (Waldbronn, Germany)
Fraction collector (FC Proteineer)	Bruker (Bremen, Germany)
Electrophoresis system	Thermo Life Science (Frankfurt, Germany)
Tank blotting system	Thermo Life Science (Frankfurt, Germany)
NanoPro1000	Proteinsimple (California, USA)

2.1.8 Plastic material

Following plastic materials were used for cell culture and experiments:

Table 6: Plastic materials.

Material	Supplier
Filter (0,22µm) & disposable syringes (20ml)	Roth (Karlsruhe, BRD) & B.Braun (Melsungen, Germany)
Eppendorf tubes (0.5ml; 1,5ml; 2ml)	Eppendorf (Hamburg, Germany)
Cryotubes CryoPure	Sarstedt (Nümbrecht, Germany)
Plastic pipettes	Corning (Corning, NY, USA)
Filtertips for pipettes (1-10µl; 2-20µl; 20-200µl; 100-1000µl)	Eppendorf (Hamburg, Germany); Sarstedt (Nümbrecht, Germany)
Combitips plus (10ml; 5ml; 2,5ml; 1ml)	Eppendorf (Hamburg, Germany)
T25 / T75 / T175- Cell culture flasks	Corning (Corning, NY, USA)
35mm; 60mm; 100mm Cell culture dishes	Corning (Corning, NY, USA)
Cell scraper	Sarstedt (Nümbrecht, Germany)
Cell Strainer (70µm & 100µm)	BD Biosciences (San Jose, CA, USA)
Lobind deepwell 96 plates	Eppendorf (Hamburg, Germany)
384 well plates	Corning (Corning, NY, USA)
Polished steel targets	Bruker (Bremen, Germany)
PAC (Disposable AnchorChip)	Bruker (Bremen, Germany)

2.1.9 Risk and Safety statements

The following hazardous materials were used for experiments and handled according to their Risk and Safety statements.

Table 7:Hazardous materials

Substance	Danger symbol	R-phrases	S-phrases
5-Fluorouracil	Xn	R 22	-
Amphotericin B	Xi	R 36/37/38	-
Bicinchoninic acid	-	R 36	S 26-36
Bis-Tris	Xi	R 36/37/38	S 26-36
Calciumchloride	Xi	R 36	S 22-24
Cell Conditioner „CC1s“	-	R 22-36-37-38-43	-
Collagenase NB6	Xn	R 36/37/38-42/43	S 22-24-26-36/37-45
DAB MapTM Kit	-	R 22-31-37-38-41	-
Bisodium carbonate	Xi	R 36	S 22/26
Bisodium-EDTA	Xn	R 22	S 2-4
Dithiothreitol	Xn	R 22-36/38	S 22-36/37/39
Dimethylsulfoxid	Xi	R 36/38	S 26

Acetic acid	C	R 10-35	S 23-26-45
Ethanol	F	R 11	S 7-16
Liquid nitrogen	-	-	S 9-23-26
Formalin 4%	T	R 20/21/22-40-43	S 36/37
Gentamicin	Xn	R 42/43	S 23-36/37-45
Haematoxylin	Xi	R 36/37/38	S 26-36
Hoechst 33342	Xn	R 22-37/38	S 36/37
Hydrocortisone	Xn	R 63	S 36/37
Isopropanol	Xi, F	R 11-36-67	S 7-16-24/25-26
Copper sulfate	Xn, N	R 22-36/38-50/53	S 22-60-61
Leucovorin	Xn	R 36/37/38-42/43	S 26-36
Magnesium chloride	Xi	R 36/37	S 26-39
Methanol	F, T	R 11-23/24/25-39/23/24/25	S 7-16-36/37-45
Sodiumhydrogen carbonate	Xi	R 36	S 22/26
Sodium hydroxide	C	R 35	S 26-37/39-45
Oxaliplatin (Eloxatin®)	Xn	R 36/37/38-42/43-40	S 26-36
Paraformaldehyde	Xn	R 20/22-37/38-40-41-43	S 26-36/37/39-45
Penicillin G & Streptomycinsulfate	Xn & T	R 42/43 & R 61-22	S 36 & S 45-36/37/39-22
Phosphatase-Inhibitor-Cocktail I	-	-	S 23-24/25
Phosphatase-Inhibitor-Cocktail II	-	-	S 23-24/25
Roti®-Histokitt II	Xn	R 10-20/21-38	S 25-36/37
Hydrochloric acid 37%	C	R 34-37	S 26-36/37/39-45
SDS	Xn	R 22-36/38	S 2-46
SuperSignal West Dura Trial Kit	Xn	R 22	-
Triiodothyronin	Xn	R 20/21/22	S 36
Tris	Xi	R 36/38	S 26
Triton X-100	Xn	R 22-41	S 26-36-23
Trypan blue	T	R 45	S 53-45
Trypsin	Xn	R 42	S 22
Xylene	Xn	R 10-20/21-38	S 25
β-Mercaptoethanol	F, Xn, N	R 11-20-50/53	S 16-25-60-61

2.2 Methods

2.2.1 Sampling of tumor material

Tumor tissues of colorectal adenocarcinoma patients were collected immediately after resection according to standardized operating procedures and either rapidly frozen in liquid nitrogen (cold ischemia <14 min) or transported in ice cold cell culture

media (D-MEM/F12 medium, supplemented with 10% FCS, 2 mM L-glutamine, 1% MEM-vitamins, 1% penicillin / streptomycin, 0.2% gentamicin, 5 µg/mL transferrin, 12.5 µg/mL fetuin and 20 µg/mL insulin). Subsequently, the vital material was used for the preparation of primary cell cultures.

2.2.2 Establishment and cultivation of primary cell cultures and secondary cell lines

Primary mixed cultures were obtained by mechanical disruption of tissues followed by enzymatic digestion for 45min with 2 mg/mL NB6 collagenase dissolved in D-PBS. Cell suspensions were washed twice with cell culture medium as well as D-PBS using 500 xg centrifugation for cell sedimentations after filtration through a 420 µm pore steel mesh, 100 µm and 70 µm cell strainer meshes. Erythrocytes were subsequently lysed using the EasyLyse kit from Dako (Hamburg, Germany) according to the manufacturer's instructions. Cell cultures were seeded in collagen I coated flasks in full media containing D-MEM/F12 medium, supplemented with 10% FCS, 2 mM L-glutamine, 1% MEM-vitamins, 1% penicillin / streptomycin 0.2% gentamicin, 5 µg/mL transferrin, 12.5 µg/mL fetuin and 20 µg/mL insulin). Primary cultures were incubated under a humidified atmosphere containing 5% CO_2 and routinely passaged applying 1x trypsin-EDTA and 1:4 dilutions. Primary mixed cell cultures were defined as a mixture of epithelial cancer cells, containing a maximum of 10% fibroblasts. For the establishment of primary clonal cell lines, the limiting dilution method was used. Primary clonal cell lines are defined as originating from one epithelial cancer cell and being free of other cells. Secondary cell lines were cultivated according to suppliers` instructions, using supplemented D-MEM/F12 or RPMI media. Cell cultures were passaged according to their growth properties.

2.2.3 Establishment of 5-Fluorouracil-resistant secondary cell lines

In order to generate drug resistant cell lines, we selected for cell clones with the ability to acquire drug resistance. This was done by using a combination of low concentration drug treatment and growth recovery cycles. Secondary cell lines were treated under standard culture conditions with the anticancer drug 5-Fluorouracil. Treatment started when the cell lines reached sub confluence growth. The concentration of 5-Fluorouracil was chosen individually for each cell line according to the previously determined IC50 for this drug. The cell lines were then incubated for 48h under drug treatment. Subsequently, the culture media containing 5-Fluorouracil was discarded; cells were washed with standard culture media and further cultivated under drug free conditions. As soon as the previously drug treated cell lines reached sub confluence growth again, drug treatment was repeated. The concentrations of 5-Fluorouracil were adjusted in each cycle of drug treatment according to the degree of developed resistance, observed by growth rates. After a median treatment and recovery time corresponding to approx. 12 cycles of drug treatment the drug resistant cell lines were harvested, cell lysates were prepared and vital aliquots were deep frozen for further experiments. The degree of acquired chemoresistance to 5-Fluorouracil was determined by cell viability measurement under treatment and a comparisons to the parental cell line.

2.2.4 Cell viability assay

Cell viability after drug treatment was assessed by intracellular ATP-level analysis according to the manufacturer’s protocol using the ATPlite Luminescence ATP Detection Assay System (PerkinElmer, Boston, MA). Cells were seeded in 384-well microtiter plates at densities adjusted to the individual growth rate of the cell lines, ranging from 500-1500 cells per well and pre incubated for 24h. The cells were then

treated with various concentrations of FOLFOX combination treatment and further incubated for additional 48h, 72h and 96h following which ATP content was measured. The concentrations of the individual drugs used were summarized in fold FOLFOX dilutions, wherein 1 fold FOLFOX corresponds to 500 µM 5-Fluorouracil, 100 µM Leucovorin and 20 µM Oxaliplatin. Samples were tested in quadruplicate. The resulting luminescence was read using a FLUOstar OPTIMA® system (BMG Laboratories, Offenburg, Germany). Data are presented as means ± S.D. and were analysed using GraphPad Prism® Version 5.0 (GraphPad Software, San Diego, CA, USA). The results were expressed as the percentage of viability at a given concentration in reference to the untreated control.

2.2.5 Cell culture lysate preparation for proteomic analysis

Cells were lysed in an organic solution consisting of 50% acetonitril (ACN) and 0.5% trifluoroacid (TFA). Lysis was performed for 10min on ice followed by a 10 min ultrasonic treatment. Lysates were then centrifuged for 5min at 12,000 xg (4℃) and the supernatant was immediately transferred to LoBind reaction tubes (Eppendorf, Hamburg, Germany). Lysates were then dried in a vacuum centrifuge 5301 (Eppendorf, Hamburg, Germany) and resuspended in 0.1% FA for measurement of protein concentration and further analysis. Protein concentration was determined using the Bicinchoninic Acid Protein assay.

For the Top Down analysis of intact proteins cell lysates were then directly subjected to the LC-MALDI workflow. For the Bottom Up analysis of tryptic peptides cell lysates were subsequently prepared for tryptic digestion. Briefly, cell lysates were dried in a vacuum centrifuge (Eppendorf Vacuum concentrator, 5301) and resolved in 50 mM ammonium bicarbonate for 3min by mixing at RT. DTT (100 mM) as reducing agent was added to a final concentration of 12.5 mM and reduction was maintained at 60

℃ for 30min followed by alkylation with iodoacetam ide (15 mM final concentration) for 30min in the dark (RT). Trypsin at a concentration of 0.2 µg/µl was added and enzymatic digestion was performed overnight at 37 °C. TFA was then added to a final concentration of 1% to stop further trypsin digestion and to degrade the acid labile detergent *Rapi*Gest™ according to the manufactures instructions. After 45min the samples were centrifuged at 12,000 x*g* for 10min at 4 ℃ to remove remaining cell debris, the supernatant was carefully removed and stored in aliquots at -80 ℃.

2.2.6 Reverse Phase-High Performance Liquid Chromatography (RP-HPLC) and Capillary-High Performance Liquid Chromatography (CAP-HPLC)

For the Top Down study of intact proteins, whole cell lysates were separated by reverse phase HPLC system 1200 (Agilent, Böblingen, Germany) using a 4.6 x 50 mm column (Agilent, Böblingen, Germany). Solvent A was 0.1% TFA in ultrapure water, solvent B was 0.1% TFA in 99.9 % AcN. 75 µg of protein was injected at a LC flow rate of 300 µl/min. The column was heated constantly to 60 ℃ and proteins were eluted by a 67min gradient from 2 % to 40 % solvent B during the first 51min followed by a 15min increase to 60% solvent B. UV absorption at 214 nm was used to monitor the separation and quality of the protein / peptide separation. After each sample separation at least four successive cycles of blank injections (50 µl of 0.1% TFA in ultrapure water) followed by short gradient separations (25min) were run through the LC system in order to equilibrate the column and remove remaining proteins. Sample LC fractions were collected every 36.6sec (= 183 µl) into a LoBind deepwell plate (Eppendorf, Hamburg, Germany) resulting in a total number of 94 fractions per sample. 50 µl of each LC fraction was then transferred to a 96-well plate dried in a vacuum concentrator 5301 (Eppendorf, Hamburg, Germany). Each dried fraction was resuspended in 3.5 µl Sinapinic acid and 3 µl per fraction were spotted

onto a polish steel target, shortly before MALDI-MS acquisition. The polish steel targets were cleaned with hot water and by sonification in a solution of 50% methanol and 5% acetic acid for 10min. Subsequently the polish steel targets were wiped with 100% acetone and 100% methanol.

For the Bottom Up studies of tryptic peptides, cell lysates were separated by capillary RPHPLC (cap-LC, 1200 Agilent system) using a 0.3 x 15 mm C18 mRP column (Agilent). Solvent A was 0.1% TFA in ultrapure water, solvent B was 0.1% TFA in 99.9 % AcN. Four µl of the tryptic digest (see 2.2.5), corresponding to 2 µg of protein was injected at a LC flow rate of 4 µl/min. The column was heated constantly to 60 ℃ and tryptic peptides were eluted by a 90min grad ient from 2% to 30% solvent B during the first 80min followed by a 10min increase to 50% B. UV absorption at 214 nm was used to monitor the separation and quality of the peptide separation. LC fractions were spotted every 15 sec (= 1 µl) by a fraction collector (FC Proteineer, Bruker Daltonics) on spots of a-cyano-4-hydroxycinnamic acid matrix Prespotted AnchorChip (PAC) target resulting in a total number of 300 target spots per sample. After each sample separation at least two successive cycles of blank injections (3 µl of 0.1% TFA in ultrapure water) followed by short gradient separations (30min) were run through the LC system in order to equilibrate the column and remove remaining tryptic peptides. The PAC target spots were dried down at RT and sealed in plastic bags, stored in the dark and short before MALDI acquisition targets were dipped two times carefully for 5sec in 500 ml of 10 mM ammonium phosphate buffer containing 0.1% TFA (4-8 ℃). The PAC targets were then analyz ed by MALDI-MS and MALDI-MS/MS measurements.

2.2.7 MALDI-MS measurement and data analysis

An ultraflex III MALDI-MS instrument equipped with a 200 Hz smartbeam laser was used during the entire Top Down as well as the Bottom Up study. All software packages including MALDI measurement, spectra processing and statistical analysis were from Bruker Daltonik (Bremen, Germany).

For the Top Down LC-MALDI study polish steel targets and CPS calibrants (monoisotopic masses: Angiotension II, 1046.54; Angiotensin I, 1296.68; Neurotensin, 1672.91; Renin Substrate, 1758.93; ACTH clip 1-17, 2093.08; ACTH clip 18-39, 2465.19; ACTH clip 1-24, 2932.58; ACTH clip 7-38, 3657.92; Insulin, 5734.51; Ubiquitin, 8565.76; Cytochrom C, 12360.97; Myoglobin, 16952.30) were used for calibration. Additionally, an external standard consisting of a whole cell lysate with insulin spiked in was used to adjust the laser energy to reach an intensity value for insulin between 3000-6000 arbitrary units and a resolution of over 600 with 3000 applied laser shots prior to each MS measurement. Subsequently, sample measurements were performed under these adjusted laser conditions by accumulating 3000 laser shots on random positions of each target spot in the linear mode.

For the both Bottom Up LC-MALDI studies prespotted PAC target calibrants (monoisotopic masses: Angiotension II, 1046.54; Angiotensin I, 1296.68; Neurotensin, 1672.91; Renin Substrate, 1758.93; ACTH clip 1-17, 2093.08; ACTH clip 18-39, 2465.19; ACTH clip 1-24, 2932.58; ACTH clip 7-38, 3657.92) were used for near neighbour calibration during MS acquisition every four spots. Prior to each MS measurement the calibrant peptide ACTH clip 18-39 was used to adjust the laser energy to reach an intensity value between 6000-10 000 arbitrary units for 1000 applied laser shots and a resolution between 18,000 (+/- 10%). Subsequently, sample measurements were performed under these adjusted laser conditions by

accumulating 2500 laser shots on random positions of each target spot in the reflector mode. During both studies three replicates per sample were processed to reveal the technical reproducibility of the workflow. Initially, after LC-MALDI data acquisition all peaks above signal to noise threshold of 3 were considered for analysis. Due to the fact that most of the peaks are detectable not only in a single LC fraction, a non-redundant compound list was generated by the software WARP-LC. By definition a new compound in the list was generated if a gap of more than 5 fractions was between adjacent chromatographic fractions and if the mass differs by more than 100 ppm from other masses, although the averaged measured mass accuracy has been in average below 15 ppm. All measurements were controlled by the software WARP-LC 1.2 and peak detection, spectra smoothing and baseline correction were done in FlexAnalyis software 3.0. WARP-LC was used to generate non-redundant compound lists which served as input files for the statistical data analysis by ProfileAnalysis (Version 2.0; Bruker Daltonik, Bremen, Germany).

2.2.8 Statistical analysis

ProfileAnalysis was used to align the compound lists to generate buckets with defined retention time and *m/z* value, which allowed the comparison over multiple sample data sets. Normalization of peak intensities was done on the total intensity of all selected buckets. Differential peptide analysis was then performed with the goal to discover robust and significant expression differences between groups. Only *m/z* ions displaying a minimum 1.5 fold difference and a *p*-value < 0.05 between the groups were considered for further targeted identification of peptides from the Bottom Up study. The m/z ions displaying a minimum 1.5 fold difference and a p-value < 0.05 from the Top Down study were identified by using an in gel digestion approach. Statistical data analysis of biomarker candidate expression was subsequently

performed using GraphPad Prism® Version 5.0 (GraphPad Software, San Diego, CA, USA)

2.2.9 Targeted identification of peptides from the Bottom Up study by MS/MS

Target peptides, which showed peak abundance differences and statistical significance according to the data analysis, were identified by MALDI MS/MS in the LIFT mode by a semi-automated spectra accumulation procedure. Respective precursor masses were selected in a timed ion gate at 8 kV and detected by accumulating 400-800 laser shots manually. In the LIFT mode, post source decay (PSD) fragments were further accelerated by 19 keV. Depending on the peak abundance between 1500-5000 laser shots were accumulated in the LIFT mode to reach high quality MS/MS spectra. Biotools 3.2. (Bruker Daltonics) was used to submit MS/MS peak lists to database searches using MASCOT (Matrix Science*)*. For the database search the following criteria were used: enzyme, trypsin; variable modifications, oxidation M; mass tolerance, 50 ppm; MS/MS tolerance 0.7 Da; peptide charge, +1; two missed cleavages were allowed. Ion scores of a minimal probability of 95% ($p < 0.05$) were accepted and regarded as significant hits.

2.2.10 Identification of proteins from the Top Down study by in gel digestion and MS/MS

RP-HPLC fractions containing the target protein were dried in a vacuum centrifuge (Eppendorf Vacuum concentrator, 5301) and separated in a 4-12% SDS Bis-Tris gel, separation was performed in an electrophoresis system. Gel bands at the molecular size of interest were excised and washed. DTT (100 mM) was added to a final concentration of 10mM and reduction was maintained at 56 ℃ for 45min followed by alkylation with Iodoacetamide (15 mM final concentration) for 30min in the dark (RT).

Trypsin at a concentration of 0.2 µg/µl was added and enzymatic digestion was performed overnight at 37 ℃. TFA was then added un til a final concentration of 1% to stop further trypsin digestion. Peptides were subsequently extracted from the gel bands using sonification and extraction buffer (50% acetonitrile / 1% TFA). After 45min the samples were centrifuged at 12,000 x*g* for 10min at 4 ℃ to clarify lysates and stored in aliquots at -80 ℃.

Peptides resulting from the in gel digestion were subsequently subjected to capillary HPLC using a 0.3 x 15 mm C18 mRP column. Solvent A was 0.1% TFA in ultrapure water, solvent B was 0.1% TFA in 99.9 % AcN. Four µl of tryptic digest was injected at a LC flow rate of 4 µl/min. LC fractions were spotted every 15 sec (= 1µl) by a fraction collector on spots of a-cyano-4-hydroxycinnamic acid matrix Prespotted AnchorChip (PAC) target. After each sample separation at least two successive cycles of blank injections (3µl of 0.1% TFA in ultrapure water) followed by short gradient separations (30 min) were run through the LC system in order to equilibrate the column and remove remaining tryptic peptides. The PAC target spots were dried down at RT and sealed in plastic bags, stored in the dark and dipped two times carefully for 5 sec in 50 ml of 10 mM ammonium phosphate buffer containing 0.1% TFA (4-8℃) shortly before MALDI acquisition. Targe t peptides were identified by MALDI MS/MS in the LIFT mode using a LC-MALDI MS/MS workflow with subsequent semi-automated spectra accumulation procedure. Respective precursor masses were selected in a timed ion gate at 8 kV and detected by accumulating 400-800 laser shots. In the LIFT mode, post source decay (PSD) fragments were further accelerated by 19 keV. Depending on the peak abundance between 1500-5000 laser shots were accumulated in the LIFT mode to reach high quality MS/MS spectra. Biotools version 3.2. (Bruker Daltonics) was used to submit MS/MS peak lists to database searches using MASCOT (Matrix Science*)*. For the database search the

following criteria were used: enzyme, none or trypsin; variable modifications, oxidation M; carbamidomethyl; mass tolerance, 50 ppm; MS/MS tolerance 0.7 Da; peptide charge, +1; two missed cleavages were allowed. Ion scores of a minimal probability of 95% ($p < 0.05$) were accepted and regarded as significant hits.

2.2.11 Western blotting

Immunological validation of selected marker candidates was done by western blotting. Protein concentrations of lysates were determined using BCA protein assay according to the manufacturer's instructions. Briefly, 25 µg of protein were subjected to a 4-12% SDS Bis-Tris gel. Separation was performed in an electrophoresis system, and electrotransferred to PVDF membranes using a tank blotting system according to the manufactures instructions. Membranes were blocked by incubation for 2h with 5% skim milk (w/v) in phosphate buffered saline containing 0.1% Tween-20. Immunoblot analysis was carried out with the antibodies raised against the corresponding proteins in a dilution recommended by the supplier and a dilution of 1:4000 for GAPDH (Ambion), respectively, in the TRIS-buffered saline containing 0.1% Tween-20. GAPDH was used as loading control. Proteins were detected by enhanced chemiluminescence using the Raytest detection system "Darkroom Evo III.

2.2.12 Cu/Zn SOD activity assay

The Superoxide Dismutase Assay Kit (Cayman Chemical) was used for the analysis of Cu/Zn SOD activity. SOD activity was assessed by measuring the dismutation of superoxide radicals generated by xanthine oxidase and hypoxanthine. A standard curve provided a means to accurately quantify the activity of all three types of SOD (Cu/Zn-, Mn-, and Fe-SOD). Experiments were conducted according to the instructions of the supplier.

2.2.13 Analysis of somatic mutations in primary cell cultures

In contrast to the secondary cell lines, whose mutation status is listed in the Catalogue Of Somatic Mutations In Cancer (COSMIC; www.sanger.ac.uk/genetics/), the mutation status of the primary cell cultures was analyzed by Sanger sequencing. Mutation analysis of proteins from cellular signaling pathways implicated in tumorigenesis and drug reponse of colorectal cancer was provided as a service by the Inostics GmbH (Hamburg, Germany). Frozen cell pellets from the cell cultures were prepared and sent to Inostics. The detection of somatic mutations in cell lines represents a multistep process that has been optimized for the selected gene set. In the first step, DNA was purified from the cells and a quantitative real-time PCR reaction was performed for each sample in order to determine the yield of the purification. In the second step the purified DNA was subjected to PCR amplification of 11 selected exons and the quality of the resulting PCR products was verified by DNA agarose electrophoresis. In the final step, the PCR products were purified, sequenced in two directions by direct sequencing and analyzed by comparing the sequence to a reference sequence.

2.2.14 NanoPro1000 technology

The NanoPro1000 instrumentation from ProteinSimple (California, USA) provides a protein / phosphoprotein assay with many similarities to Western blot analysis. This technology combines a physical separation of native proteins with the specificity of antibody-based detection. For this purpose, NanoPro1000 assays apply a capillary-based isoelectric focusing for the separation of proteins and thus are able to resolve various protein modification states [66]. The antibody based detection of proteins is performed using luminol and peroxide to generate chemiluminescent light, which is then captured by a CCD camera. Because of a unique capillary-based design,

NanoPro assays are highly quantitative, fully automated, and extremely sensitive. The workflow of the NanoPro technology is shown in figure 1.

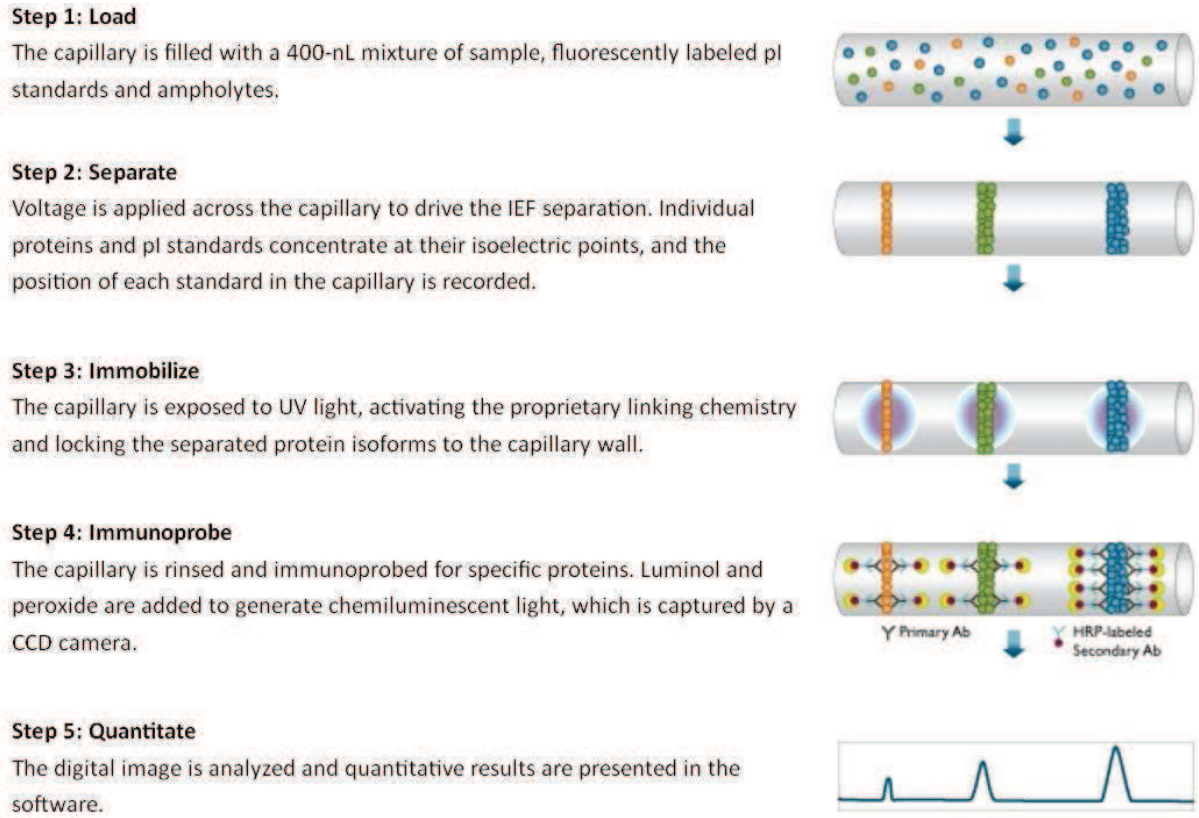

Figure 1. Schematic workflow of the NanoPro1000 technology (modified after Proteinsimple)

Herein, only nanograms of protein are needed for analysis. This enables a detailed characterization of protein modifications and protein expression in small, clinical samples. Furthermore, it is necessary to micro dissect epithelial cancer compartments from the heterogeneous microenvironment of a tumor in order to analyze the distinct expression of a biomarker candidate in a clinical sample. In contrast to traditional protein analysis techniques which require thousands to millions of cells, NanoPro assays are reported to require as few as 25 cells per assay [67]. Thus, the NanoPro technology is planned to be used for a validation of the predictive biomarker candidates, which potentially result from the Top Down and Bottom Up proteomic studies, in clinical samples. In the Assay Development experiments for the

adaption of antibodies corresponding to biomarker candidates, the MSD lysis buffer was used for sample preparation and 150 ng final protein concentration were loaded on the capillary system. The pI 5-8 nested or the pI 3-10 G2 Premix gradient was used for protein separation according to the pI of the biomarker candidate to be analyzed. Antibodies against the predictive biomarker candidates were tested for compatibility with the NanoPro1000 technology according to the Assay Development instructions.

2.2.15 Meso Scale Discovery technology

Meso Scale Discovery (MSD) technology is a multiplexed antibody based technology that uses electrochemiluminescence for the detection of proteins. In this technology the whole cell lysate is subjected to an ELISA-system of multiwellplate-coupled primary antibodies. The detection of antibody bound proteins is carried out using a secondary antibody, which is coupled to an aromatic complex called Ruthenium(II)-tris-bipyridin-(4-methylsulfonat)-NHS-ester („SULFO-TAG™“). Since the bottom of the multiwellplates consist of carbon coated foil, the voltage applied by the MSD Sector Imager 6000 stimulates the aromatic SULFO-TAG™ complex, which subsequently emits light at 620 nm, as shown in figure 2. This light is detected by a camera and counted in Relative Light Units. The intensity of light correlates with the amount of antibody bound proteins. Multiple excitation cycles of each label amplify the signal to enhance light levels and improve sensitivity. Since this is a multiplexing technology one is able to screen up to 5 different target proteins and their activation states. The activation of the EGF-receptor and cellular signaling proteins, such as AKT, GSK3β, p70S6K, ERK1/2, MEK were analyzed. The determination of activation states of signaling proteins is performed by using a combination of antibodies detecting phosphorylated and unphosphorylated versions of the target protein.

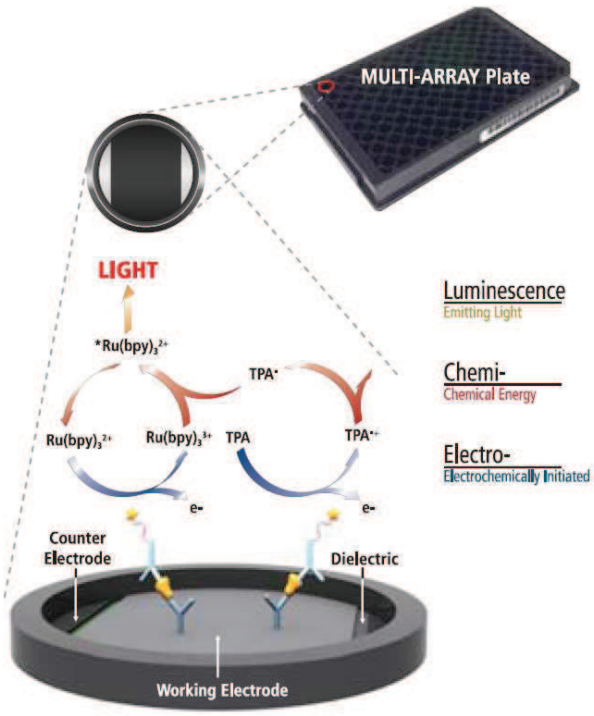

Figure 2: Schematic detection of proteins by the MSD technology.

A total protein content of 10 µg to 20 µg protein per well are needed, to analyze up to five different proteins quantitatively. The assays were conducted according to the supplier instructions. Statistical data analysis was performed using GraphPad Prism® Version 5.0 (GraphPad Software, San Diego, CA, USA).

3 Results

The studies for the discovery of protein biomarker candidates, predictive for the response to FOLFOX chemotherapy, were based on a diverse panel of twenty colorectal cell cultures. This panel included commercially available secondary cell lines as well as newly established primary cell cultures and their primary clonal cell lines. Primary cell cultures were continuously established during the time in which this thesis was prepared. The cell cultures were further on characterized in respect to their genetic identities, growth rates, mutation status and chemosensitivity to FOLFOX chemotherapy. Subsequently, intrinsic protein expression profiles of the individual cell cultures were generated by Top Down and Bottom Up proteomic analysis using a LC-MALDI workflow. After statistical analysis significantly regulated peaks were identified by either in gel digestion and subsequent LC-MALDI-MS/MS or direct identification of peptides by MALDI-MS/MS.

3.1 Establishment of primary cell cultures

Primary cell cultures were established according to Standard Operating Procedures of Indivumed. Patients gave full consent for the use of their tumor material. From four of these primary mixed cultures, six primary mixed cell cultures were successfully prepared by using the limiting dilution method (see table 1). Subsequently, four primary clonal cell lines could be established. Growth of clonal cell lines was controlled by microscopical examination to ensure the mono clonality of the culture. Since the preparation of primary cell cultures included steps to eliminate fibroblasts from the culture, the primary mixed cultures consisted mainly of epithelial cancer cells. During first *in vitro* passages of the primary cultures, differential trypsination was applied to prevent excessive growth of fibroblasts in the cultures. The content of fibroblasts within the cultures was determined by microscopical examination and IHC

staining against marker for fibroblasts (Vimentin) and epithelial cells (pan-cytokeratin) using Ventana technology, see figure 3. As expected, all epithelial cancer cells in these cultures showed a strong pan-cytokeratin staining and were negative for Vimentin. Fibroblasts within these cultures were negative for pan-cytokeratin and positive for Vimentin. Primary mixed cell cultures used for experiments contained a maximum of 10% fibroblasts.

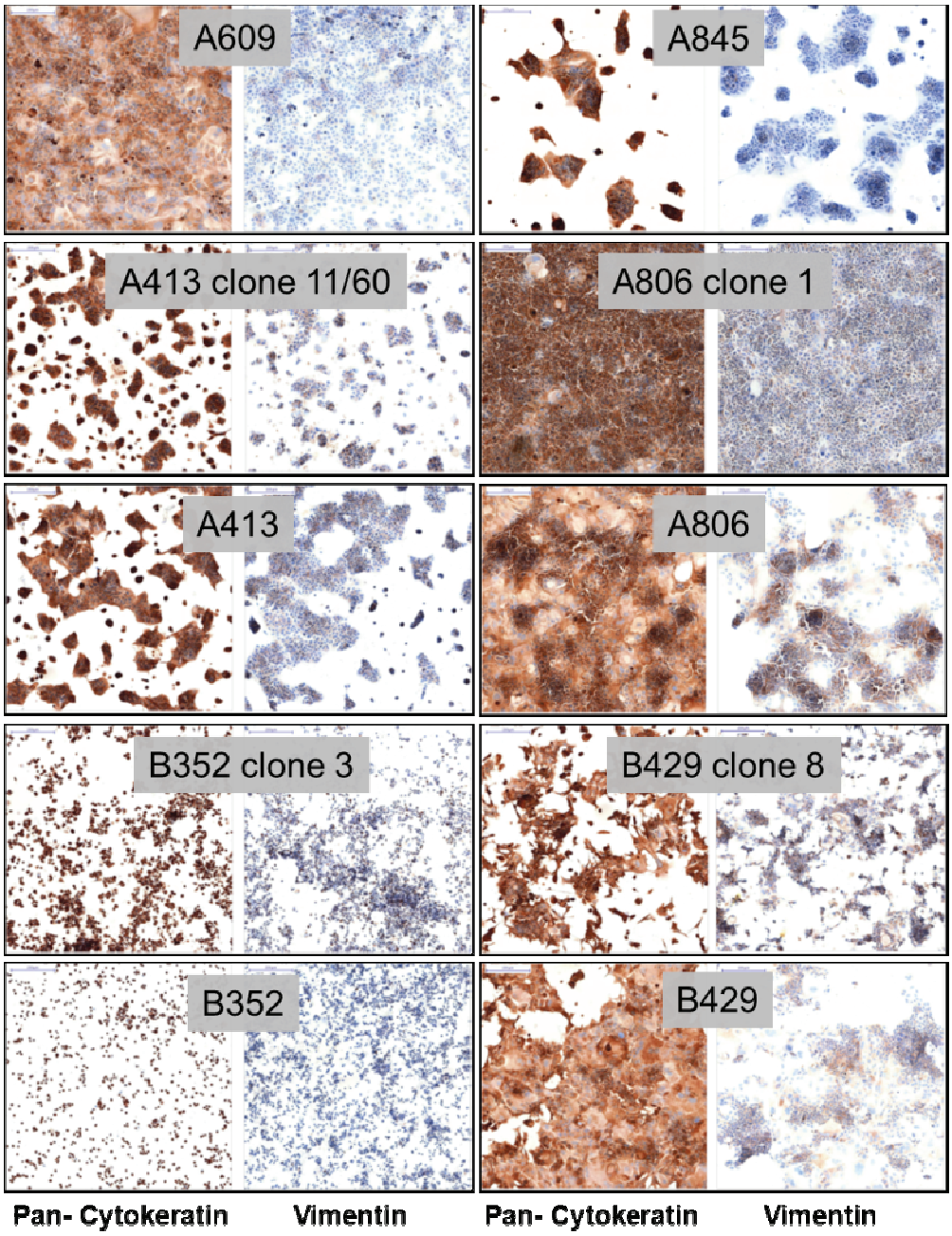

Figure 3: Pan-Cytokeratin and Vimentin IHC staining of primary cell cultures and their clonal cell lines.

3.2 Mutation status of primary and secondary cell cultures

For mutation analysis of the primary cell cultures the genes BRAF, PIK3CA, KRAS, APC and TP53 were sequenced in selected hotspot regions of exons. These genes encode for three key cell signaling proteins (BRAF, PIK3CA, KRAS), involved in ErbB-receptor related cell signaling and two tumor suppressor proteins (APC, TP53). The ErbB-receptor family (including EGFR, HER-2, HER-3 and HER-4) and downstream signaling proteins such as BRAS, PI3K and KRAS are promoting cell proliferation and survival and thus represent molecular targets for therapy. In regard to the new generation, targeted drugs, the ErbB-receptor family is a main target for therapeutic antibodies and small molecules. Therefore, information on the mutation status of the cell cultures is mandatory for the interpretation of data resulting from studies analyzing signaling pathway activation and inhibition. The APC gene is a gatekeeper gene in carcinogenesis of colorectal carcinomas, which prevents the uncontrolled growth of cells that may result in cancerous tumors. The TP53 gene regulates the cell cycle and functions as a tumor suppressor. TP53 has been described as being involved in response to chemotherapeutics because of its role in conserving genome stability and induction of apoptosis. Mutation analysis of ten primary cell cultures has successfully been performed in DNA isolated from ten cell cultures. A total of 19 different genetic alterations have been found. Four different genetic alterations were found in KRAS, one in BRAF, seven in TP53, and seven in APC (see table.8).

Overall, twenty three mutations were detected in the ten primary cell cultures. No PI3KCA mutation was present in these cell cultures, one clonal cell line carried a BRAF mutation and five of the cell cultures carried a KRAS mutation. There was no BRAF-KRAS double mutant present. Since the mutation of APC is an early event in

Table 8: Mutation status of primary and secondary cell cultures. Hotspot regions of selected genes were sequenced.

		Mutations	BRAF	KRAS	PIK3CA	APC	TP53
Primary cell cultures	1	A413 clone 11/60	1799 T< T/A			4661 ins A	818 G<A
	2	A413MK		35 G<G/A		4099 C> C/T	476 C<T
	3	B352 clone 3				3945 C>C/A 4227 ins GAACC	
	4	B352MK				3945 C>C/A 4227 ins GAACC	701 A>G
	5	A806 clone 1		35 G>C		4661 ins A	773 G>A
	6	A806MK		35 G>C			773 G>A
	7	B429 clone 8				4627 G>G/T	
	8	B429MK				4632 G>G/T	639 C> C/T
	9	A845MK		38 G>G/A		3747 C> C/A	589 G>A
	10	A609MK		35G>A		4099 C> C/T	476 C>T
Secondary cell lines	11	HT-29	p.V600E c. 1799T>A	p.Q61L c.182A>T	p.P449T c.1345C>A	p.T1556fs*3 c.4666_4667insA p.E853* c.2557G>T	p.R273H c.818G>A
	12	LS174T		p.G12D c.35G>A	p.H1047R c.3140A>G		
	13	SW480		p.G12V c.35G>T		p.Q1338* c.4012C>T	
	14	Colo320		p.G12D c.35G>A		p.S811* c.2432C>G	p.R248W c.742C>T
	15	Colo678		p.G12D c.35G>A		p.T1556fs*3 c.4666_4667insA	
	16	HCT-15		p.G13D c.38G>A	p.E545K c.1633G>A p.D549N c.1645G>A	p.I1417fs*2 c.4248delC p.R2166* c.6496C>T	p.S241F c.722C>T p.? c.1101-2A>C
	17	HCT-8		p.G13D c.38G>A			
	18	Caco-2				p.Q1367* c.4099C>T	
	19	Lovo		p.G13D c.38G>A		p.R1114* c.3340C>T	
	20	LS513		p.G12D c.35G>A			

The mutation status of secondary cell lines was obtained from the Catalogue of Somatic Mutations in Cancer (COSMIC) internet database. Equally to the primary cell cultures twenty three mutations were present in the ten secondary cell lines. Among these cell lines also only one of ten cell lines had a mutation in the BRAF gene, nine cell lines carried a KRAS and three cell lines a PI3KCA mutation. The APC gene was mutated in seven of ten and the TP53 gene in only three of ten cell lines.

The mean number of mutated genes per cell culture was 2.3 for the primary as well as secondary cell cultures, whereas the distribution of mutations differed slightly with a median of 2.5 for the primary and 2.0 for the secondary cell cultures. Most of the primary cell cultures carried two or a maximum of 3 mutations, with just one cell culture carrying only one mutation. In the panel of secondary cell lines a maximum of 5 mutations was observed, with three cell lines carrying only one mutation. As well the number of mutations per gene is higher in the secondary cell lines. In regard to the distribution of mutations between primary and secondary cell cultures, the primary cell cultures seem to be more often mutated in the APC and TP53 genes, whereas secondary cell lines seem to have more mutations in genes involved in cell signaling. Nevertheless the number of cases is most likely to small to draw any final conclusions.

3.3 Chemosensitivity of primary and secondary cell cultures to FOLFOX treatment

In order to define a chemosensitive and a chemoresistant group of cell cultures, which were the basis for the proteomic studies, the *in vitro* chemosensitivity of the twenty cell cultures to FOLFOX treatment was characterized. The ATP-Lite assay was used to detect cell death/loss of viability induced by drug treatment. The effect of FOLFOX treatment was analyzed in four different drug dilutions at 48, 72 and

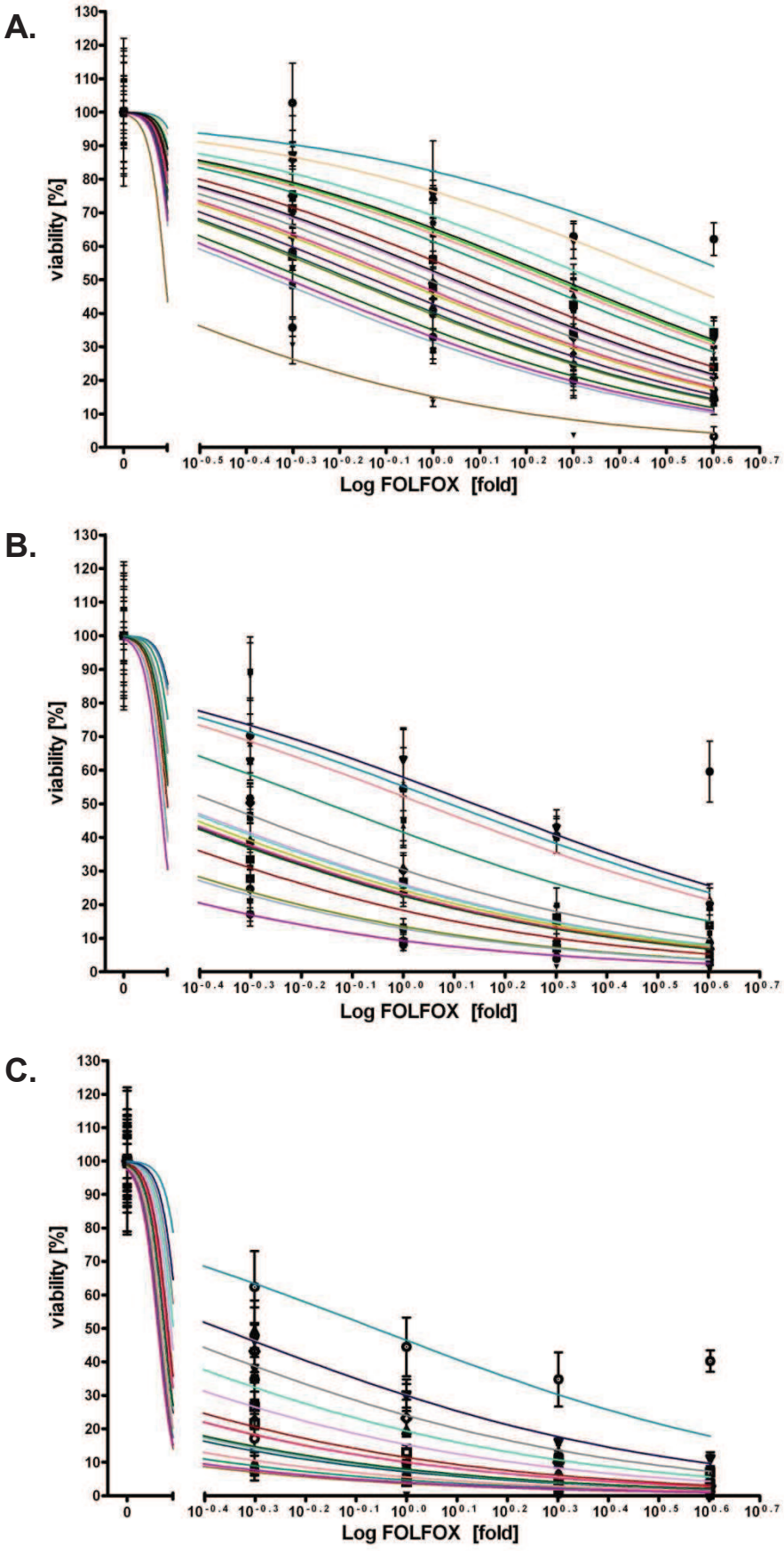

Figure 4: Dose-response curves of the twenty FOLFOX treated cell cultures after 48h (A), 72h (B) and 96h (C). The legend for cell cultures identification has been removed to enhance lucidity in reference to figure 6.

96 hours after adding the compound. The cell cultures showed dose-time dependent responses to FOLFOX treatment as shown in figure 4. Generally, cell death was induced by FOLFOX treatment in a dose dependent manner, whereas the cyto- and genotoxic effects seemed to accumulate over time resulting in more impact of long term treatment. The calculation of IC50 values (corresponding to the concentration of FOLFOX resulting in 50% cell death) revealed differential chemosensitivity of the cell cultures to drug treatment.

As shown in figure 4, there was no trend evident of primary cell cultures being more chemoresistant or chemosensitive than secondary cell cultures. Although, four of six primary mixed cell cultures were relatively chemoresistant. Primary clonal cell lines seem to differ in chemosensitivity from their correspondent primary mixed cell cultures. Cell cultures, such as LS513 and B352MK were very sensitive to drug treatment, whereas other cell cultures e.g. A806MK and Colo678 were many folds less sensitive. Based on the differential chemosensitivity of the cell cultures a chemosensitive and a chemoresistant group was composed by dividing the groups in reference to the median chemosensitivity. These groups differed significantly (p-value ≤ 0.001) in their chemosensitivity at every time point as shown in figure 5.

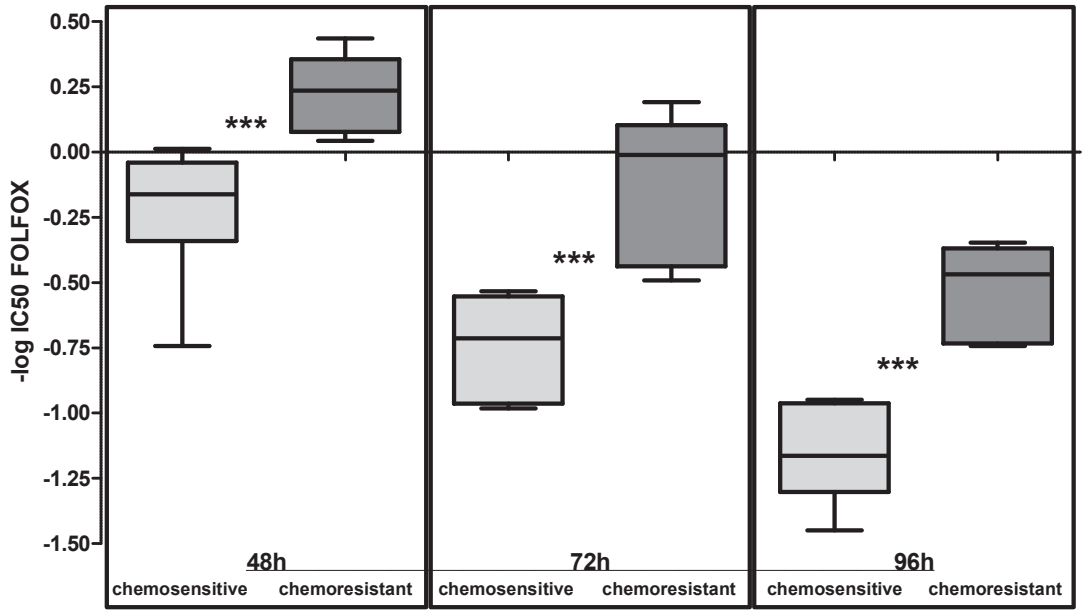

Figure 5: Chemosensitivity of sensitive and resistant groups of cell cultures to FOLFOX treatment. The chemosensitivity differed significantly, p-value= 0.0007 for 48 hours; 0.0003 for 72 hours and p-value= < 0.0001 for 96 hours, respectively.

Since there were cell cultures with a chemosensitivity close to the median of the whole cell culture panel, these cell cultures may have switched between groups on different time points. Therefore, a cell culture was defined as chemosensitive and chemoresistant, if it belonged to a group two of three times. The final assembly of groups with corresponding IC50 values at different time points was summarized in figure 6. The appointed chemosensitive and the chemoresistant group was used as a basis for further Top Down and Bottom Up proteomic analysis to discover differential expressed proteins or peptides between those groups. This cell culture panel was used in the Top Down and Bottom Up studies of intrinsic chemoresistance to FOLFOX treatment.

A.

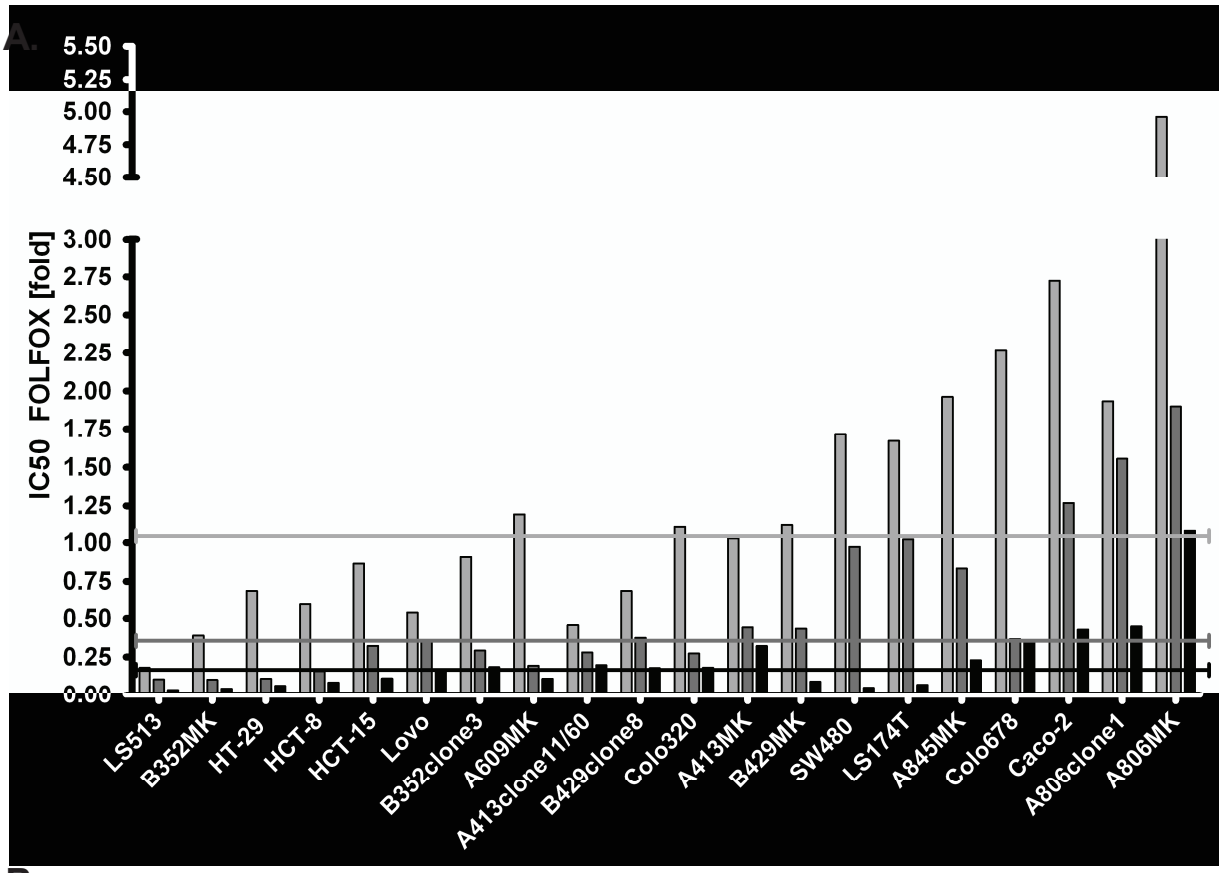

B.

		IC 50 [fold FOLFOX]					IC 50 [fold FOLFOX]		
	Cell Cultures	48h	72h	96h		Cell Cultures	48h	72h	96h
Chemosensitive	LS513	0.1808	0.1042	0.0355	Chemoresistant	Colo320	1.1020	0.2741	0.1810
	B352MK	0.3898	0.1027	0.0445		A413MK	1.0290	0.4417	0.3206
	HT-29	0.6883	0.1087	0.0628		B429MK	1.1160	0.4346	0.0899
	HCT-8	0.6043	0.1574	0.0829		SW480	1.7160	0.9741	0.0497
	HCT-15	0.8653	0.3226	0.1122		LS174T	1.6700	1.0210	0.0685
	Lovo	0.5371	0.3554	0.1663		A845MK	1.9610	0.8333	0.2295
	B352 clone 3	0.9088	0.2922	0.1847		Caco-2	2.7240	1.2690	0.4273
	A609MK	1.1960	0.1929	0.1088		Colo678	2.2640	0.3655	0.3397
	A413 clone 11/60	0.4559	0.2796	0.1981		A806 clone 1	1.9310	1.5540	0.4497
	B429 clone 8	0.6883	0.3734	0.1778		A806MK	4.9610	1.8970	1.0770

Figure 6: Final assembly of chemosensitive and chemoresistant groups, including calculated IC50 values of the twenty FOLFOX treated cell cultures after 48h, 72h and 96h. The data were plotted as a bar chart (A.; grey = 48h, dark grey = 72h and black = 96h) and were summarized in figure (B).

3.4 Establishment of a Top Down proteomic workflow

For the discovery of predictive biomarker candidates a proteomic workflow for the detection of low molecular weight proteins and peptides was developed. In contrast to most proteomic approaches, which apply tryptic digestion of proteins, cell lysates of cell cultures were analyzed without prior tryptic digestion. This enabled the access to low molecular proteins, which can potentially not be detected in Bottom Up

proteomic workflows. By using this workflow cell lysates were pre-fractionated by RP HPLC and subsequently analyzed by MALDI MS in order to generate protein expression profiles in a mass range of 2.5 kDa up to 30 kDa, reflecting the low molecular proteome, as shown in figure 7.

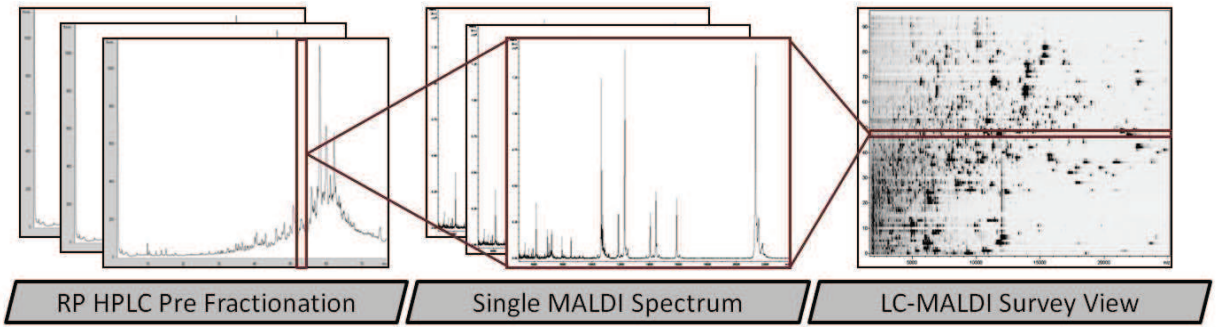

Figure 7: Schematic illustration of the established Top Down proteomic workflow. In the HPLC chromatogram the time [min] is plotted on the X-axis and the intensity [arb.units] on the Y-axis. In the MALDI spectrum the mass [kDa] is plotted on the X-axis and the intensity [arb.units] on the Y-axis. The survey view of LC-MALDI data shows the LC fractions on the X-axis and the mass [kDa] is plotted on the Y-axis.

The establishment of the workflow included several steps in which methods were adjusted to this new approach. In the first step, the optimal parameter for the pre-fractionation of proteins were determined by adjusting the RP-HPLC gradient and the temperature of the column. In the second step, the parameter for the acquisition of MALDI data were adapted to the newly established RP HPLC conditions. In a third step, the statistical analysis of data from the Top Down study was used to evaluate the reproducibility and accuracy of the workflow. On this basis, the statistical analysis revealed several significant regulated biomarker candidates. Since these biomarker candidates could not be directly identified by MS/MS analysis, due to their molecular weight above 4000 Da, an “in gel” digestion approach was applied to purify and final identification of the biomarker candidates.

3.5 Top Down proteomic study of intrinsic chemoresistance to FOLFOX therapy

Fourteen cell cultures were used for the Top Down study of intrinsic chemoresistance. This cell culture panel included nine secondary cell lines and five primary cell cultures (see table 9). After initial establishment of the workflow, the samples were randomly assigned to the LC-MALDI acquisition to prevent bias in sample preparation and technical conduction of the workflow. For illustration of the LC-MALDI data figure 8 shows exemplary survey views of replicates of LC-MALDI data from one cell line. The LC fractions are plotted on the y axis and the mass range on the x axis. Intensity of peaks is displayed by density.

Table 9: Chemosensitive and chemoresistant groups of cell cultures used in the Top Down study.

Chemosensitive	Chemoresistant
LS513	Colo320
HT-29	A413MK
HCT-8	SW480
HCT-15	LS174T
B352 clone 3	Colo678
A609MK	Caco-2
A413 clone 11/60	A806 clone 1

Although, no exact quantitative information can be derived from those pictures the survey views give a first overview on retention time, signal intensity and general pattern reproducibility. For optimization of MALDI measurement reproducibility, the laser intensity for MALDI MS measurements was adjusted to an external standard consisting of a whole cell lysate with insulin spiked in prior to every measurement. Assessment of reproducibility for sample screening has been derived from the number of measured peaks (compounds) and the signal intensities of the same peaks within the technical replicates. The number of non-redundant compounds between individual samples ranged from 2500-3000, whereas the averaged CV for the number of compounds within the replicates was 11%.

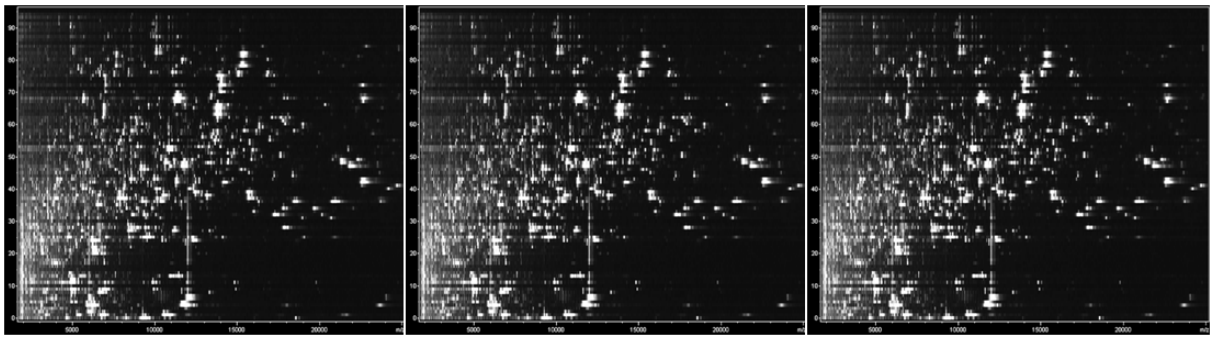

Replicate 1 Replicate 2 Replicate 3

Fig. 8: Three exemplary technical replicates of the cell line HCT-8, shown as LC-MALDI survey views to visualize the reproducibility of the workflow.

Statistical analysis of the LC MALDI data sets by the Principal Components Analysis showed a weak clustering of chemoresistant against chemosensitive cell lines, as shown in figure 9. This clustering of groups suggests that there are differences in the protein expression patterns between groups, although the studied cell lines were all colorectal cancer cell lines.

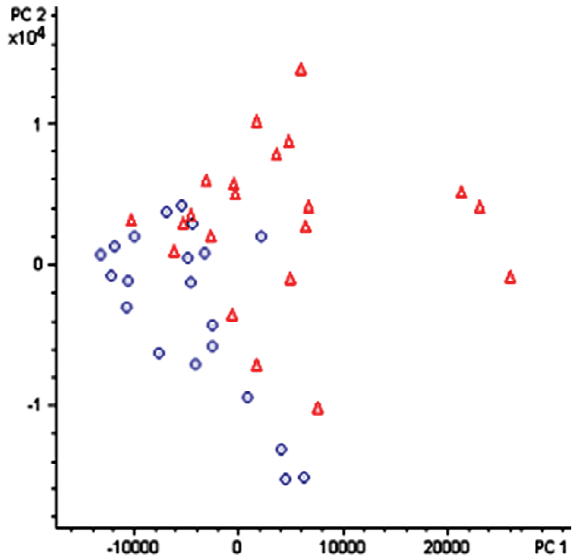

Figure 9: PCA analysis of the generated proteomic profiles. Chemoresistant cell cultures (red) cluster against chemosensitive cell cultures (blue) with a slight overlapping of groups.

By comparing the protein expression profiles of the panel of fourteen colorectal cancer cell cultures defined into a chemoresistant and a chemosensitive group, 88 compounds were found to be significantly ($p = \leq 0.01$) regulated more than 1.5 fold between groups. Table 10 displays the results of the T-test analysis. The compounds are presented as buckets, which are defined as combination of LC-retention time and

molecular weight. Furthermore, the significance of regulation and the degree of regulation are displayed. The p-values of the compounds were analyzed by the Bonferroni correction in order to minimize false positive classifications. The results are shown as p-value for the False Discovery Rate (FDR).

For the identification of biomarker candidates (Buckets) it was necessary to isolate the mass of interest from the diverse mixture of proteins, present in a single HPLC-fraction. Therefore, a pre-fractionation of LC-fractions by SDS-Page was chosen. Further on, the intact protein needs to be enzymatically digested and identified via MALDI-MS/MS. This was done using an in gel digestion approach.

Table 10: Results of the T-test analysis of LC-MALDI data performed in ProfileAnalysis. Compounds, which were significantly (p= ≤ 0.003) regulated are displayed. Buckets consist of the LC retention time and the molecular weight.

	Bucket	p-Value	Fold change	p-Value (FDR)
1	1397.0s : 6434.92m/z	0.000	2.260	0.000
2	2487.1s : 4867.67m/z	0.000	-1.860	0.002
3	2584.9s : 5150.19m/z	0.000	-1.810	0.008
4	610.3s : 6772.71m/z	0.000	2.680	0.008
5	2470.4s : 15858.49m/z	0.000	-1.860	0.008
6	2433.8s : 7926.52m/z	0.000	-1.820	0.008
7	1475.4s : 6170.38m/z	0.000	3.610	0.009
8	2660.9s : 13727.06m/z	0.000	-3.390	0.012
9	2666.4s : 4994.65m/z	0.000	-1.800	0.012
10	982.0s : 5119.86m/z	0.000	1.780	0.017
11	2251.6s : 5463.08m/z	0.000	-1.950	0.017
12	969.6s : 4895.30m/z	0.000	1.830	0.017
13	965.6s : 5105.57m/z	0.000	1.700	0.018
14	1945.5s : 9250.26m/z	0.000	2.050	0.018
15	1376.0s : 6392.31m/z	0.000	2.220	0.018
16	2798.9s : 6539.56m/z	0.000	-2.190	0.018
17	2557.6s : 4312.05m/z	0.001	-1.650	0.020
18	1519.6s : 9523.48m/z	0.001	2.720	0.020
19	3302.4s : 14183.44m/z	0.001	-2.700	0.020
20	2232.1s : 5209.18m/z	0.001	-2.290	0.021
21	2365.2s : 10937.19m/z	0.001	-2.200	0.023
22	3138.7s : 5736.20m/z	0.001	-2.080	0.027
23	1665.6s : 8373.76m/z	0.001	1.810	0.027
24	2701.7s : 6772.77m/z	0.001	-1.850	0.027
25	627.0s : 6929.77m/z	0.001	1.670	0.027
26	1511.1s : 4763.83m/z	0.001	2.130	0.027
27	2643.1s : 7276.63m/z	0.001	-3.560	0.027
28	628.8s : 6962.06m/z	0.001	1.960	0.027
29	3552.1s : 7769.72m/z	0.001	-3.250	0.027
30	2728.1s : 8078.86m/z	0.001	-1.890	0.027
31	1483.1s : 3115.38m/z	0.001	1.870	0.027
32	2473.4s : 7330.49m/z	0.001	-1.580	0.027
33	630.2s : 5308.26m/z	0.001	-3.080	0.027
34	2406.9s : 6921.07m/z	0.001	-1.790	0.027
35	964.0s : 7205.46m/z	0.002	1.950	0.028
36	3799.8s : 5697.37m/z	0.002	-3.280	0.028
37	2817.1s : 8867.83m/z	0.002	-2.080	0.028
38	1373.5s : 6243.81m/z	0.002	10.590	0.028
39	632.2s : 5268.21m/z	0.002	-1.940	0.028
40	2999.6s : 6896.16m/z	0.002	-1.780	0.029
41	2787.8s : 9210.91m/z	0.002	-2.160	0.029
42	2347.0s : 10641.47m/z	0.002	-2.470	0.029
43	970.0s : 4924.44m/z	0.002	1.620	0.029
44	3151.4s : 5698.26m/z	0.002	-1.640	0.029
45	3360.1s : 13857.37m/z	0.002	-1.880	0.029
46	2394.6s : 21301.57m/z	0.002	-2.660	0.030
47	2852.0s : 6332.14m/z	0.002	-1.950	0.030
48	2562.7s : 4484.53m/z	0.003	-1.660	0.032
49	2661.3s : 6861.09m/z	0.003	-2.030	0.032
50	628.8s : 6946.15m/z	0.003	1.770	0.032
51	3329.6s : 14497.96m/z	0.003	-2.310	0.032
52	3057.5s : 11204.68m/z	0.003	-2.250	0.032
53	1491.5s : 12332.08m/z	0.003	4.940	0.032
54	2673.0s : 8144.58m/z	0.003	-2.140	0.034
55	2670.6s : 3038.88m/z	0.003	-1.760	0.034

3.5.1 In gel digestion workflow for the identification of biomarker candidates

The molecular identities of the Buckets from the T-test analysis were unknown at this point of the study. The knowledge of the protein identity of a biomarker candidate is essential for a further antibody based validation. Furthermore, the final translation of the predictive biomarker to the clinical situation is mostly accompanied by the development of an antibody based ELISA assay.

Since nearly all of the Buckets from table 10 displayed a molecular weight above 4000 Da, a direct identification of the biomarker candidates via MS/MS analysis, similar to a Bottom Up workflow, was technically not possible. As a first step for the identification of those biomarkers, a pre-fractionation of the HPLC-fractions from the initial study containing the Bucket of interests, was performed by SDS page. Therefore, LC-fractions of interests from a cell line with a high expression of the biomarker were separated in a 4-12% SDS Bis Tris gel and gel bands at the molecular size of the biomarker candidate to be identified were excised. Subsequently, in gel digestion of proteins within gel bands was performed, the tryptic peptides were eluted and subjected to cap-RP-HPLC. The resulting LC-fractions were spotted on PAC targets and peptides were identified by MS/MS analysis. The MS-MS spectra were analyzed by a database search on the MASCOT server. Figure 9 gives a schematic overview on the in gel digestion workflow.

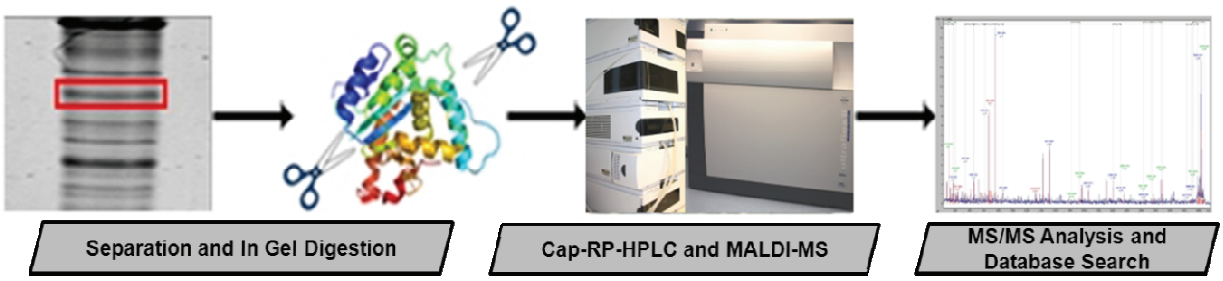

Figure 10: Schematic overview on the in gel digestion workflow. Gel bands were excised, in gel digestion was performed and subsequently LC-MALDI-MS/MS analysis revealed the protein identity.

An example for a MS/MS spectrum, which resulted in the identification of the Superoxide dismutase [Cu/Zn] is shown in figure 11. The spectrum was generated from one (3720.81m/z, corresponding to the bucket 5 of the initial study) of the three peptides that were detected during the identification of the protein. The MASCOT database search for this peptide resulted in a MASCOT score of 151, and thus identified the SOD 1 with great confidence. In the In gel digestion experiments, several peptides corresponding to the SOD 1 were detected with high intensities, which indicates a high abundance of the protein in the LC-Fraction.

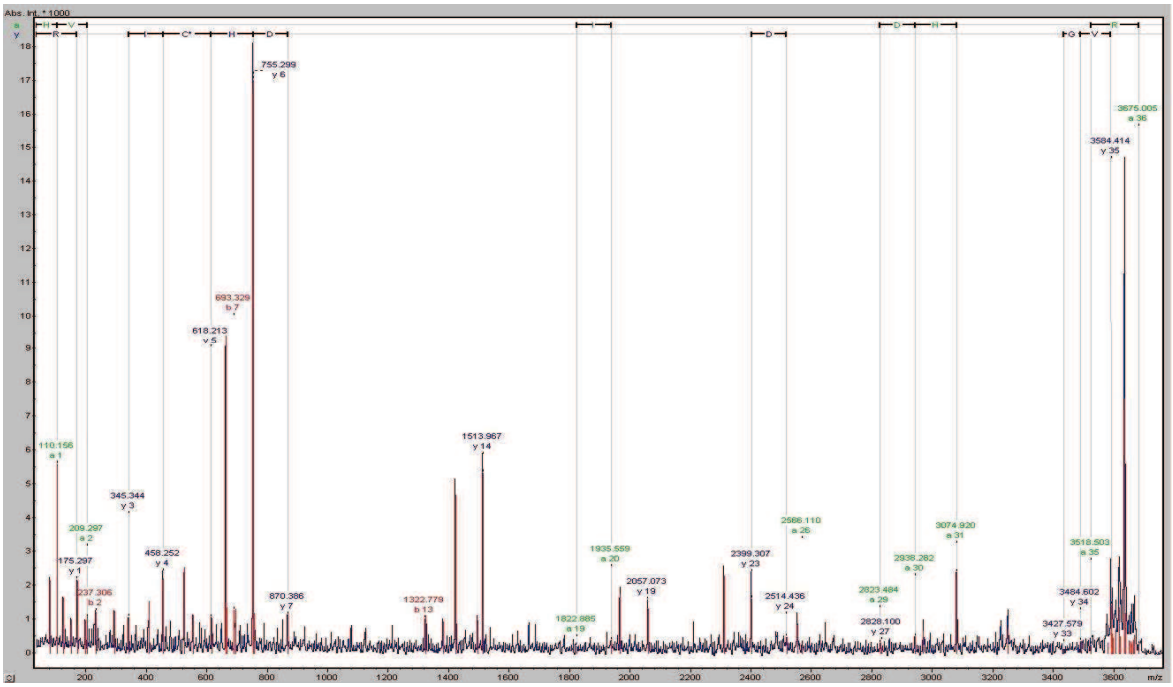

Figure 11: MALDI-MS/MS spectra of one (3720.81m/z) of the three peptides used for the identification of the Superoxide dismutase [Cu/Zn]. The relative intensity is plotted on the y-axis, the molecular mass is plotted on the x-axis. Peptides that could be linked to fragments are indicated by the lines below.

This was initially stated by the MALDI-MS spectrum of the corresponding cell line from the basic data set of the study. Other significantly ($p \leq 0.05$) regulated biomarker candidates which were identified by using this approach are shown in table 11. The identification approach using in gel digestion resulted in the identification of twenty one biomarker candidates from various cellular compartments, with several biological functions. Among those were for example nuclear proteins, such as the DNA-directed

RNA polymerase, the small nuclear ribonucleoprotein Sm D3 and the Histone H2B type 1. Furthermore, enzymes located in the cytoplasm like the Superoxide dismutase [Cu/Zn], the Ubiquitin-60S ribosomal protein L40 and the mitochondrial ATPase inhibitor, were identified.

Although all of these twenty one biomarker candidates may have a potential in predicting the response to FOLFOX treatment or give insight in mechanisms of chemoresistance, it was not possible to validate them all during this thesis. For this reason, a literature search on all identified biomarker candidates was conducted in order to select the most promising biomarker candidates. As a result of this literature search, three biomarker candidates were selected for further validation. This set of biomarkers included the Superoxide dismutase [Cu/Zn] (SOD1), the Ubiquitin-60S ribosomal protein L40 (UBA52) and the mitochondrial ATPase inhibitor (ATPIF1). The SOD1 has already been described in the context of chemoresistance to cisplatin and has been found to be regulated similar to the findings in this study. This biomarker, which in general supports/confirms the results from this study, has been used as an internal control. The biomarker candidates UBA52 and ATPIF1 are undescribed in the context of chemoresistance and thus potentially represent valuable, newly discovered predictors of response to FOLFOX chemotherapy.

Table 11: List of biomarker candidates from the Top Down study, identified by the in gel digestion approach. Expression differences of the biomarker candidates are displayed as Fold change in relation to the S = chemosensitive vs. R = chemoresistant group.

T-test Bucket	Identity of Biomarker Candidates	UniProt identifier	p-value	Fold change S/R
2470.4s:15858.49m/z	Superoxide dismutase [Cu-Zn]- Homo sapiens (Human)	SODC_HUMAN	**0.0001**	**-1.86**
1491.5s:12332.08m/z	ATPase inhibitor, mitochondrial- Homo sapiens (Human)	ATIF1_HUMAN	**0.0027**	**4.94**
1475.4s:6170.38m/z	Ubiquitin-60S ribosomal protein L40- Homo sapiens (Human)	RL40_HUMAN	**0.0001**	**3.61**
2337.5s:11204.95m/z	Dermcidin (Preproteolysin)- Homo sapiens (Human)	DCD_HUMAN	**0.0063**	**3.31**
3000.2s:13926.29m/z	Thioredoxin domain-containing protein 17- Homo sapiens (Human)	TXD17_HUMAN	**0.0054**	**2.68**
2406.9s : 6921.07m/z	DNA-directed RNA polymerases I, II, and III subunit RPABC4 OS=Homo sapiens	RPAB4_HUMAN	**0.0015**	**-1.79**
2660.9s : 13727.06m/z	Histone H2B type 1 (H2B.1 A)- Homo sapiens (Human)	H2B1C_HUMAN	**0.0002**	**-3.39**
1665.6s : 8373.76m/z	Cysteine-rich protein 1 (Cysteine-rich intestinal protein) (CRIP) - Homo sapiens (Human)	CRIP1_HUMAN	**0.0011**	**1.81**
2817.1s : 8867.83m/z	Cytochrome c oxidase polypeptide VIc precursor (EC 1.9.3.1) - Homo sapiens (Human)	COX6C_HUMAN	**0.0017**	**-2.08**
2673.0s : 8144.58m/z	Uncharacterized protein C20orf52 - Homo sapiens (Human) ROMO1	CT052_HUMAN	**0.0030**	**-2.14**
2738.9s : 18435.83m/z	Thioredoxin, mitochondrial precursor (Mt-Trx) (MTRX) (Thioredoxin-2) - Homo sapiens (Human)	THIOM_HUMAN	**0.0049**	**-2.1**
2626.6s : 11040.89m/z	Loss of heterozygosity 3 chromosomal region 2 gene A protein - Homo sapiens (Human)	L3R2A_HUMAN	**0.0121**	**-2.11**
2571.6s : 13985.36m/z	Small nuclear ribonucleoprotein Sm D3 (snRNP core protein D3) (Sm-D3) - Homo sapiens (Human)	SMD3_HUMAN	**0.0130**	**-1.73**
2632.0s : 15209.69m/z	Fatty acid-binding protein, epidermal (E-FABP) - Homo sapiens (Human)	FABPE_HUMAN	**0.0130**	**-2.18**
2591.4s : 10292.36m/z	Dynein light chain 1, cytoplasmic (Dynein light chain LC8-type 1) - Homo sapiens (Human)	DYL1_HUMAN	**0.0134**	**-1.64**
2369.0s : 21805.30m/z	NADH dehydrogenase [ubiquinone] 1 beta subcomplex subunit 9 OS- Homo sapiens	NDUB9_HUMAN	**0.0139**	**-2.27**
2646.1s : 7939.90m/z	40S ribosomal protein S28 - Homo sapiens (Human)	RS28_HUMAN	**0.0147**	**-1.66**
2636.3s : 6929.97m/z	NADH dehydrogenase [ubiquinone] 1 beta subcomplex subunit 1 (EC 1.6.5.3) - Homo sapiens (Human	NDUB1_HUMAN	**0.0200**	**-1.52**
2789.8s : 12777.80m/z	SH3 domain-binding glutamic acid-rich-like protein - Homo sapiens (Human)	SH3L1_HUMAN	**0.0272**	**-2.17**
2843.5s : 17899.84m/z	Ubiquitin-conjugating enzyme E2 L3 (EC 6.3.2.19) - Homo sapiens (Human)	UB2L3_HUMAN	**0.0302**	**-1.96**
2376.1s : 21973.62m/z	Peptidyl-prolyl cis-trans isomerase F, mitochondrial OS=Homo sapiens (Human)	PPIF_HUMAN	**0.0361**	**-3.26**

In order to visualize and statistically analyze the value of those three biomarker candidates, visualization by box and whisker plots and T-tests with adjusted raw data were generated. The analysis of LC-MALDI data using Profile Analysis is hindered by the fact that replicates of samples are recognized as independent samples. Therefore, statistical significances of selected biomarker candidates were independently verified in the GraphPad Prism® Version 5.0 software using the means of replicates, as shown in figure 12.

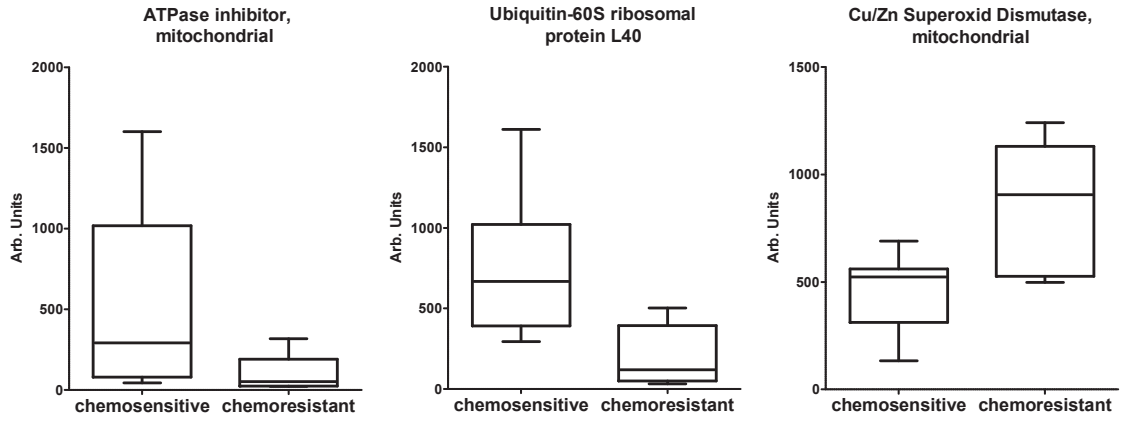

Figure 12: Box and whisker plots for the three biomarker candidates from the Top Down study, chosen for further validation. The means of replicates were plotted with the 5-95 percentile.

The ATPase inhibitor was up regulated 4.94 fold (p-value = 0.0265) in the chemosensitive group, the Ubiquitin- 60S ribosomal protein L40 was up regulated 3.61 fold in the chemosensitive group and the Superoxide dismutase [Cu/Zn] was 1.86 fold up regulated (p-value = 0.0045) in the chemoresistant group. These biomarker candidates were subjected to a technical validation of the workflow by western blotting and NanoPro1000 assays were developed for antibodies directed against the corresponding biomarkers.

3.6 Bottom Up proteomic study of intrinsic chemoresistance to FOLFOX therapy

Following the initial Top Down study of the low molecular weight proteome, a Bottom Up study was conducted to expand the discovery of predictive biomarker candidates to the high molecular weight proteome. The cell culture panel from the Top Down study was extended with six additional cell cultures and was analyzed using a cap-RP-HPLC MALDI-MS/MS based Bottom Up proteomic workflow. A schematic illustration of the Bottom Up proteomic workflow is shown in figure 13. In summary, whole cell lysates of the cell cultures were digested enzymatically and resulting digests were subjected to the workflow. Since the tryptic digestion of high molecular weight proteins results in a higher number of peptides than the digestion of low molecular weight proteins, the complex patterns of protein expression generated by this workflow are dominated by the former. This enabled the extension of analysis to high molecular weight proteins, which are potentially not detected in the Top Down proteomic workflow. By using this workflow digests of cell lysates were pre fractionated by cap-RP HPLC and subsequently analyzed by MALDI-MS/MS in order to generate protein expression profiles in a mass range of 0.8 kDa up to 4 kDa, representing the most abundant peptides in the digests.

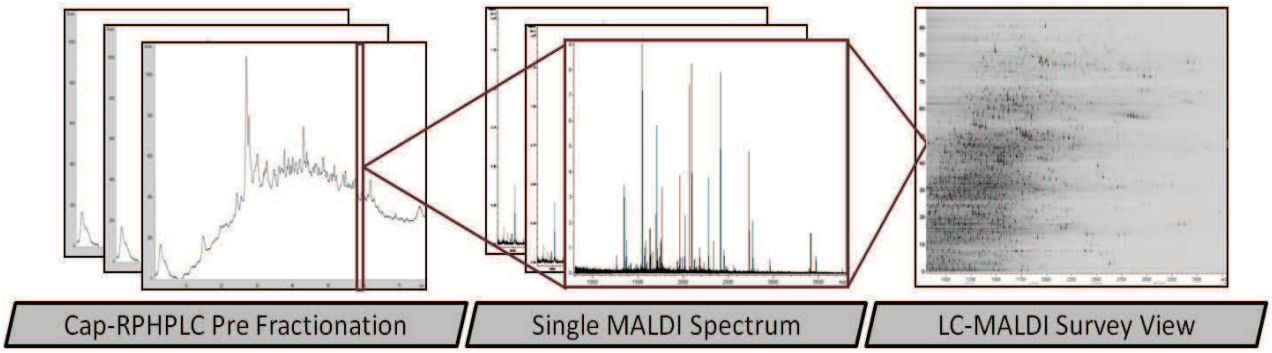

Figure 13: Schematic illustration of the Bottom Up proteomic workflow. In the cap-RP-HPLC chromatogram the time [min] is plotted on the X-axis and the intensity [arb.units] on the Y-axis. In the MALDI spectrum the mass [kDa] is plotted on the X-axis and the intensity [arb.units] on the Y-axis. The survey view of LC-MALDI data shows the LC fractions on the X-axis and the mass [kDa] is plotted on the Y-axis.

The conditions for the pre fractionation of tryptic peptides in the cap-RPHPLC and subsequent MALDI measurements were guided by the Standard Operating Procedures of the Indivumed GmbH. Twenty cell cultures were used for this Bottom Up study of intrinsic chemoresistance. This cell culture panel included the nine secondary cell lines and five primary cell cultures from the previous Top Down study as well as one additional secondary cell line, one primary clonal cell line and four primary mixed cell cultures (see table 12). The cell cultures were grouped into chemosensitive and chemoresistant according to their previous classification by chemosensitivity testing.

Table 12: Chemosensitive and chemoresistant groups of cell cultures used in the Bottom Up study.

Chemosensitive	Chemoresistant
LS513	Colo320
B352MK	A413MK
HT-29	B429MK
HCT-8	SW480
HCT-15	LS174T
Lovo	A845MK
B352 clone 3	Caco-2
A609MK	Colo678
A413 clone 11/60	A806 clone 1
B429 clone 8	A806MK

The samples were randomly assigned to the cap-RP-HPLC-MALDI acquisition to prevent bias in sample preparation and in the technical conduction of the workflow. For illustration of the data figure 14 shows exemplary survey views of three replicates from one cell line. The cap-RP-HPLC fractions were plotted on the y axis and the mass range on the x-axis. Intensity of peaks is displayed by density. Here again, no exact quantitative information can be derived from those pictures, but the survey views give a first overview on retention time, signal intensity and general pattern reproducibility. The amount of acquired data, which more than twice as high as in the Top Down study, even complicates the visual estimation of reproducibility. Therefore, the assessment of reproducibility for samples has been derived from the number of

measured peaks (compounds) and the signal intensities of the same peaks within the technical replicates. The number of non-redundant compounds between individual samples ranged from 4900-7800, whereas the averaged CV for the number of compounds within the replicates was 10%.

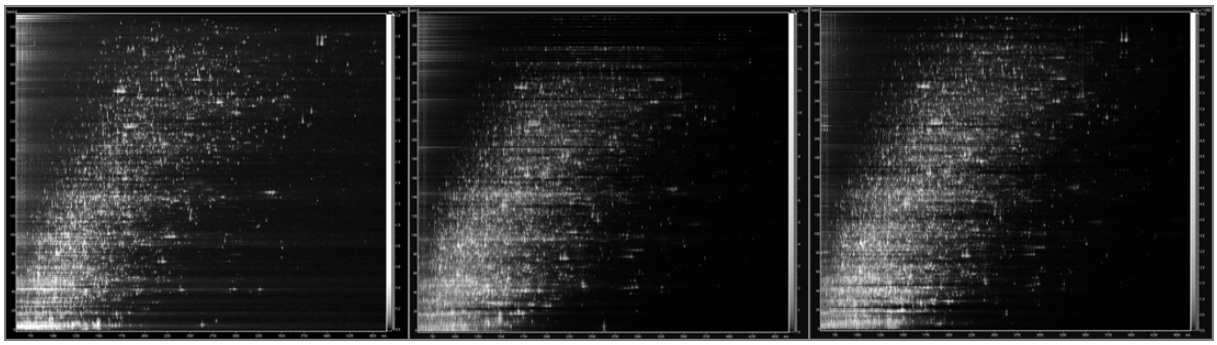

Replicate 1 Replicate 2 Replicate 3

Figure 14: Three exemplary technical replicates of the cell line HCT-8, shown as cap-RP-HPLC-MALDI survey views to visualize the reproducibility of the workflow.

Statistical analysis of the LC-MALDI data sets by the Principal Components Analysis (PCA) showed no clustering of chemoresistant against chemosensitive cell lines, as shown in figure 15. This lack of clustering of groups suggests that the recorded data is similar in most parameters. Overall differences in the protein expression patterns between groups are unincisive, although single parameters are significantly regulated. The statistical analysis of data was carried out just as in the Top Down study. The analysis of data revealed several significant regulated peptides, corresponding to biomarker candidates. By comparing the protein expression profiles of the panel of twenty colorectal cancer cell cultures defined into chemoresistant and chemosensitive groups, 44 compounds were found to be significantly ($p = \leq 0.02$) regulated more than 1.5 fold between groups. Table 13 shows the results of the T-test analysis of the data from the Bottom Up study.

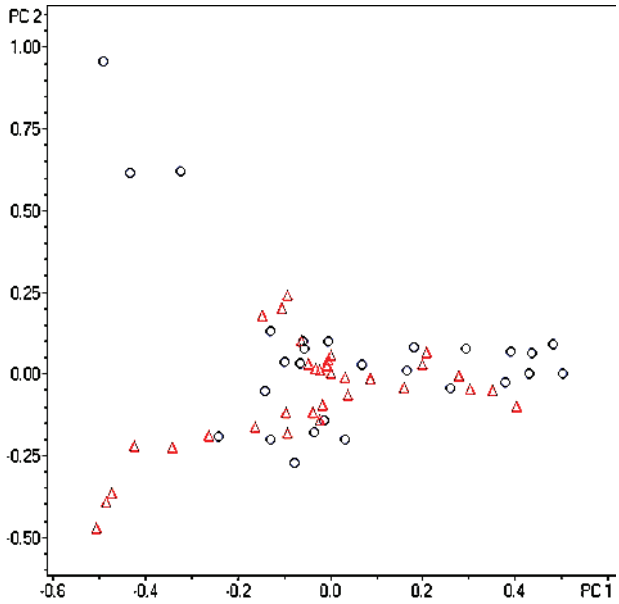

Figure 15: PCA analysis of the generated proteomic profiles from the Bottom Up study. The chemoresistant cell lines (red) did not cluster against the chemosensitive cell lines (blue) in the overall analysis of similarities.

The compounds are again presented as Buckets, which are defined as a combination of the cap-HPLC-retention time and the molecular weight. Furthermore, the significance of regulation and the degree of regulation are displayed. Additionally, the p-values of the Buckets were analyzed by the Bonferroni correction in order to minimize false positive classifications in a very stringent way. The results are shown as p-Value (FDR). To reveal the molecular identity of significantly, regulated Buckets, corresponding m/z ions had to be identified by MALDI-MS/MS analysis and a subsequent database search. Since these peptides can be directly identified by MS/MS analysis, due to their molecular weight below 4000 Da, there was a direct access to the molecular identity of the biomarker candidates.

Table 13: Results of the T-test analysis of LC-MALDI data performed in ProfileAnalysis. Compounds, which were significantly (p= ≤ 0.02) regulated are displayed.

	Bucket	p-Value	Fold change	p-Value (FDR)
1	1698.5s : 1363.68m/z	0.000	-2.420	0.130
2	1640.0s : 1075.58m/z	0.000	-2.240	0.156
3	1765.4s : 1354.72m/z	0.001	-2.630	0.156
4	3326.3s : 1490.79m/z	0.001	-2.300	0.156
5	2813.6s : 1433.75m/z	0.001	-1.790	0.207
6	1696.4s : 1403.75m/z	0.001	-2.720	0.207
7	1647.5s : 1341.68m/z	0.002	-3.010	0.223
8	2998.6s : 1197.72m/z	0.002	2.070	0.223
9	2526.4s : 1276.73m/z	0.002	-2.870	0.223
10	3356.8s : 1503.80m/z	0.002	-1.870	0.223
11	2952.1s : 1649.84m/z	0.003	-2.040	0.223
12	2948.7s : 1390.79m/z	0.004	-2.700	0.292
13	4013.3s : 1979.98m/z	0.005	-2.420	0.296
14	2753.6s : 1414.78m/z	0.005	-1.640	0.296
15	2367.7s : 801.53m/z	0.005	2.490	0.296
16	4709.0s : 1704.95m/z	0.006	2.520	0.317
17	2625.2s : 1424.73m/z	0.006	-1.530	0.317
18	3342.5s : 1516.80m/z	0.006	-1.570	0.317
19	3727.0s : 1623.87m/z	0.006	-1.580	0.317
20	5008.1s : 2997.43m/z	0.009	2.940	0.371
21	1711.4s : 1503.86m/z	0.009	-3.170	0.371
22	4289.1s : 1664.84m/z	0.009	-1.690	0.371
23	2634.6s : 1028.61m/z	0.009	1.590	0.373
24	4246.1s : 1768.95m/z	0.011	-1.720	0.381
25	2959.6s : 1588.89m/z	0.012	1.810	0.381
26	2403.5s : 1367.72m/z	0.014	-2.160	0.381
27	2690.6s : 1100.67m/z	0.015	1.960	0.381
28	1867.1s : 1053.62m/z	0.015	1.770	0.381
29	2520.5s : 955.55m/z	0.015	1.760	0.381
30	2719.6s : 1108.61m/z	0.015	1.920	0.381
31	3014.6s : 1248.05m/z	0.016	-1.810	0.381
32	3539.9s : 1537.80m/z	0.016	-1.760	0.381
33	2743.2s : 1164.67m/z	0.016	-1.640	0.381
34	2575.3s : 1071.59m/z	0.016	1.570	0.381
35	3320.4s : 1534.80m/z	0.016	-2.750	0.381
36	4280.4s : 1830.97m/z	0.016	-1.800	0.381
37	2879.9s : 1168.65m/z	0.017	-1.800	0.381
38	3413.0s : 1039.63m/z	0.018	2.560	0.381
39	2961.3s : 1448.78m/z	0.018	-2.020	0.381
40	2540.5s : 1296.72m/z	0.018	1.820	0.381
41	3619.8s : 2179.08m/z	0.019	-1.870	0.381
42	2148.3s : 1180.65m/z	0.019	1.750	0.381
43	3077.2s : 1127.68m/z	0.019	1.870	0.381
44	3349.1s : 1114.67m/z	0.019	1.700	0.381

Some of the Buckets from the T-test could not be identified due to a low abundance of the peptides or because the peptides did not carry enough information for a significant database search hit. The identified Buckets are summarized in table 14.

Among the identified Buckets, representing biomarker candidates were again proteins with various cellular localizations and biological functions. For example cell structure related proteins like Vinculin, a membrane-cytoskeletal protein and the tubulin beta-2C chain, involved in microtubules formation, have been identified. Examples for proteins involved in protein expression are the MYM-type zinc finger protein 2 and the eukaryotic translation initiation factor 2C1 (Ago 1). Furthermore, the heat shock protein 27 and the heat shock cognate 71kDa protein (HSC70), as example for stress induced proteins have been identified. Another interesting biomarker candidate is the UBX domain containing protein 1 (UBXN), which is a component of a complex required to couple deglycosylation and proteasome-mediated degradation of misfolded proteins and is involved in ubiquitin-proteasome systems.

In comparison to the Top Down study, less significant differences in the protein expression profiles were detected in the Bottom Up study. This may indicate that fewer differences can be detected by using this workflow in the analysis of the high molecular weight proteome. High molecular weight proteins result in a high number of peptides when being digested, those amounts of peptides from very few different proteins may hinder the detection of peptides from small, low abundant proteins.

Table 14: List of biomarker candidates from the Bottom Up study, identified by direct fragmentation of target m/z ions by MALDI-MS/MS. Expression differences of the biomarker candidates are displayed as Fold change in relation to the S = chemosensitive vs. R= chemoresistant group.

T-test Bucket	Identity of Biomarker Candidates	Uniprot Identifier	p-value	Fold change S/R
5008.1s:2997.43m/z	Heat shock cognate 71 kDa protein (Heat shock 70 kDa protein 8) - Homo sapiens (Human)	HSP7C_HUMAN	**0.0086**	**2.94**
2998.6s:1197.72m/z	UBX domain-containing protein 1 - Homo sapiens (Human)	UBXD1_HUMAN	**0.0024**	**2.06**
1696.4s:1403.75m/z	Eukaryotic translation initiation factor 2C 1 (eIF2C 1)- Homo sapiens (Human)	I2C1_HUMAN	**0.0013**	**-2.72**
3326.3s:1490.79m/z	Uncharacterized protein C20orf52 - Homo sapiens (Human)	ROMO1_HUMAN	**0.0004**	**-2.22**
3173.6s:1163.66m/z	Heat-shock protein beta-1 (Heat shock 27 kDa protein) (HSP 27) - Homo sapiens (Human)	HSPB1_HUMAN	**0.0137**	**-2.82**
2948.7s:1390.79m/z	Microtubule-associated serine/threonine-protein kinase 4 - Homo sapiens (Human)	MAST4_HUMAN	**0.0047**	**-2.69**
2952.1s:1649.84m/z	SWI/SNF-related matrix-associated actin-dependent regulator of chromatin subfamily C member 2 (SWI/SNF complex 170 kDa subunit)- Homo sapiens (Human)	SMRC2_HUMAN	**0.0029**	**-2.02**
3320.4s:1534.80m/z	Homeobox protein Nkx-3.1 - Homo sapiens (Human)	NKX31_HUMAN	**0.0158**	**-2.75**
4013.3s:1979.98m/z	Uncharacterized protein C3orf19 - Homo sapiens (Human)	CC019_HUMAN	**0.0045**	**-2.42**
2994.1s:1919.95m/z	Endothelial PAS domain-containing protein 1 (EPAS-1) (Member of PAS protein 2) (HIF2 alpha) (HIF-1 alpha-like factor) (HLF) - (Basic-helix-loop-helix-PAS protein MOP2) (Hypoxia-inducible factor 2 alpha) - Homo sapiens (Human)	EPAS1_HUMAN	**0.0173**	**-2.57**
3571.6s:1462.81m/z	Ceramide kinase-like protein- Homo sapiens (Human)	CERKL_HUMAN	**0.0204**	**2.16**
2526.4s:1276.73m/z	Rab3 GTPase-activating protein non-catalytic subunit (Rab3 GTPase-activating protein 150 kDa subunit)- Homo sapiens (Human)	RBGPR_HUMAN	**0.0022**	**-2.86**
1957.3s:845.52m/z	Tumor necrosis factor receptor type 1-associated DEATH domain protein- Homo sapiens (Human)	TRADD_HUMAN	**0.019**	**2.69**
4078.9s:2101.08m/z	Lariat debranching enzyme (EC 3.1.-.-)- Homo sapiens (Human)	DBR1_HUMAN	**0.044**	**2.22**
4174.1s:2002.06m/z	Import inner membrane translocase subunit TIM50, mitochondrial precursor - Homo sapiens (Human)	TIM50_HUMAN	**0.0416**	**-2.61**
4709.0s:1704.95m/z	MYM-type zinc finger protein 2 (Zinc finger protein 198) - Homo sapiens (Human)	ZMYM2_HUMAN	**0.0059**	**2.52**
3413.0s:1039.63m/z	Tubulin beta-2C chain (Tubulin beta-2 chain)- Homo sapiens (Human)	TBB2C_HUMAN	**0.0161**	**2.47**
2961.3s:1448.78m/z	Cytohesin-1 (PH, SEC7 and coiled-coil domain-containing protein 1)- Homo sapiens (Human)	CYH1_HUMAN	**0.0179**	**-2.02**
1765.4s:1354.72m/z	Tryptase gamma precursor (EC 3.4.21.-) (Transmembrane tryptase)- Homo sapiens (Human)	TRYG1_HUMAN	**0.0005**	**-2.63**
1698.5s:1363.68m/z	Sodium-dependent phosphate transport protein 2B- Homo sapiens (Human)	NPT2B_HUMAN	**0.0001**	**-2.42**

Similar to the Top Down study, a literature search on the identified biomarker was carried out to select the most promising biomarker candidates. As a result of this literature search, again three biomarker candidates were selected for a further validation. These three biomarker candidates were the heat shock cognate 71 kDa protein, the UBX domain containing protein 1 and the eukaryotic translation initiation factor 2C 1.

The heat shock cognate 71kDa protein has been mentioned in a few publications in the context of chemoresistance, but it function related to drug response has not been intensively described. Similar to the SOD 1, this biomarker in general supports the results from this study and has been used as an internal control. In contrast, the UBX domain containing protein 1 and the eukaryotic translation initiation factor 2C 1 have not been described in the context of chemoresistance. These two biomarker candidates thus potentially represent valuable, newly discovered predictors of response to FOLFOX chemotherapy. In order to visualize and statistically analyze the value of those three biomarker candidates, visualization by box and whisker plots and t-tests with adjusted raw data were generated. As mentioned, the analysis of LC-MALDI data using Profile Analysis is hindered by the fact that replicates of samples are recognized as independent samples. Therefore, statistical significances of selected biomarker candidates were independently verified in the GraphPad Prism® Version 5.0 software using the means of replicates, as shown in figure 16.

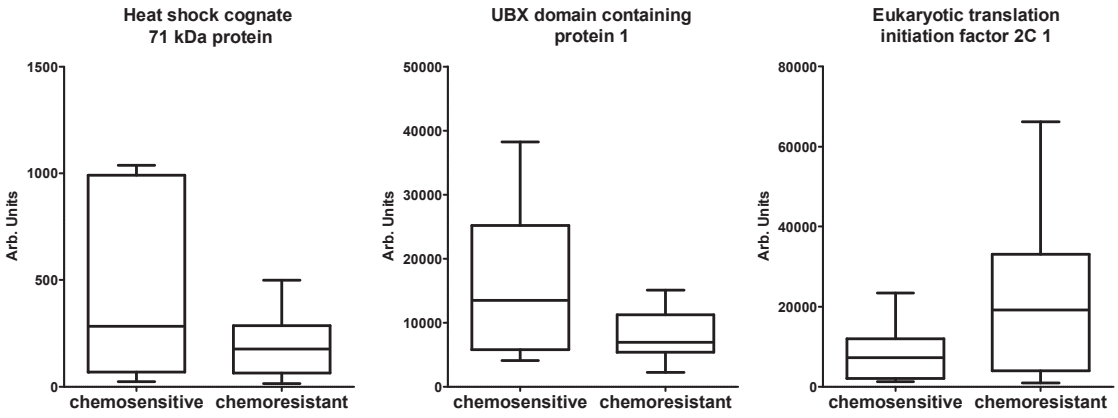

Figure 16: Box and whisker plots for the three biomarker candidates from the Bottom Up study, chosen for further validation. The means of replicates were plotted with the 5-95 percentile.

The heat shock cognate 71kDa protein (HSC70) was found to be up regulated 2.94 fold (p-value= 0.0358) in the chemosensitive group, the UBX domain containing protein 1 (UBXN) was up regulated 2.06 fold (p-value= 0.0277) in the chemosensitive group and the eukaryotic translation initiation factor 2C 1 (Ago 1) was 2.72 fold up regulated (p-value= 0.0273) in the chemoresistant group. These biomarker candidates were, similar to the selected biomarker candidates form the Top Down study, subjected to a technical validation of the workflow by western blotting. For a further validation in micro dissected tumor specimen, here also NanoPro1000 assays were developed for antibodies directed against the corresponding biomarkers.

3.7 Validation of biomarker candidates from the Top Down and Bottom Up proteomic studies

The Top Down and Bottom Up proteomic studies of intrinsic chemoresistance to FOLFOX therapy resulted in the discovery and identification of several biomarker candidates. The six most promising biomarker candidates were subjected to a more detailed statistical analysis and an extensive literature search on these proteins was performed. These biomarker candidates are potentially predictive for a response to FOLFOX chemotherapy and may ultimately be used for the patient tailored therapy in

the clinical setting. After the initial discovery of biomarker candidates using a newly established workflow, it is important to validate the biomarker candidates, prior to their adaption to the clinical setting. The process of validation used here can be summarized in two steps. The first step was the technical validation of the biomarker candidates. In this step results from the newly established workflows of the studies should be verified by an independent, traditional technique. In a second step, the relevance of the biomarker candidates, which were discovered in a panel of cell cultures, had to be verified in an independent set of clinical samples. This will provide the important information on whether the biomarker candidates can predict chemosensitivity to FOLFOX therapy not only in the panel of cell cultures, but in the clinical setting, in clinical relevant patients` tumors.

3.7.1 Technical validation of the selected biomarker candidates

In this first step, traditional western blotting was performed, in order to technically validate the differential expression of the biomarker candidates found in the LC-MALDI discovery studies. Therefore, antibodies raised against the corresponding biomarker candidate were purchased. The expression of the biomarker candidates were exemplarily analyzed in six cell cultures from the initial cell culture panel for every biomarker. Based on the data from the both discovery studies, these six cell cultures consisted of three cultures with a high biomarker candidate expression and three cultures with a low expression, respectively (see table 15). The western blotting experiments in general confirmed the results from the LC-MALDI discovery studies. The differential expression of biomarker candidates in the selected six cell cultures was also detectable with an independent technique.

Table 15: Summary of cell cultures used for the technical validation of biomarker candidates.

		ATPIF 1	UBA52	SOD 1	AGO 1	UBXN	HSC70
High	**Lane 1**	A609MK	A609MK	A413MK	Colo320	HCT-15	Lovo
	Lane 2	HT-29	HCT-15	Colo320	B429MK	HCT-8	HCT-8
	Lane 3	HCT-15	HT-29	Colo678	LS174T	HT-29	B352MK
Low	**Lane 4**	Colo678	A413MK	LS513	HCT-15	A845MK	A845MK
	Lane 5	Caco-2	Colo320	HCT-8	Lovo	A860clone1	Colo320
	Lane 6	A806clone1	Colo678	B352clone3	B352MK	LS174T	Colo678

Figure 17 shows western blots for the technical validation of biomarker candidates from the Top Down study. The western blots for ATPIF 1 confirmed a high expression of the biomarker in the chemosensitive cell cultures HT-29, HCT-15 and especially in A609MK. The three other, chemoresistant cell cultures showed a low expression of the biomarker, as expected. The western blot for UBA52 also verified an upregulation of the biomarker candidate in the chemosensitive cell cultures, although the chemoresistant cell culture A413MK showed a higher expression than the chemosensitive cell line HT-29. The western blotting experiments for the validation of the SOD 1 only resulted in weak expression differences between cell cultures. Nevertheless, the mean regulation of 1.86 could be verified in this experiment.

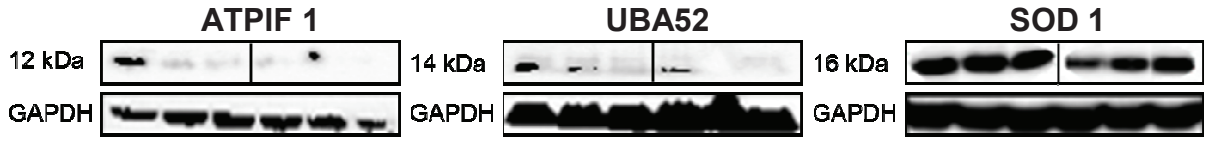

Figure 17: Western blots for the technical validation of biomarker candidates from the Top Down study. GAPDH was used for loading control.

Figure 18 shows western blots for the technical validation of biomarker candidates from the Bottom Up study. Here again, the differential expression of cell cultures for the corresponding biomarker candidates could verified. The western blot for Ago 1 displayed a high expression of the biomarker candidate in the chemoresistant cell cultures, whereas the chemosensitive cell cultures only showed low expression. The western blot for UBXN showed strong expression differences between the high expressing chemosensitive cell cultures and the low expressing chemoresistant cell

cultures. The two chemoresistant cell cultures A845MK and A806clone1 showed almost no expression of the biomarker candidate. The regulation of HSC70 between chemosensitive and chemoresistant cell cultures could also clearly be verified. As expected, all three chemosensitive cell cultures showed a high expression of the biomarker and in comparison, the corresponding expression of the biomarker in the chemoresistant cell cultures was low.

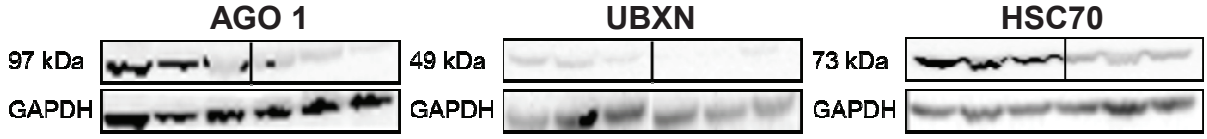

Figure 18: Western blots for the technical validation of biomarker candidates from the Bottom Up study. GAPDH was used for loading control.

Since the validation of the differential expression of biomarker candidates was conducted by western blotting, the specificity and sensitivity of the used antibodies is of great importance. Unspecific binding of the antibody can partly mask the real expression of the targeted proteins and is especially important when these antibodies should be adapted to other techniques such as IHC, ELISA, MSD or NanoPro1000.

In order to visualize the affinity of the antibodies to unspecific binding of proteins the complete molecular range of the western blots was analyzed. Within this molecular range, the antibodies raised against the SOD 1 and Ago 1 showed several unspecific signals (data not shown). In contrast, the antibodies for ATPIF, UBA52, UBXN and HSC70 showed almost no unspecific signals beside those of the molecular size of the biomarker candidates.

3.7.2 NanoPro1000 assay development for selected biomarker candidates

In order to validate the discovered biomarker candidates in an independent cohort of real clinical samples from patients` tumors, adequate technical assays had to be developed. This assay must be suitable for the robust detection of the biomarker candidates in low amounts of sample, typically available in the clinical situation. The validation study will provide information on the predictive power of the biomarkers outside of the training set of cell cultures and thus allows a decision on whether the biomarker candidate can potentially be useful in the clinical situation. Since patient derived clinical samples are very heterogeneous in regard to the tumor content and tumor morphology, in contrast to *in vitro* cell cultures, the compartments of epithelial cancer cells should be isolated from the tumor. The isolation of distinct regions within the tumor is possible by using “laser capture micro dissection” (LCM). A disadvantage of using this method is the resulting, mostly small amount of pure cell populations from which only small quantities of protein can be extracted.

The NanoPro1000 technology has the ability to detect proteins and protein isoforms in small quantities of proteins that can be extracted from micro dissected clinical samples. In order to use this technology, the antibodies used for the technical validation had to be checked for compatibility within the new system. It might possible that these antibodies will not bind to their target protein, because the NanoPro technology uses a novel protein immobilization technique in which steric consequences may hinder binding. Compatibility of antibodies was verified according to the assay development program of the supplier. Two cell cultures, each with a high and a low expression of the biomarker candidate were subjected to the NanoPro1000 analysis. An antibody dilution and a comparison of both control cell cultures were carried out in order to check compatibility with the system.

Four of the six antibodies used in the technical validation of the biomarker candidates were compatible with the NanoPro1000 technology. The antibodies raised against the SOD 1, UBXN, Ago 1 and HSC70 detected their target in the NanoPro1000 system. It was determined if the signals from the antibodies could be cleary appointed to the corresponding target by checking the pI of the signal in comparison to the theoretical pI of the target and by using control cell lines with high and low expression of the target.

For SOD 1 assay development experiments the cell line LS513 was used as negative control and LS174T as positive control. The antibody against the SOD 1 showed several signals in a pI range of 4.5 to 6.5, as shown in figure 19. The theoretical pI of SOD 1 is 5.73. The antibody dilution revealed that signals are detectable down to a dilution of 1:500, whereas a saturation of the antibody is probably not reached at a dilution of 1:50. Nevertheless, a 1:50 dilution of the antibody produced high intensity, well resolved signals, suitable for analysis. The mean reproducible peak pattern in the spectrum are at a pI= 4.9 and at a pI= 6.1, which both decreased in intensity with the increasing antibody dilution. The results from the high and low biomarker expressing cell cultures indicate that the peak pattern at pI= 6.1 represents the SOD 1, since this patterns are regulated according to the expected expression. The peak pattern at pI= 4.9 was inversely correlated to the peak pattern at pI= 6.1, this has been verified in four other cell cultures (data not shown). The identity of the peak pattern at pI= 4.9 is unknown, initial peak identification experiments suggested that this detected isoform may be an active, dimer form of the SOD 1 (data not shown).

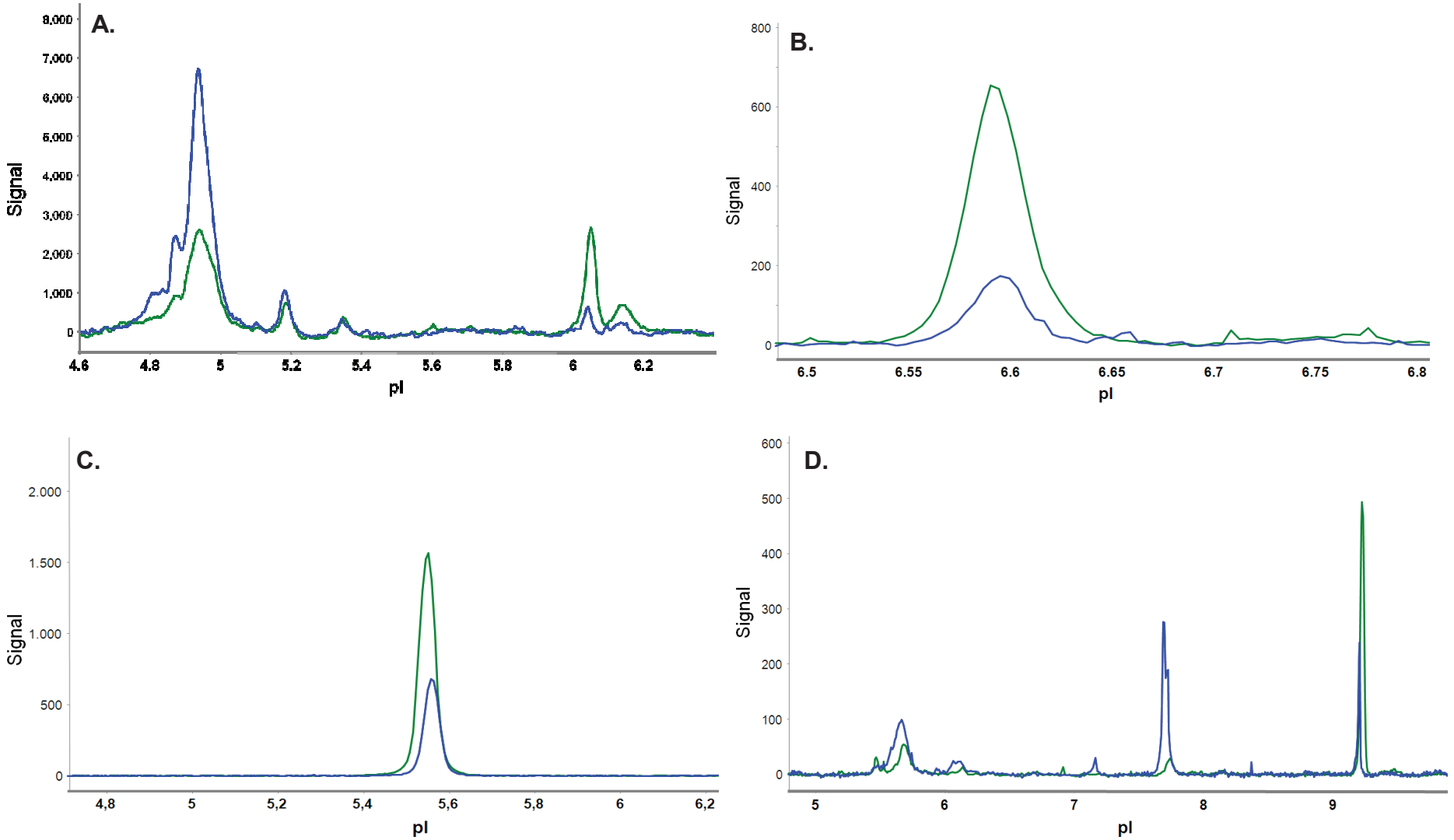

Figure 19: Assay developments for four antibodies corresponding to biomarker candidates. Signals of high (blue) and low (green) expressing control cell cultures are displayed. The assay development for SOD 1 is shown in panel A, UBXN is shown in panel B, HSC70 in panel C and AGO 1 in panel D.

The antibody against the UBXN showed a distinct signal at a pI of 6.59, as shown in figure 19, clearly corresponding to the theoretical pI of 6.46. The antibody dilution revealed that signals were detectable down to a dilution of 1:500, although the signal intensities were quite low. A 1:50 dilution of the antibody produced reproducible signal intensities, suitable for analysis. The signals from the high (HCT-15) and low (LS174T) expressing control cell cultures indicated the peak identity, due to their expected regulation. The theoretical pI of HSC70 is 5.37 and the HSC70 directed antibody showed a single signal at a pI of 5.56, as shown in figure 19. The recorded signals at a 1:50 dilution of the antibody were reproducible and suitable for analysis. The results from the high (Lovo) and a low (Hela) expressing control cell cultures confirmed the peak identity, by comparison of the theoretical pI and the experimental one. In addition, the peaks showed the expected regulation. The theoretical pI of Ago 1 is 9.27 and the antibody against Ago 1 showed several signals in a pI range of 5.5 to 9.5, as shown in figure 19. The antibody dilution revealed that signals are detectable down to a dilution of 1:500 (data not shown), whereas a saturation of the antibody was reached at the dilution of 1:50. The results from the high (Colo320) and low (Lovo) expressing control cell cultures indicate that the peak at the pI= 9.25 represents the Ago 1, since this peak is close to the theoretical pI and regulated according to the expectations.

In summary, the initial assay development of protocols for each of the four antibodies was successful. The assay development for UBXN and HSC70 was uncomplicated. In contrast, the assay development for the SOD 1 and Ago 1 required further elucidation of the spectra. The antibodies for the corresponding biomarker candidates showed several signals beside the expected signal at the theoretical pI. For a final establishment of NanoPro1000 protocols for the biomarker candidates, the recorded spectra have to be analyzed and elucidated in detail. In order to establish

NanoPro1000 protocols for the biomarker candidates, whose antibodies were not compatible with the system, new antibodies, directed against other domains of the corresponding proteins have to be purchased. Furthermore, the protocols have to be adapted to small amounts and characteristics of laser micro dissected clinical samples. Based on fully developed NanoPro1000 assays for the corresponding biomarker candidates enable a future validation study in clinical samples. This validation study could not be performed in this thesis, although an independent cohort of patients has already been defined (data not shown).

3.8 Bottom Up proteomic study of established chemoresistant cell lines and their parental counterparts

Six biomarker candidates from the initial Top Down and Bottom Up discovery studies of intrinsic chemoresistance to FOLFOX chemotherapy were technically validated and the basis for a validation in an independent set of clinical samples was established. In order to investigate aspects of the biological background of the biomarker candidates, the influence of continuous 5-FU treatment on the expression of the biomarker candidates and thus their potential involvement in acquired chemoresistance was analyzed. A further regulation of the biomarker candidates by drug treatment would suggest a functional contribution of the biomarker candidate in chemoresistance.

In order to establish an *in vitro* model for acquired chemoresistance five 5-FU resistant cell lines were established from five secondary cell lines by a mean of twelve cycles of drug treatment and recovery phases. These newly established 5-FU resistant cell lines and their parental cell lines were used for a comparative Bottom Up proteomic study of acquired resistance. The secondary cell lines from which drug resistant sub cell lines have been successfully established were HT-29, LS174T,

Colo320, Colo678 and SW480. The degree of acquired chemoresistance to 5-Fluorouracil was determined by the comparisons of the IC50 values for 5-FU treatment in parental and 5-FU-resistant cell lines, as shown in figure 20. The IC50s were calculated from dose-response curves after 48h, 72h and 96h of treatment. All chemoresistant cell lines showed a minimum degree of resistance to 5-FU of a two fold change in the IC50s. On this basis, a comparative Bottom Up proteomic study of the chemoresistant cell lines and their parental counterparts was performed. Subsequently, statistical analysis of the LC-MALDI data revealed significantly regulated Buckets, which were directly identified by MALDI-MS/MS.

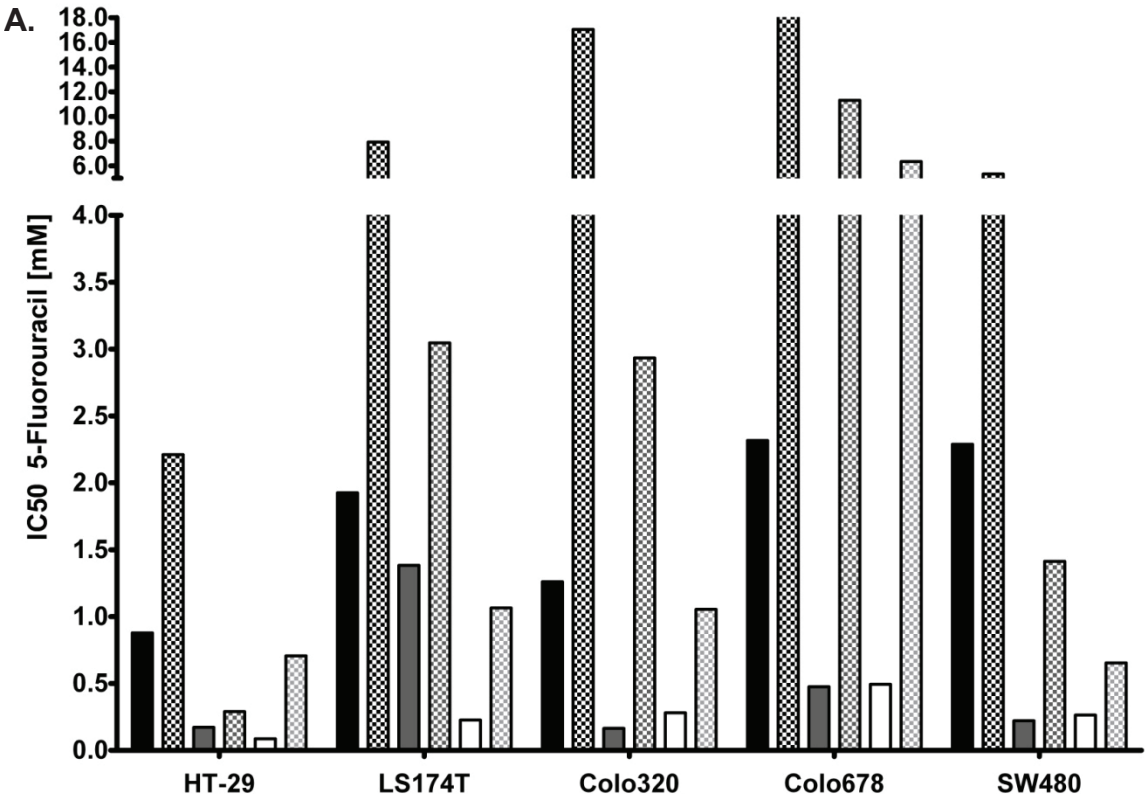

B.

	48h		72h		96h	
	IC50 parental	IC50 resistant	IC50 parental	IC50 resistant	IC50 parental	IC50 resistant
HT-29	0.8781	**2.2110**	0.1719	**0.2893**	0.0876	**0.7063**
LS174T	1.9255	**7.9260**	1.3837	**3.0460**	0.2263	**1.0640**
Colo320	1.2610	**17.0400**	0.1647	**2.9340**	0.2808	**1.0540**
Colo678	2.3170	not calculatable	0.4763	**11.3100**	0.4933	**6.3510**
SW480	2.2890	**5.3360**	0.2214	**1.4130**	0.2637	**0.6536**

Figure 20: IC50 values of parental and corresponding 5-FU resistant cell lines. A. Chemosensitivity of the cell lines to 5-FU treatment was determined after 48 hours (black = parental and black-caro = resistant), 72 hours (dark grey= parental and dark gray-caro= resistant) and 96 hours (white= parental and white-caro= resistant) of 5-FU treatment. B. IC50 values of parental and 5-FU resistant cell lines for 5-FU.

The resistant sub cell lines from Colo320 and Colo678 developed a very strong resistance to 5-FU. The IC50s of Colo320 reached a maximum of a seventeen fold change between the parental and resistant cell line. Colo678 even reached a 23 fold change in the IC50s. Colo678 displayed a very high degree of resistance after 48 hours of treatment, in consequence an IC50 could not be calculated for this time point. The cell line HT-29 showed a mean fold change of 4.1 in the IC50s between the parental and the resistant cell line, LS174T showed mean fold change of 3.8 and SW480 a mean fold change of 3.7. In general, the combination of 5-FU, Leucovorin and Oxaliplatin called FOLFOX treatment was more effective than 5-FU single treatment. This is displayed by the lower IC50 values for FOLFOX in comparison to 5-FU in the parental cell lines, as shown in figure 20 and 21. In reference to the implication of 5-FU resistance in chemoresistance to FOLFOX therapy the chemosensitivity of the 5-FU-resistant sub cell lines to FOLFOX was also determined after 48h, 72h and 96h of FOLFOX treatment. All five 5-FU-resistant cell lines showed also chemoresistance to FOLFOX treatment in comparison to their parental cell lines, as shown in figure 21.

A.

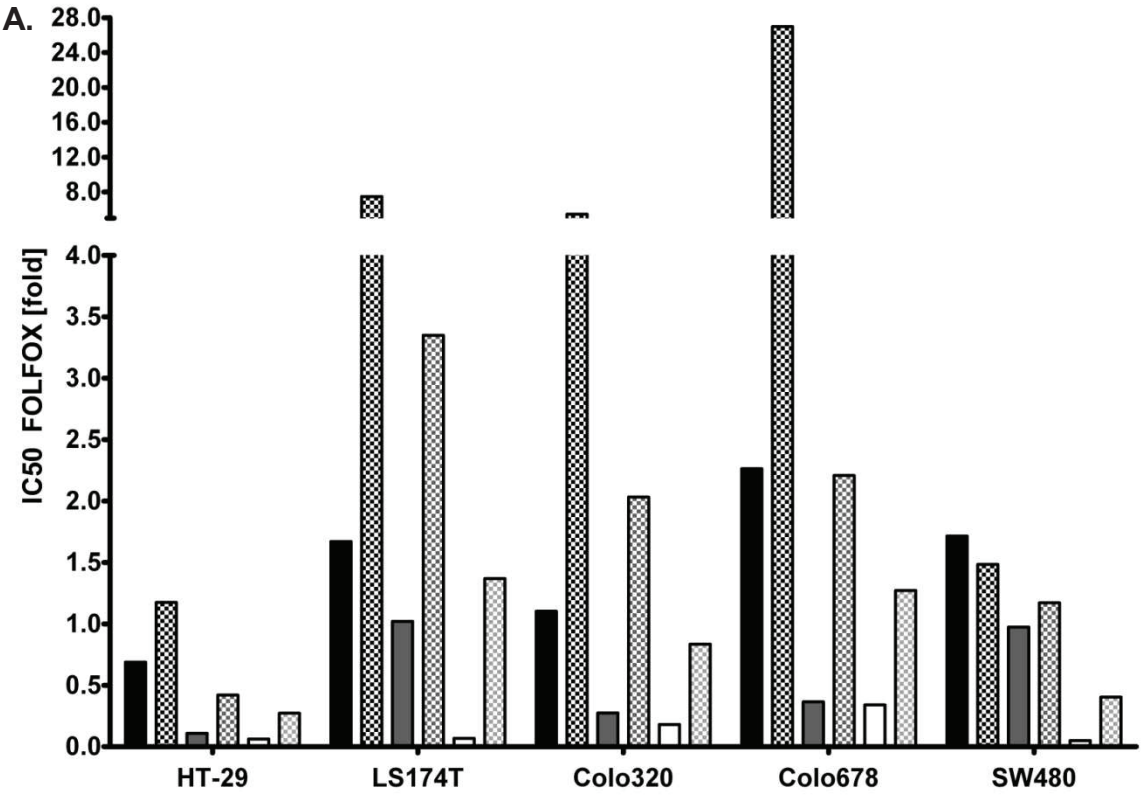

B.

	48h		72h		96h	
	IC50 parental	IC50 resistant	IC50 parental	IC50 resistant	IC50 parental	IC50 resistant
HT-29	0.6883	**1.1740**	0.1087	**0.4209**	0.0628	**0.2727**
LS174T	1.6700	**7.4860**	1.0210	**3.3500**	0.0685	**1.3690**
Colo320	1.1020	**5.4700**	0.2741	**2.0320**	0.1810	**0.8347**
Colo678	2.2640	**26.9800**	0.3655	**2.2080**	0.3397	**1.2710**
SW480	1.7160	**1.4840**	0.9741	**1.1720**	0.0497	**0.4041**

Figure 21: IC50 values for FOLFOX of parental and corresponding 5-FU resistant cell lines. A. Chemosensitivity of the cell lines to FOLFOX treatment was measured after 48 hours (black = parental and black-caro = resistant), 72 hours (dark grey= parental and dark gray-caro= resistant) and 96 hours (white= parental and white-caro= resistant) of 5-FU treatment. B. Table with IC50 values of parental and 5-FU resistant cell lines for FOLFOX.

The mean degree of fold change in chemosensitivity to FOLFOX was lower than the degree of chemoresistance to 5-FU. Similar to the chemoresistance to 5-FU, the resistant sub cell lines of Colo320 and Colo678 showed a high degree of resistance to FOLFOX. Notably, the 5-FU resistant sub cell line of LS174T was even more resistant to FOLFOX treatment than to 5-FU treatment. This cell line showed a mean fold change of IC50s for 5-FU of 3.8 and a 9.3 fold change for FOLFOX treatment. The resistant sub cell lines of HT-29 and SW480 displayed a mean fold change of 3.3 and 3.4 in the IC50s for FOLFOX treatment.

The established chemoresistant cell lines and their parental counterparts, shown in table 16, were then subjected to the Bottom Up proteomic wokflow. The samples were lysed, digested with trypsin and then randomly assigned to the cap-RP-HPLC-MALDI acquisition.

Table 16: Summary of the parental, chemosensitive and the established, corresponding chemoresistant cell lines used in the Bottom Up study of acquired chemoresistance.

Parental	Chemoresistant
HT-29	HT-29 - R
LS174T	LS174T - R
Colo320	Colo320 - R
Colo678	Colo678 - R
SW480	SW480 - R

The assessment of reproducibility for samples has been derived from the number of measured peaks (compounds) and the signal intensities of the same peaks within the technical replicates. The number of non-redundant compounds between individual samples ranged, similar to the initial Bottom Up study, from approx. 4500 to 7500. The averaged CV for the number of compounds within the replicates was 11%. The statistical analysis of the LC MALDI data set by the PCA showed a strong clustering of parental against chemoresistant cell lines, as shown in figure 22.

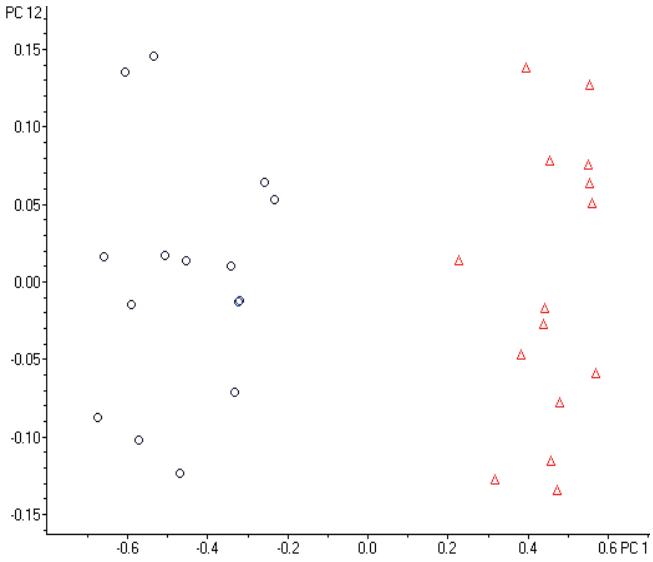

Figure 22: PCA analysis of the generated proteomic profiles from the Bottom Up study of acquired chemoresistance. The parental cell lines (blue) clustered against their chemoresistant counterparts (red).

This clustering of groups suggests that the establishment of chemoresistance resulted in changes in protein expression in the chemoresistant cell lines compared to their parental cell lines. The statistical analysis of data was carried out similar to both discovery studies, as described earlier. The analysis of data revealed several significant regulated peptides, corresponding to biomarker candidates for acquired chemoresistance. By comparing the protein expression profiles of the five parental, colorectal cancer cell lines to their chemoresistant counterparts,162 compounds were found to be significantly ($p = \leq 0.01$) regulated more than 1.5 fold between groups. Table 17 shows the results of the t-test analysis of the data. The compounds are presented as Buckets, which are defined as a combination of the cap-HPLC-retention time and the molecular weight. Furthermore, the significance of regulation and the degree of regulation are displayed. The molecular identity of selected, significantly regulated Buckets was revealed by MALDI-MS/MS analysis and a subsequent database search.

Table 17: Results of the T-test analysis of LC-MALDI data performed in ProfileAnalysis. Compounds, which were significantly (p= ≤ 0.0003) regulated are displayed.

	Bucket	p-Value	Fold change	p-Value (FDR)
1	5264.2s : 2071.21m/z	0.00000	-15.330	0.000
2	3670.9s : 2033.08m/z	0.00000	-4.470	0.000
3	2122.2s : 850.53m/z	0.00000	12.030	0.000
4	3606.5s : 1617.91m/z	0.00000	-22.610	0.000
5	3168.3s : 1385.79m/z	0.00000	-8.940	0.000
6	3994.7s : 1668.88m/z	0.00000	-9.660	0.000
7	1837.9s : 1568.80m/z	0.00000	12.430	0.000
8	2600.9s : 995.60m/z	0.00000	-6.110	0.000
9	3015.0s : 1249.72m/z	0.00000	-4.460	0.000
10	3508.0s : 1560.86m/z	0.00001	-15.680	0.000
11	3063.0s : 1025.62m/z	0.00001	-32.020	0.000
12	2886.9s : 860.49m/z	0.00001	-20.900	0.000
13	2997.2s : 1044.65m/z	0.00001	-8.160	0.000
14	3346.0s : 1490.82m/z	0.00001	-8.790	0.000
15	4567.6s : 2045.09m/z	0.00002	-3.810	0.000
16	3336.5s : 1552.84m/z	0.00002	-2.960	0.000
17	1683.0s : 1054.61m/z	0.00002	7.350	0.000
18	2061.1s : 1377.73m/z	0.00002	153.240	0.000
19	3595.3s : 1684.88m/z	0.00002	28.430	0.000
20	3261.7s : 1425.80m/z	0.00002	-2.660	0.000
21	3134.9s : 1563.83m/z	0.00003	-8.860	0.001
22	2704.1s : 1349.77m/z	0.00003	4.640	0.001
23	3916.7s : 1414.81m/z	0.00004	-7.970	0.001
24	2958.8s : 1160.68m/z	0.00005	-5.110	0.001
25	3260.8s : 1492.84m/z	0.00005	-12.630	0.001
26	2547.9s : 1129.68m/z	0.00005	7.590	0.001
27	2905.0s : 1256.75m/z	0.00007	-4.150	0.001
28	4035.1s : 2556.36m/z	0.00007	-6.100	0.001
29	3759.4s : 1329.73m/z	0.00007	11.980	0.001
30	4394.4s : 1887.04m/z	0.00009	-3.390	0.001
31	3616.8s : 1473.80m/z	0.00010	-5.190	0.001
32	1922.6s : 1148.69m/z	0.00010	3.890	0.001
33	1849.4s : 1079.61m/z	0.00011	4.950	0.001
34	3687.2s : 2210.16m/z	0.00013	-23.710	0.001
35	4702.5s : 1931.08m/z	0.00013	33.540	0.001
36	2771.7s : 1360.76m/z	0.00014	-3.420	0.002
37	3159.2s : 1356.77m/z	0.00017	-12.740	0.002
38	4407.1s : 1715.96m/z	0.00018	7.830	0.002
39	4012.2s : 1643.91m/z	0.00020	-26.190	0.002
40	2927.8s : 2330.26m/z	0.00023	-4.000	0.002
41	4209.3s : 2306.18m/z	0.00024	-6.710	0.002
42	2196.8s : 1067.64m/z	0.00024	-7.840	0.002
43	4897.8s : 1959.03m/z	0.00024	8.960	0.002
44	3432.0s : 1449.81m/z	0.00025	-2.510	0.002
45	3025.9s : 1547.83m/z	0.00029	12.51	0.003

Table 18: Exemplary list of identified Biomarker candidates from the Bottom Up study of acquired chemoresistance.

T-test Bucket	Identity of Biomarker Candidates	Uniprot Identifier	p-value	Fold change
3670.9s : 2033.08m/z	Alpha-enolase- Homo sapiens	ENOA_HUMAN	**0**	**-4.47**
2600.9s : 995.60m/z	Vam6/Vps39-like protein- Homo sapiens	VPS39_HUMAN	**0**	**-6.11**
3260.8s : 1492.84m/z	Rho GTPase-activating protein- Homo sapiens	SYDE1_HUMAN	**0.0001**	**-12.63**
3606.5s : 1617.91m/z	Carbohydrate sulfotransferase 3- Homo sapiens	CHST3_HUMAN	**0**	**-22.61**
3346.0s : 1490.82m/z	Prefoldin subunit 6- Homo sapiens	PFD6_HUMAN	**0.00001**	**-8.79**
3616.8s : 1473.80m/z	Centromere protein S- Homo sapiens	CENPS_HUMAN	**0.0001**	**-5.19**
2886.9s : 860.49m/z	10 kDa heat shock protein - Homo sapiens	CH10_HUMAN	**0.00001**	**-20.9**

The MALDI-MS/MS experiments resulted in the identification of biomarker candidates, predictive for acquired chemoresistance. All exemplarely identified biomarker candidates were strongly up regulated in the chemoresistant group. Amoung these candidates, the carbohydrate sulfotransferase 3 was the most regulated protein between groups with a 22.61 fold up regulation in the chemoresistant group. The alpha-enolase was the less regulated protein, still displaying a 4.47 fold up regulation in the chemoresistant group. The biomarker candidates UBXN and HSC70, from the Bottom Up discovery study, were detected to be further regulated. As a matter of the stringency of statistical analysis these biomarker candidates are not shown in the T-test. The T-test only shows Buckets present in all studied cell cultures and the expression levels of the two biomarkers were below the level of detection in the chemoresistant cell lines. In the initial Bottom Up discovery study, the biomarker candidates HSC70 and UBXN were found to be up regulated in the chemosensitive group, thus it was expected, that the levels of UBXN further decrease by the acquisition of chemoresistance. The biomarker candidate Ago 1 has initially been found to be up regulated in the chemoresistant group, a further up regulation was not detected in the cell lines with acquired chemoresistance. The involvement of the biomarker candidate in acquired chemoresistance can nevertheless not be proven wrong. Potentially, the biomarker candidate may be regulated by short term drug treatment, resulting in a

chemoresistant phenotype of the cell lines. Thus the involvement must not be present in the current chemoresistant phenotype, but may be inducer of drug resistance.

3.9 Characterization of biological features of the biomarker candidate Superoxide Dismutase [Cu/Zn]

As an example for a further characterization of biological features of a biomarker candidate, the SOD 1 was chosen. The SOD1 is a ubiquitously expressed, anti-oxidant enzyme, which is mainly involved in the conversion of toxic superoxide anions into molecular oxygen and hydrogen peroxide, to regulate the intracellular oxidative stress. Therefore, it was analyzed if the enzyme activity of the SOD 1 is, similar to the expression of the enzyme, significantly regulated between chemosensitive and chemoresistant cell cultures from the Top Down discovery study, as shown in figure 23. The biological, functional background of biomarker candidates is very important, in order to elucidate whether the biomarker candidate is just indicative of, or causally involved in chemoresistance. In these experiments, the enzyme activity of the SOD 1 was measured, to investigate the relation of enzyme activity to chemoresistance. enzyme activity correlates with the protein expression. The cell cultures showed differential enzyme activity, with the cell line LS174T showing the highest activity of 61.57 U/ml and the cell culture A806 clone 1 showing the lowest activity of 12.55 U/ml.

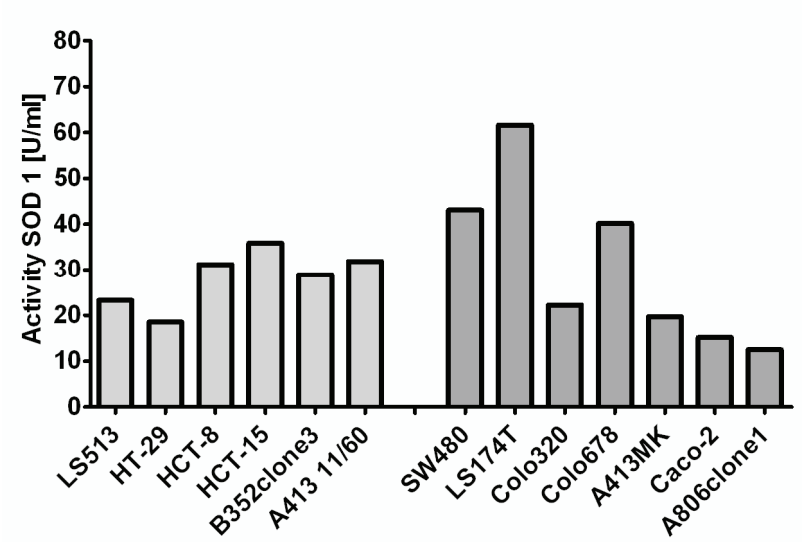

Figure 23: Enzyme activity of the SOD 1 in different cell cultures. The bars of the chemosensitive group are light grey, the bars of the chemoresistant group are dark grey. The grouping of cell cultures refers to figure 6.

Especially for the SOD 1, but in general for enzymes it is important to determine if the Statistical analysis revealed that there was no significant difference in enzyme activity between the chemosensitive and the chemoresistant group. Figure 24 shows, that there was also no correlation of the SOD 1 enzyme activity to either the expression data from the LC-MALDI analysis in the Top Down study, or to the densiometrically determined expression intensity of the western blotting.

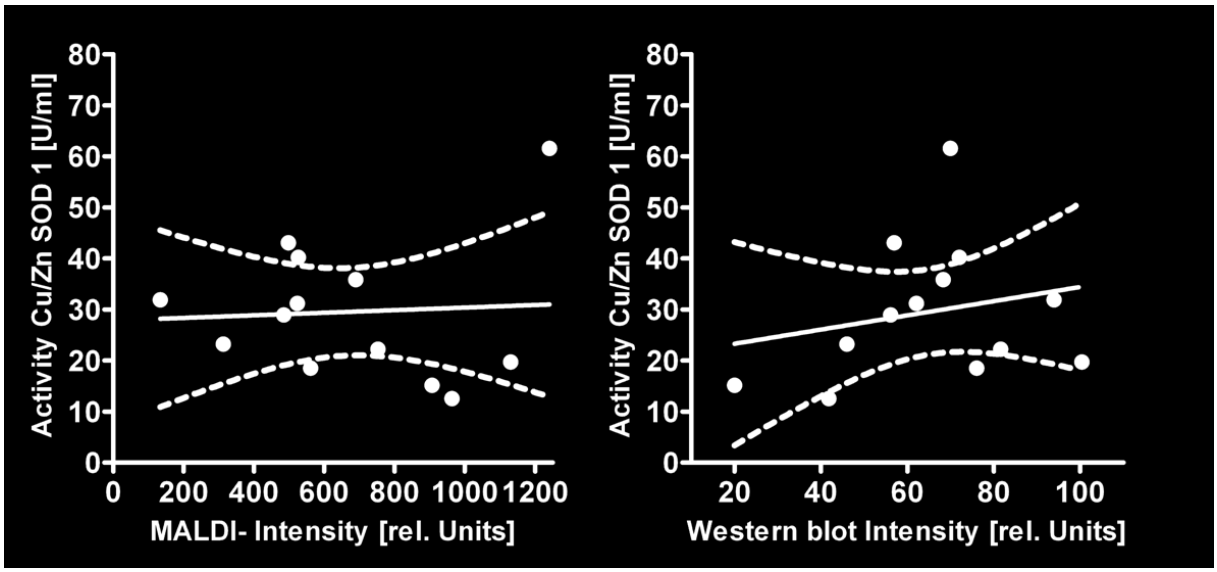

Figure 24: Correlation of SOD 1 enzyme activity to expression data from the LC-MALDI discovery study as well as to the expression data resulting from western blotting experiments. The dotted lines are representing the 5-95% confidence intervals.

3.9.1 Analysis of EGFR related pathway activation in the cell culture panel

Since there was no correlation between the protein expression and enzyme activity of the SOD 1, another related biological aspect of the cellular influences of the SOD 1 was analyzed. Several examples of scientific literature are demonstrating that oxidative stress influences the Epidermal growth factor receptor related signaling pathways, such as the MAPK signaling pathways. The effect of oxidative stress can results in the activation of the MAP kinase pathways, as well as in their inhibition. The intrinsic activation or inhibition of the signaling pathways can result in either pro-apoptotic, or anti-apoptotic cellular responses. Therefore, it was interesting, if there were significant differences in the intrinsic activation of the cellular signaling between chemosensitive and chemoresistant cell cultures. The activation status of key phosphoproteins of the EGFR related signaling pathways, in this case the MAPK and the AKT signaling pathway, were analyzed. In detail, the EGFR, AKT, GSK3β, mTOR, p70S6K, ERK and MEK were measured in the whole panel of twenty cell cultures, as shown in figures 25-27. Regarding the activation of the EGFR, most of the cell cultures showed an activation below 10%, except of the cell line Colo320 with an activation of 85% and the cell line SW480 with an activation of 20%. The downstream AKT signaling pathway, including AKT, GSK3β, mTOR and p70S6K, was differentially activated in the individual cell cultures, but these regulations did not reach statistical significance ($p = 0.05$). Similar to the activation of the EGFR and the AKT signaling pathway, the MAPK pathway, represented by ERK and MEK, also did not show any significant regulations between the chemosensitive and the chemoresistant group.

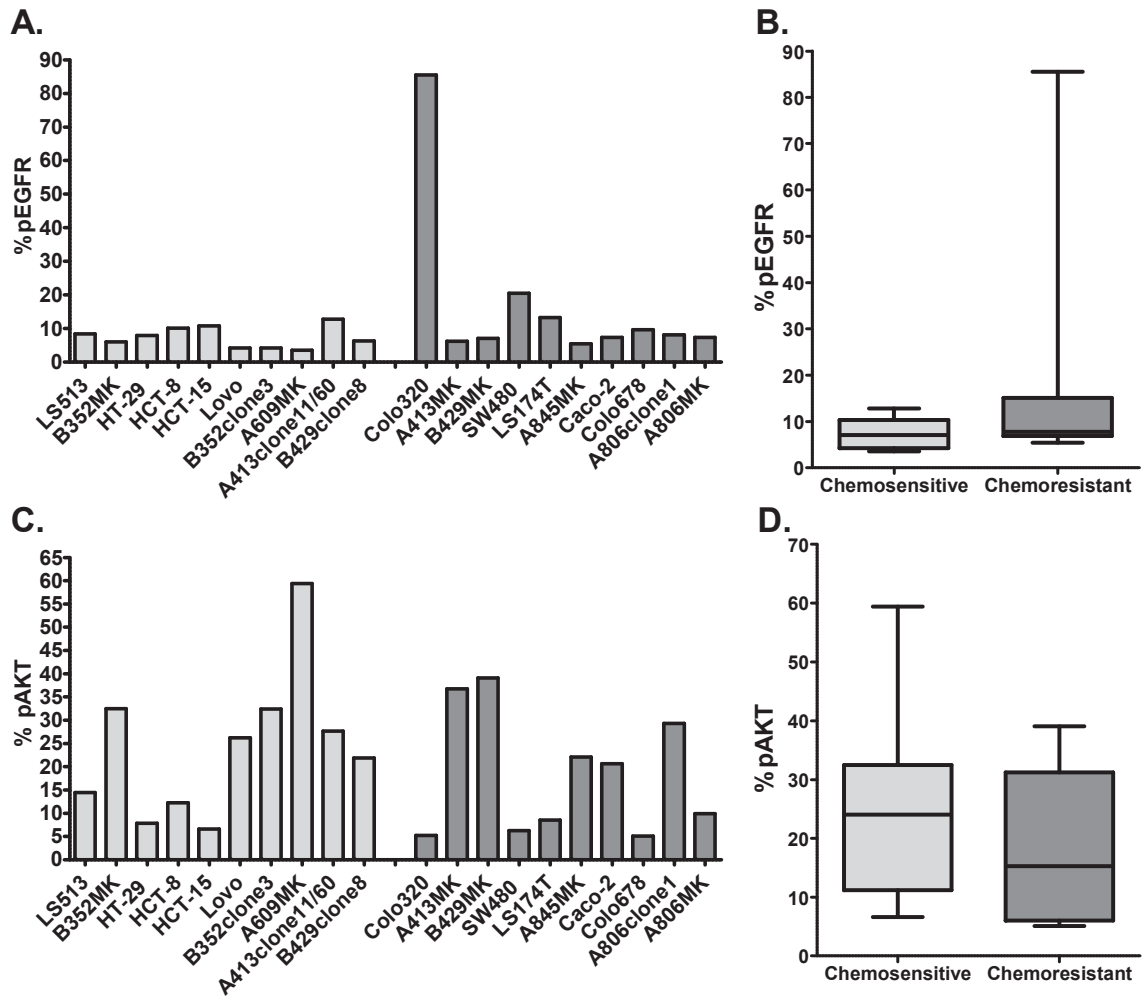

Figure 25: The activation status of EGFR and related pathways are presented as bar charts and box plots. The activations of the EGFR (A,B), AKT (C,D) are shown.

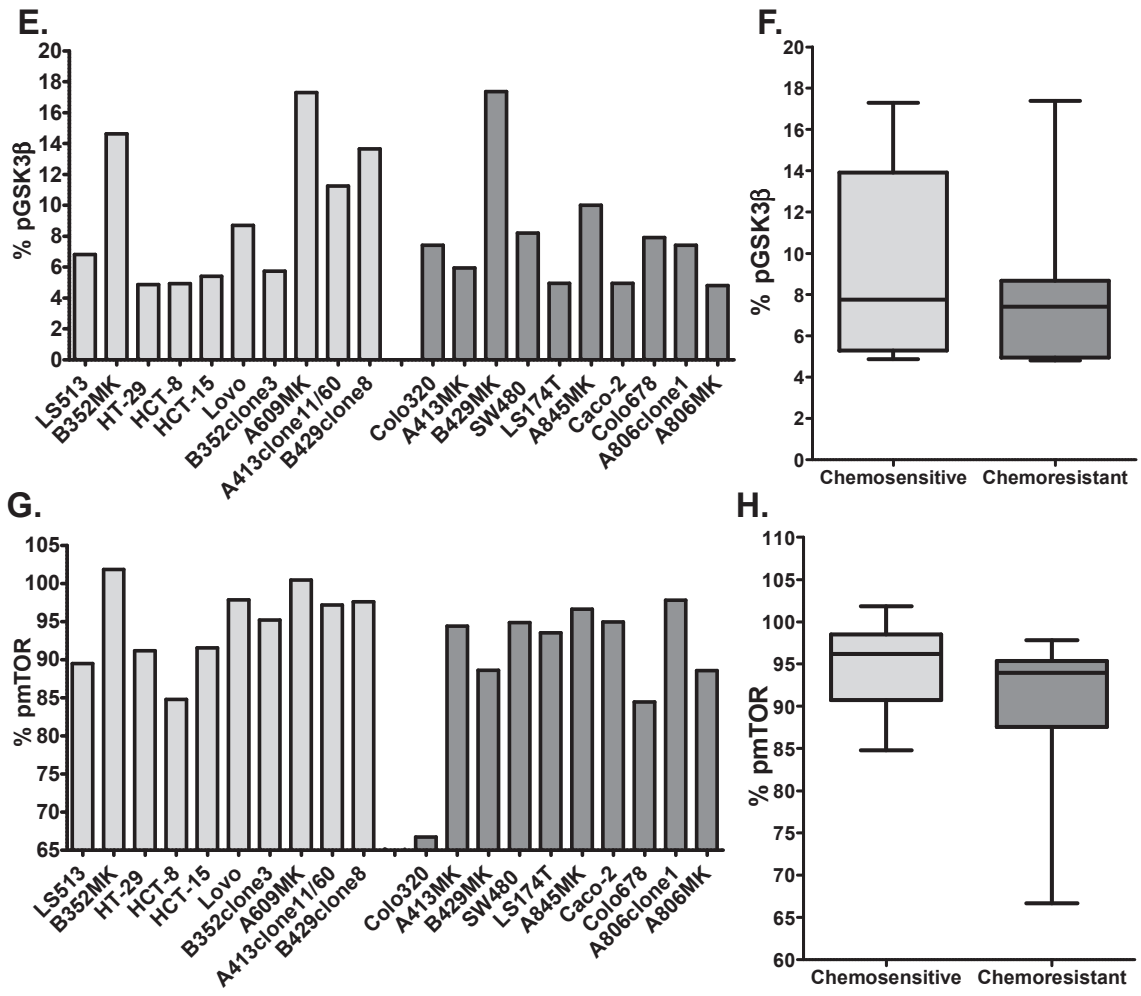

Figure 26: The activation status of EGFR and related pathways are presented as bar charts and box plots. The activations of the GSK3β (E,F), mTOR (G,H) are shown.

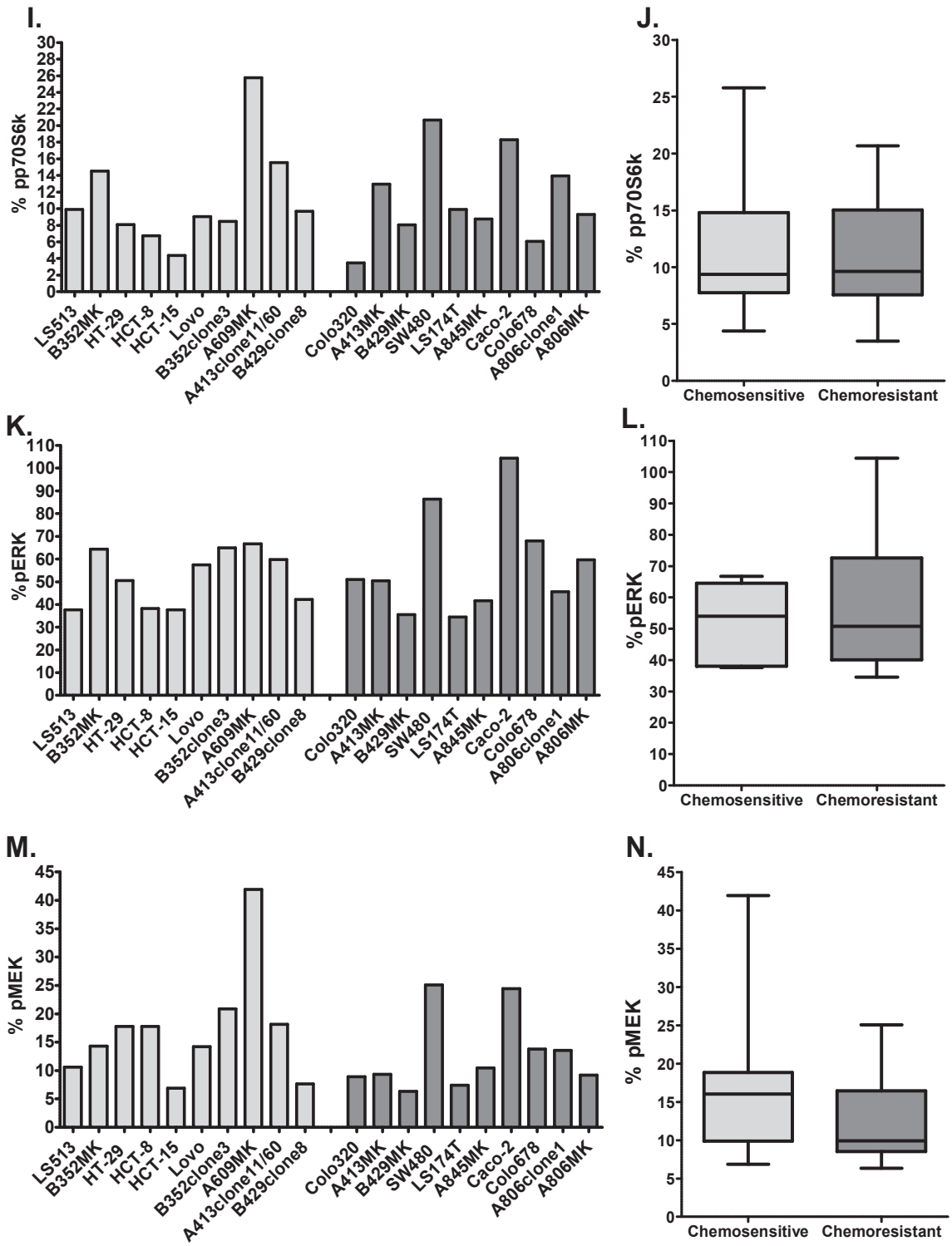

Figure 27: The activation status of EGFR and related pathways are presented as bar charts and box plots. The activations of the P70S6K (I,J), ERK1/2 (K,L) and MEK1/2 (M,N) are shown.

In summary, it is unclear whether the selected EGFR related pathways are influenced by reactive oxygen species under drug treatment, but the intrinsic activation of these pathways did not significantly differ between the chemosensitive

and the chemoresistant group. Therefore, these experiments did not prove any correlation of the biological expression of the SOD 1 and the activation of the EGFR related pathways. There was also no correlation between the chemosensitivity of the cell cultures and the activation status of the signaling pathways. Of note, mutations of these signaling proteins are known to be mostly activating mutations (kras), but a correlation of the mutation status of the selected signaling proteins from the pathways and their activation did not exist (data not shown).

Since therapeutic compounds such as oxaliplatin, which is a part of FOLFOX therapy, produce reactive oxygen species in the cell, which mostly lead to DNA damage, there is an implicated relation of the mode of action of the compound and the biomarker candidate SOD 1. These first experiments for a further biological characterization of the SOD 1 , the enzyme activity and the related activation of EGFR related signaling pathways, did not indicate a causal involvement of the SOD 1 in intrinsic chemoresistance. This does not prove, that there is no causal involvement, but after having analyzed this parameters, there is a good basis for further experiments regarding the analysis of the SOD 1 biological features under drug treatment and further strongly indicative experiments, such as SOD 1 knock down in the cell cultures and the determination of the modulation of chemosensitivity by the knock down.

4 Discussion

The discovery and final adaption of protein biomarker candidates, predictive for the response to FOLFOX combination chemotherapy, to the clinical setting will ultimately enable a personalized chemotherapy of colorectal cancer patients. The molecular characterization of patients will shift the concept of anticancer therapy from standardized treatment of patient groups to specialized treatment concepts for molecular defined subgroups of patients [68]. These subgroups will most likely be defined by patterns of combinations of biomarkers. Therein, the expression status of the corresponding biomarkers will either indicate a chemoresistance to treatment, enabling to choose an alternative treatment option, or will indicate a chemosensitivity to a certain therapeutic, especially if a biomarker also represents a drug target [69]. This individualization of anticancer therapy will increase survival and life quality of patients, by being able to provide maximal effective therapies and sparing them from ineffective therapies and side effects [70]. Currently, it is mandatory to identify biomarkers for molecular subgroups of patients benefiting from treatment, during the development of targeted drugs. Nevertheless, no biomarkers predictive for the response to the conventional FOLFOX chemotherapy have been fully validated and integrated into clinical practice. Therefore there is a great need for biomarkers predicting response to chemotherapy [71;72;73].

In translational research, the discovery of such predictive biomarkers is mostly based on primary and/or secondary cell lines or on human tumor specimen. The cell cultures represent easy-to-handle *in vitro* systems, but only partly reflect the origin tumor. A reason for the lack of biomarkers could also be that the number of cell cultures used in proteomic studies is usually too low (below five) to reflect the heterogeneity of colorectal tumors. The discovery of biomarkers based on human tumors is currently predominantly performed retrospectively, using residual tissue

specimens obtained from surgical resection procedures. Often these tissue samples are obtained by core needle biopsies, e.g. fine needle aspiration, resulting in small sample amounts, which are often insufficient for comprehensive molecular analysis with currently available technologies. Furthermore, several studies have shown that tissue samples change their molecular profiles and start degrading immediately after resection from the patient‘s blood supply [74]. The routine establishment of primary cell cultures, the comprehensive panel of secondary cell lines and especially the collection of high quality fresh frozen tumor samples, including patients` follow up data of the Indivumed GmbH offered an excellent basis for the discovery of predictive biomarkers. The cell cultures were used for the discovery of biomarkers and generation of hypotheses regarding their clinical relevance. Furthermore, these cell cultures were used for the development of technical assays, which are necessary for a further validation, e.g. NanoPro1000 technologie, ELISA. The high quality tissue samples and follow up data can be used for the validation of those hypotheses by studies in patient populations.

4.1 Characterization of the cell cultures panel in regard to chemosensitivity

A diverse panel of cell cultures was used in this thesis. This panel consisted of twenty secondary as well as primary mixed cell cultures. This high number of heterogeneous cell cultures more closely reflects the clinical situation and thus enabled the discovery of robust biomarker candidates in a defined *in vitro* setting. In consequence, the discovered biomarker candidates should be better translatable to the clinic than results from studies using single or low numbers of cell lines.

The used primary cell culture panel has initially been characterized in regard to the mutation status of selected genes (Kras, Braf, PIK3CA, APC, TP53). These genes are implicated in pro- and anti-apoptotic cell signaling and are relevant in the concept

of targeted therapy of colorectal cancer. Screening for mutations in the EGFR related signaling pathways in colorectal cancer patients may provide additional information on optimizing treatment options with targeted therapies. There was no difference in the frequency of mutations in the selected genes between the chemosensitive and the chemoresistant group in this study. This is in accordance with the limited number of studies, which have assessed the predictive value of such mutations in response to conventional chemotherapy [48].

In lung cancer, mutations in the TP53 gene are described to have neither prognostic for survival nor a predictive value of a differential benefit from adjuvant chemotherapy [75]. This has also been found for the panel of colorectal cancer cell cultures, although there is evidence that Dukes' C tumors with mutated TP53 have significantly better prognosis when treated with adjuvant chemotherapy [76]. The overall frequency of the corresponding mutations found in the panel of cell cultures does not fully reflect the frequency of those mutations found in studies of clinical specimen. This must be due to the relative low number of twenty cell cultures.

The classification of the cell cultures into chemosensitive and chemoresistant to FOLFOX treatment using a cell viability assay was the basis for all further comparative proteomic studies. In theory, the overall effects of drug induced cytotoxicity by chemotherapeutics are the sum of all specific cellular effects underlying multi factorial mechanisms. Therefore, *in vitro* chemosensitivity testing reveals the chemosensitivity of cells to anticancer therapy either by determination of the death of all cancer cells or at least by growth inhibition. The ATP-TCA (Tumor Chemosensitivity Assay) used in this study, is superior to other assay in sensitivity and handling [77]. Furthermore, this assay has already been applied to the clinical situation for several tumor entities [78-82]. In order to comprehensively investigate the chemosensitivity of the cell cultures to FOLFOX therapy, *in vitro* FOLFOX

treatment as well as single agent treatment of the cell cultures with 5-FU and Oxaliplatin was performed. Those experiments confirmed the synergistic drug interaction of 5-FU, Oxaliplatin and Leucovorin reported before [83].

Furthermore, three time points (two, three and four days) of drug treatment were analyzed, in contrast to most other studies in which only one time point of chemosensitivity measurement is conducted. The order in the allocation of cell cultures in respect to their chemosensitivity differed slightly for the three different time points. This indicates that the classification of the panel of cell cultures based on several durations of drug treatment gives a more comprehensive picture of the time dependent chemosensitivity of cell cultures to drug treatment and enables a more robust classification of chemosensitivity. In addition, different mathematical methods were in tested this thesis for the extraction of the degree of chemosensitivity from dose response curves. Several methods, like the “AUC” Area under the curve calculation, the “SI” Sensitivity Index and the “IC50” Half Maximal Inhibitory Concentration resulted in almost the same grouping of cell cultures (data not shown). Finally, the median chemosensitivity based on the IC50`s was used for the classification of cell cultures in chemosensitive and chemoresistant groups, which is in accordance with most of the published literature [84]. The predictive value of the ATP-TCA can help to guide individualized anticancer therapy, especially in second line treatment where the guidelines for therapy are not always clearly defined [85]. The ultimate goal for individualized anticancer therapy should however be the identification of predictive biomarkers and the elucidation of mechanisms of chemoresistance rather than the exclusive detection of chemosensitivity. Only this knowledge can ultimately lead to rational drug design and scientific based concepts of individual chemotherapy.

4.2 Proteomic studies for the discovery of predictive biomarker candidates

The technical basis for the analysis of the low molecular weight, intact proteome of cell cultures was provided by the establishment of the Top Down proteomic workflow. This workflow enabled the discovery of low abundant and low molecular weight biomarker candidates, might not be detectable in proteomic workflows applying tryptic digestion of proteins. Another feature of this workflow is the possibility to detect post translational modifications of the native protein, as well as cleaving products of proteins and degraded proteins. Additionally, the already, at the Indivumed GmbH, established Bottom Up workflow was applied to the analysis of the high molecular weight proteome.

Both workflows were designed to minimize the occurance of bias during sample preparation and detection. This included sample randomization, measurement adjustments by using an external standard, visual control of LC-MALDI spectra and controlled experimental conditions (temperature, moisture, etc.) Similar to the Bottom Up proteomic workflow, the newly designed Top Down workflow applied a label free separation and subsequent detection of proteins. Several studies showed the possibilities for label free relative quantification [86;87]. For example, Neubert et al [88] demonstrated that LC-MALDI peptide quantification between samples is possible over three orders of magnitude and the average reproducibility within technical replicates below 25 % CV. The averaged CVs for the individual samples in the Top Down and Bottom Up studies ranged from 9 % to 17 % and resulted in total averages of about 14 % over all 102 measurements. These results were in accordance with the reproducibility of those LC-MALDI studies previously mentioned. The field of mass spectrometry-based, label-free, quantitative proteomics has been reviewed by Zhu *et al* [89].

Both proteomic studies for the discovery of biomarker candidates, predictive for intrinsic chemoresistance to FOLFOX therapy resulted in several biomarker candidates, of whom six were identified by literature search as the most promising. Two of these biomarker candidates were already described in the literature, supporting our findings in general, as well as undescribed candidates being even more interesting. The already described biomarker candidate SOD 1, which is an antioxidant enzyme of 16 kDa that protects the cell by decreasing ROS levels. The SOD 1 catalyzes the conversion of single electron reduced species of molecular oxygen to hydrogen peroxide and oxygen. The SOD 1 is activated by the formation of a homodimer of 32 kDa. There are three classes of SODs (Cu/Zn SOD, Mn SOD, Fe SOD), that differ in their metal binding ability, distribution in different cell compartments, and sensitivity to various reagents. Among these, SOD 1 is widely distributed and comprises 90% of the total SOD. This ubiquitous enzyme, which requires Cu and Zn for its activity, has great physiological significance and therapeutic potential [90]. The SOD 1 is described in the context of chemoresistance to platinum compounds in several tumor entities [91;92;93]. For example, Kim et al [94] found the SOD 1 to be 1.47 fold upregulated in ovarian, cisplatin resistant cell lines, which is very similar to the findings in the Top Down study. Another published study suggests a mechanism of resistance involving the Ape/Ref1 protein of the base excision repair (BER) pathway, which is also regulated by intracellular ROS. By overexpression of SOD 1, the ROS level decreased and Ape/Ref1's ability to repair DNA and protect cells from apoptosis could also be restored [95].

The second biomarker candidate that has been already described in the context of chemoresistance, was the Heat shock cognate protein 70 (HSC70). Hsc70 is a member of the heat shock protein 70 family. Human HSC70 is a 73 kDa molecular chaperone and is involved in a multitude of housekeeping and chaperoning functions,

including polypeptide folding, protein translocation across membranes and prevention of protein aggregation under stress conditions [96;97]. HSC70 is essential for the survival of normal and tumor cells [98] and has an important role in stabilizing the folding of newly synthesized polypeptides [99]. In response to different types of stress, including heat shock and oxidative stress, HSC70 accumulates in the nucleus. However its functions still remains to be completely elucidated [100;101]. Recent reports revealed that HSC70 has specific functions in each tissue and cell, and is active in various aspects such as intercellular signaling [102]. HSC70 has, in contrast to the results from this thesis, been found to be overexpressed in chemoresistant cancer cells [103;104;105]. This biomarker candidate has been described to be upregulated in the cervix squamous cell carcinoma cell line A431 with acquired chemoresistance to cisplatin [106]. Furthermore, HSC70 has been shown to be induced by treatment of human neuroblastoma derived SH-SY5Y cells with staurosporin, which is another chemotherapeutic agent [107]. It is unclear why HSC70 was found to be down regulated in the chemoresistant group, although there is evidence of this protein to be upregulated in chemoresistant cancer cells. Nevertheless, the involvement of HSC70 in intrinsic chemoresistance of colorectal cancer cells to FOLFOX treatment has not yet been studied in detail.

The remaining four of the six biomarker candidates are mostly rarely described in the literature and could not be linked to chemoresistance in cancer. Therefore, those proteins are even more interesting, because they are here newly described in the context of chemoresistance in colorectal cancer. In this study, the first of these four biomarker candidates was the Eukaryotic translation initiation factor 2C 1 (AGO 1), which is a 97 kDa, RNAi- and miRNA-binding repressor ribonucleoprotein. AGO 1 is present in all RNA-induced silencing complexes reported to date [108]. Ago 1 is located in the cytoplasm and has several biological functions. Based on results from

tissue microarrays, Li et al proposed that AGO 1 might represent a novel colon cancer marker with early diagnostic significance [109]. Although AGO 1 is described to play an important role in stem cell self-renewal, RNA interference and translational regulation [110], very little is known about his involvement or function in cancer. Since Ago 1 has been found to be upregulated in chemoresistant cell cultures, it may be possible that AGO 1 is involved in chemoresistance through silencing of pro-apoptotic miRNAs or RNAi. Thereby, high intrinsic levels of AGO 1 may enhance the ability of cancer cells to compensate drug induced effects and thus contribute to a chemoresistant phenotype.

The second biomarker candidate, that was significantly regulated, was the 49 kDa UBX domain-containing protein 1 (UBXN). UBXN is a component of the ubiquitin conjugation pathway and is localized in the cytoplasm, cytoskeleton and the nucleus [111]. UBXN plays a role in endoplasmic reticulum (ER)-associated degradation (ERAD). It functions to recruit ubiquitylated substrates to the cytoplasmic ATPase valosin containing protein and other ERAD components such as ubiquitin ligases [112]. Thus, UBXN ensures that misfolded or unassembled proteins are retained in the ER and then directed for degradation by ERAD [113;114]. Recent studies indicated that the endoplasmic reticulum (ER) can sense and transduce apoptotic signals, induced by stress that interferes with protein folding [115]. UBXN was found to upregulated in chemosensitive cell cultures, which may indicate an involvement of UBXN in ER-stress mediated survival or apoptotic signaling. In consequence, the elevated expression of UBXN may positively contribute to the transduction of pro-apoptotic signals from the ER.

Another identified biomarker candidate, that was undescribed in the context of chemoresistance, was the 14 kDa Ubiquitin-60S ribosomal protein L40 (UBA52). This protein is rarely described in the literature and most of the information was received

from the Uniprot website (http://www.uniprot.org/). The UBA52 ribonucleoprotein consists of two chains, the first chain is ubiquitin and the second chain is the 60S ribosomal protein L40. The latter one is part of the 60S ribosomal subunit. UBA52 is located in the cytoplasm as well as in the nucleus and is involved in several biological processes. Due to the ubiquitin chain, this protein is involved in protein ubiquitination and indirectly also in endoplasmic reticulum-associated degradation. Furthermore, UBA52 is involved in DNA repair, mitotic cell cycle regulation and apoptotic processes. Similar to the biomarker candidate UBXN, UBA52 may be involved in chemoresistance by the modulation of apoptotic signaling and ubiquitin related protein degradation pathways. Additionally, UBA52 may also be involved in distinct chemoresistance mechanisms with the involvement in DNA repair and subsequent signal transduction by p53 class mediators.

The last one of the further analyzed biomarker candidates was the 12kDa mitochondrial ATPase inhibitor (ATPIF1). ATPIF1 has been found on the cell membrane, where it is proposed to modulate the activity of angiostatin of endothelial cells [116]. However, it has been mainly described to be located in the mitochondrion [117]. Campanella *et al* [118] stated that, when mitochondrial function is compromised and the mitochondrial membrane potential falls below a threshold, the F(1)F(o)-ATP synthase can reverse, hydrolysing ATP to pump protons out of the mitochondrial matrix. Although this activity can deplete ATP and precipitate cell death, it is limited by the mitochondrial protein ATPIF1, as endogenous F(1)F(o)-ATPase inhibitor. Nevertheless, little is known about the complete physiological activity of ATPIF1. Emerging research suggests that ATPIF1 has a wider ranging impact on mitochondrial structure and function than previously thought. The ATPIF1 has not yet been studied in relation to chemosensitivity. As a mitochondrial protein involved in ATPase activity regulation, an involvement in mitochondrial mediated

apoptosis could be speculated. The ATPIF1 has been discovered to be upregulated in chemosensitive cell cultures, therefore the overexpression of the ATPIF1 could result in a stronger pro-apoptotic response to FOLFOX treatment. But as mentioned before, several undescribed biological functions of this biomarker candidate could contribute to chemosensitivity.

In summary, the discovery of biomarker candidates predictive for intrinsic chemoresistance to FOLFOX treatment by using a newly established Top Down and a Bottom Up proteomic workflow resulted in the discovery of several highly significant biomarker candidates. The six most promising ones consisted of two biomarker candidates already described in the context of chemoresistance, which in general supports the results and four undescribed biomarker candidates. All of those have biological backgrounds and functions that may be linked to mechanism of chemoresistance. Therefore, a further validation and investigation of the causal involvement in chemoresistance may fully elucidate the potential of these biomarker candidates. Ultimately, a combination of biomarker will have a greater predictive value for the response to FOLFOX therapy than a single marker. Nevertheless, a deeper characterization of the involvement of the biomarker in chemoresistance can potentially reveal that also other biological features than protein expression may be of predictive value.

4.3 Validation of predictive biomarker candidates

Validation of a biomarker involves a systematic evaluation to assure that the technique used to assay the biomarker is reliable to perform its task [119]. Biomarker validation should furthermore be guided by the established principles of bio-analytical method validation [120,121]. However, the identification of clinically useful predictive biomarkers for solid tumors has been proven difficult [122]. Many of the initially

promising biomarkers failed to translate into clinically useful applications [123]. Interestingly, the failure of a predictive biomarker has often only become apparent at a relatively late stage in investigation. This can be explained by either an insufficient preclinical validation of the biomarker candidates or inadequate biomarker assays. Recently, the field has recognized the need to develop a robust clinical biomarker development methodology, including extensive validations to facilitate the process [124]. In general, newly discovered biomarker candidates should be technically validated [125-127], in order to control the discovery workflow, and more importantly tested for their relevance in an independent cohort of patients [128;129]. Validation is of great importance, especially if the technical workflow for the discovery study has been newly established, such as the Top Down workflow in this thesis. For this purpose it is necessary to develop independent technologies and assays suitable for the measurement of the biomarker candidate and the adaption to the clinical situation [130]. These assays must be able to detect the biomarker candidates in very small sample amounts, as they are typical in the clinic. Furthermore, Wulfkuhle *et al* [131] demonstrated the requirement of laser capture micro dissection (LCM) to analyze specific changes in protein expression and modification. Micro dissection should be a basic component of molecular analysis since dramatic changes within specific protein phosphorylation levels were noted between a majority of the undissected and micro dissected samples. This integration of LCM technologies also results in small samples sizes and proves the need for adequate technologies. The recently introduced, antibody-based NanoPro1000 technique enables a detailed characterization of protein isoforms in very small sample volumes, which has not yet been possible by standard western blotting techniques [66]. In respect to antibody-based assays, Haab *et al* [132] noted that the sensitivity of individual antibody-antigen interactions for any given detection has great impact on results. Since

antibody validation is a standard operating procedure at the Indivumed GmbH, the antibodies corresponding to the six biomarker candidates were checked for sensitivity and specifitivity (data not shown). Antibodies corresponding to four of the six biomarker candidates showed signals in the NanoPro1000 technology, therefore assay developments for the four biomarker candidates were conducted. These assay developments are the basis for a further validation of the biomarker candidates in an independent cohort of patients, which will be a future project. In order to perform validation studies, the biomarkers must be qualified for a specified purpose prior to clinical implementation [133]. Qualification of a biomarker is to define its sensitivity and specificity [134;135] for clinical end-point determination and to prove its clinical utility [136;137]. Use of unqualified biomarkers can lead to incorrect treatment decisions, which will impact adversely on patient health outcomes. Therefore, biomarker candidates are finally validated in clinical studies that should fulfill all requirements to properly assess the clinical utility of a biomarker [138; 139].These trials are ideally based on cohorts of patients, which are sufficiently homogeneous and numerous for the development of therapeutically relevant classifiers [vsd]. Validation studies should then apply the classifier completely specified including cut offs, and measure the prediction accuracy [140, 141]. The size and design of the validation study should be robust, so that meaningful confidence intervals on predictive accuracy and positive and negative predictive values can be reported [142]. Furthermore, the right statistics have a fundamental role in ensuring that biomarkers and the data they generate are used appropriately and to address relevant objectives such as the estimation of biological effects [143]. Therefore, raw expression data from studies should be made publicly available to enable others to reanalyze the data [144].

Poor study design and inadequate reporting of studies have been identified as a major obstacle to progress in the field of biomarkers [145,146]. In response, the Statistics Subcommittee of the National Cancer Institute-European Organization for Research and Treatment of Cancer (NCI-EORTC) Working Group on Cancer Diagnosis developed tumor biomarker study reporting guidelines: REporting recommendations for tumor MARKer prognostic studies (REMARK guidelines) [37]. These guidelines address the reporting of study design, hypotheses, patient and bio-specimen characteristics, assay methods and statistical analysis methods used in the studies of prognostic biomarkers. Another point that needs to be addressed before implementation of the biomarker candidates in the clinical situation is whether the biomarkers are purely indicative of chemoresistance or causally involved. If a causal mechanistic relationship between a particular molecular pathway or function and the clinical outcome in individual patients is evident, the biomarker candidate could also represent a new drug target.

There are several approaches to determine, if there is a functional involvement of the biomarker in chemoresistance. One of the approaches is the use of cell lines with acquired chemoresistance, established from parental cell lines [147]. This approach has the advantage that the chemoresistant as well as the parental cell line has the same genetic background, whereas the status of chemoresistance is different. Mostly, the studies using this approach compare one parental cell line to the corresponding chemoresistant clone, which does hardly reflect the heterogeneity of tumors. This might be due to the fact that it is very difficult to establish chemoresistant cell lines. The comparative Bottom Up study of acquired chemoresistance was conducted using five parental cell lines and five chemoresistant counterparts. In this study, HSC70 and UBXN have been found to be

further downregulated in the chemoresistant cell lines. This down regulation of HSC70 and UBXN during the acquisition of chemoresistance indicates a direct involvement of the biomarker candidates in chemoresistance related mechanisms. The direct verification of the involvement of the biomarker candidates in chemosensitivity can for example be carried out by ´knock-out´ experiments, in which the expression of the biomarker in the cell will be inhibited and the consequence to the chemosensitivity of the cell can be observed [148]. Another approach for testing an involvement of the biomarker candidate in chemoresistance, beside the direct measurement of the biological activity, is the investigation of downstream effectors. This was done in the exemplary validation of the SOD 1 by examining an influence of SOD 1 expression on the activation of EGFR related pathways. Unfortunately, neither the activity of the SOD 1 nor the activation of the EGFR related pathways indicated a causal biological function of the SOD 1 in chemoresistance to FOLFOX treatment.

Nevertheless, knock out experiments or SOD 1 inhibitor studies will elucidate whether there is an active involvement of the SOD 1. Interestingly, the SOD 1 has independently been found to be a drug target in leukemia cells [149] and in lung cancer [150]. Furthermore, the newly developed small molecule ATN-224 has been shown to inhibit the SOD 1 by the depletion of copper. The inhibition of SOD 1 leads to inhibition of endothelial cell proliferation *in vitro* and attenuation of angiogenesis *in vivo* [151]. The inhibition of SOD 1 in tumor cells leads to the induction of apoptosis [152]. Based on these results, Donate *et al* [153] identified biomarker candidates for the response to the new SOD 1 inhibitor. They found the SOD activity measurement in blood cells in mice and levels of endothelial progenitor cells (EPCs) in bonnet macaques treated with ATN-224 to be of predictive value. This is a good example in

which a biomarker candidate is also a drug target and biomarker candidates for this new compound have been identified.

4.4 Future prospects

In future projects, the assay development of the NanoPro1000 assays has to be completed and the assays have to be adapted to clinical specimen. Following the establishment of robust assays to measure the expressions of biomarker candidates a first retrospective validation study in an independent cohort of patients can be conducted. Thereby, a first impression of the sensitivity and specitifity of the biomarker candidates can be achieved. Subsequently, combinations of biomarkers can be analyzed in regard to their predictive value and adequate cut off values for the biomarker assays can be defined. A next step would be the final validation of the biomarker candidates in a prospective clinical study. This will provide information on patient stratification in regard to the optimal clinical endpoints that can be defined. Furthermore, the clinical study will show how adequate the preclinical developed biomarkers are for the integration in clinical practice.

Another future project could be the deeper characterization of biological backgrounds and functions of the biomarker candidates, in regard to their involvement in chemoresistance to FOLFOX chemotherapy. The literature search on the six newly discovered biomarker candidates revealed their involvement in several biological functions, therefore the analysis of crosslinks between biological functions of the biomarker candidates would be interesting.

Further experiments using gene knock downs and small molecule inhibitors to modulate the expression or activity and the analysis of downstream effectors of the corresponding cellular signaling pathways of the biomarker candidates will ultimately elucidate their involvement in chemoresistance and possible interactions. Finally, the

newly established Top Down as well as the Bottom Up proteomic workflows have been shown to be applicable to the discovery of biomarker candidates and can also be used in other settings.

6 Summary

Since the introduction of chemotherapy for cancer treatment in the early 20th century, considerable efforts have been made to maximize drug efficiency and at the same time minimize side effects. A detailed and comprehensive understanding of drug response mechanisms is essential to ultimately guide a molecular based personalized anticancer therapy. As there is a great interpatient variability in response to chemotherapy, the development of predictive biomarker for the response to chemotherapy is an ambitious aim for the rapidly growing research area of personalized molecular medicine. The individual prediction of response will greatly improve treatment and thus increase survival and life quality of patients.

Towards this end, this thesis aimed at the discovery of protein biomarker candidates predictive for the response to FOLFOX chemotherapy in colorectal cancer. The first task of this thesis was the assembly of a diverse panel of twenty colorectal cell cultures, consisting of primary, epithelial mixed cultures, primary clonal cell lines, as well as secondary cell lines. Six primary mixed cultures and four primary, clonal cell lines were established from patients` tumors. The cell culture panel was characterized in respect to chemosensitivity to FOLFOX treatment and mutation status of selected genes. In order to discover predictive protein biomarker candidates, basal protein expression profiles of chemosensitive and chemoresistant cell cultures were measured and compared. Therefore, a Top Down proteomic workflow for the analysis of the low molecular weight proteome was newly established and validated. The high molecular weight proteome was analyzed using a Bottom Up proteomic workflow. In combination, these workflows revealed several biomarker candidates, differentially regulated between the chemosensitive and chemoresistant cell cultures. The six most promising biomarker candidates were technically validated and adequate assays for the detection of the biomarker

candidates in clinical samples were developed. These assays are the basis for a validation of biomarker candidates in an independent, clinically relevant, cohort of patients. One of the most promising biomarker candidates was the SOD 1, an enzyme involved in the detoxification of reactive oxygen species. The biological background of this biomarker candidate was exemplarily further investigated. Therein, it was tested whether the expression of the biomarker candidate correlates with enzyme activity. Additionally, downstream signaling pathways, related to the SOD 1 were analyzed.

Within the scope of this thesis, predictive biomarker candidates for the response to FOLFOX chemotherapy were discovered, using a panel of cell cultures and newly developed, as well as already established proteomic workflows. These very promising biomarker candidates and their combinations are planned to be validated in the clinical setting using large, heterogeneous groups in order to verify a clinical application in the future.

6 Zusammenfassung

Seit der Einführung der Chemotherapie zur Krebsbehandlung im frühen 20. Jahrhundert wurden erhebliche Anstrengungen unternommen, die Effizienz von Medikamenten zu maximieren und gleichzeitig Nebenwirkungen zu minimieren. Ein detailliertes und umfassendes Verständnis von Mechanismen der Resistenz gegen Medikamente ist wichtig, um letztlich eine molekular basierte personalisierte Krebs-Therapie durchführen zu können. Da es eine große Variabilität im Ansprechen auf eine Chemotherapie gibt, ist die Entwicklung von prädiktiven Biomarkern für die Vorhersage eines Ansprechens auf eine Chemotherapie ein ehrgeiziges Ziel für das rasch wachsende Forschungsgebiet der personalisierten, molekularen Medizin. Die individuelle Vorhersage des Ansprechens auf eine Therapie wird die Behandlung von Patienten erheblich verbessern und somit das Überleben und die Lebensqualität der Patienten erhöhen.

Das Ziel dieser Arbeit war daher, die Entdeckung von Protein Biomarker Kandidaten, die ein Ansprechen oder eine Resistenz gegen die FOLFOX Chemotherapie bei Dickdarmkrebs vorhersagen können. Die erste Aufgabe dieser Arbeit war die Zusammenstellung eines vielfältigen Panels von zwanzig kolorektalen Zellkulturen, bestehend aus primären, epithelialen Mischkulturen, primären klonalen Zelllinien sowie sekundären Zelllinien. Sechs primäre Mischkulturen und vier primäre, klonale Zelllinien wurden aus Tumoren von Patienten aufgearbeitet. Die zwanzig Zellkulturen wurden hinsichtlich ihrer Chemosensitivität gegenüber einer FOLFOX Behandlung untersucht. Zusätzlich wurde der Mutations-Status von ausgewählten Genen erhoben. Um prädiktive Protein Biomarker Kandidaten zu entdecken, wurden basale Protein Expressions Profile von den chemosensitiven und chemoresistenten Zellkulturen gemessen und verglichen. Hierfür wurde ein auf Massenspektrometrie basierter Top Down Proteomik Workflow für die Analyse des niedermolekularen

Proteoms neu entwickelt und validiert. Das hochmolekulare Proteom wurde mit einem Bottom Up Proteomic Workflow analysiert. Als Ergebnis beider Studien wurden mehrere Biomarker Kandidaten entdeckt, die differentiell reguliert zwischen der chemosensitiven und chemoresistenten Gruppe an Zellkulturen vorlagen. Die sechs aussichtsreichsten, hoch interessanten Biomarker Kandidaten wurden technisch validiert und angemessene technische Methode für den Nachweis der Biomarker Kandidaten in klinischen Proben wurde entwickelt. Diese Methode ist die Basis für eine Validierung der Biomarker Kandidaten in einer unabhängigen, klinisch relevanten Kohorte von Patienten. Zu den aussichtsreichsten Biomarker Kandidaten gehörte die SOD 1, ein Enzym, das an der Entgiftung von reaktiven Sauerstoffspezies beteiligt ist. Der biologische Hintergrund dieses Biomarker Kandidaten wurde exemplarisch untersucht. Hierbei wurde getestet, ob die Expression des Biomarker Kandidaten mit seiner Enzym-Aktivität korreliert. Darüber hinaus wurden nachgeschaltete Signalwege, mit Bezug auf die SOD 1 analysiert.

Im Rahmen dieser Dissertation wurden prädiktive Biomarker Kandidaten für ein Ansprechen eine FOLFOX Chemotherapie identifiziert. Hierzu wurde ein Panel von selbst etablierten und sekundären Zellkulturen benutzt. Weiterhin wurde zur Untersuchung des Proteoms, ein Workflow neu etabliert und mit einem bestehenden Workflow kombiniert. Es ist weiterhin geplant, die gefundenen, vielversprechenden Biomarker Kandidaten und Kombinationen derer, mithilfe einer großen, heterogenen Gruppen zu validieren, um eine eventuelle klinische Anwendung in der Zukunft zu überprüfen.

5 References

[1] Jemal A, Bray F, Center MM, Ferlay J, Ward EME, Forman D. Global cancer statistics. CA Cancer J Clin, 2011,61, 69–90.

[2] Cunningham D, Atkin W, Lenz HJ, Lynch HT, Minsky B, Nordlinger B, Starling N. Colorectal cancer. Lancet. 2010. 375: 1030–47.

[3] Chapuis PH, Fisher R, Dent OF, Newland RC, Pheils MT. The relationship between different staging methods and survival in colorectal carcinoma. Diseases of the Colon and Rectum. 1985, 28:158–61.

[4] Greene FL, Balch CM, Fleming ID. AJCC cancer staging handbook. 6th ed. New York: Springer, 2002.

[5] Leonard GD, Brenner B, Kemeny NE. Neoadjuvant chemotherapy before liver resection for patients with unresectable liver metastases from colorectal carcinoma. J Clin Oncol. 2005, 23:2038–48.

[6] Adam R, Delvart V, Pascal G, Valeanu A, Castaing D, Azoulay D. Rescue surgery for unresectable colorectal liver metastases down staged by chemotherapy: a model to predict long-term survival. Ann Surg. 2004, 240:644–57.

[7] Scheithauer W, Rosen H, Kornek GV, Sebesta C, Depisch D. Randomised comparison of combination chemotherapy plus supportive care with supportive care alone in patients with metastatic colorectal cancer. BMJ. 1993, 306:752-5.

[8] Cunningham D, Pyrhonen S, James RD. Randomised trial of irinotecan plus supportive care versus supportive care alone after fluorouracil failure for patients with metastatic colorectal cancer. Lancet. 1998, 352:1413-8.

[9]. Smyth JF, Hardcastle JD, Denton G, et al. Two phase III trials of tauromustine (TCNU) in advanced colorectal cancer. Ann Oncol. 1995, 6:948-9.

[10] Allen-Mersh TG, Earlam S, Fordy C, Abrams K, Houghton J. Quality of life and survival with continuous hepatic-artery floxuridine infusion for colorectal liver metastases. Lancet. 1994, 344:1255-60.

[11] Palliative chemotherapy for advanced or metastatic colorectal cancer: Colorectal Meta-analysis Collaboration. Cochrane Database. Syst Rev. 2000, 2:CD001545.

[12] Liu ZF, Guo QS, Zhang XQ, Yang XG, Guan F, Fu Z, Wang MY: Biweekly oxaliplatin in combination with continuous infusional 5-fluorouracil and leucovorin (modified FOLFOX-4 regimen) as first-line chemotherapy for elderly patients with advanced gastric cancer. Am J Clin Oncol. 2008, 31:259-63.

[13] Buroker TR, Moertel CG, Fleming TR, Everson LK, Cullinan SA, Krook JE, Mailliard JA, Marschke RF, Klaassen DJ, Laurie JA. A controlled evaluation of recent approaches to biochemical modulation or enhancement of 5-fluorouracil therapy in colorectal carcinoma. J Clin Oncol. 1985, 3:1624–31.

[14] Andre´ T, Boni C, Mounedji-Boudiaf L, Navarro M, Tabernero J, Hickish T, Topham C, Zaninelli M, Clingan P, Bridgewater J, Tabah-Fisch I, deGramont A. For the Multicenter International Study of Oxaliplatin/5-Fluorouracil/leucovorin in the Adjuvant Treatment of Colon Cancer (MOSAIC) Investigators. Oxaliplatin, fluorouracil, and leucovorin as adjuvant treatment for colon cancer. New England Journal of Medicine. 2004, 350: 2343–51.

[15] Rothenberg ML, Oza AM, Bigelow RH, et al. Superiority of oxaliplatin and fluorouracil-leucovorin compared with either therapy alone in patients with progressive colorectal cancer after irinotecan and fluorouracil- leucovorin: interim results of a phase III trial. J Clin Oncol. 2003, 21:2059-69.

[16]. Giacchetti S, Perpoint B, Zidani R, et al. Phase III multicenter randomized trial of oxaliplatin added to chronomodulated fluorouracil- leucovorin as first-line treatment of metastatic colorectal cancer. J Clin Oncol. 2000, 18:136-47.

[17] de Gramont A, Figer A, Seymour M, et al. Leucovorin and fluorouracil with or without oxaliplatin as first-line treatment in advanced colorectal cancer. J Clin Oncol. 2000, 18:2938-47.

[18] Raymond E, Buquet-Fagot C, Djelloul S, et al. Antitumor activity of oxaliplatin in combination with 5-fluorouracil and the thymidylate synthase inhibitor AG337 in human colon, breast and ovarian cancers. Anticancer Drugs. 1997, 8:876-85.

[19] Meyerhardt JA and Mayer RJ. Systemic Therapy for Colorectal Cancer. New England Journal of Medicine. 2005, 352;5.

[20] Sobrero A, Guglielmi A, Grossi F, Puglisi F, Aschele C. Mechanism of action of fluoropyrimidines: relevance to the new developments in colorectal cancer chemotherapy. Semin Oncol. 2000, 27:Suppl 10:72-7.

[21] Longley, DB, Harkin DP and Johnston PG. 5-Fluorouracil: Mechanisms of action and clinical strategies. Nature reviews cancer. 2003, 3:5 330-338.

[22] Diasio RB and Harris BE. Clinical pharmacology of 5-fluorouracil. Clin. Pharmacokinet. 1989,16, 215–237.

[23] Zhang ZG, Harstrick A, Rustum YM. Modulation of fluoropyrimidines: role of dose and schedule of leucovorin administration. Semin Oncol. 1992, 19:3,10-5.

[24] Kidani Y. Oxaliplatin. Drugs Future. 1989, 14:529-532.

[25] Mathe G, Kidani Y, Segiguchi M, et al. Oxalato-platinum or 1-OHP, a third generation platinum complex: an experimental and clinical appraisal and preliminary comparison with cis-platinum and carboplatinum. Biomed Pharmacother. 1989, 85:809.

[26] Preston TJ, Henderson JT, McCallum GP, Wells PG. Base excision repair of reactive oxygen species-initiated 7, 8-dihydro- 8-oxo-2'-deoxyguanosine inhibits the cytotoxicity of platinum anticancer drugs. Mol Cancer Ther. 2009, 8:2015–2026.

[27] Alexandre J, Nicco C, Chereau C, et al. Improvement of the therapeutic index of anticancer drugs by the superoxide dismutase mimic mangafodipir. J Natl Cancer Inst. 2006, 98:236–244.

[28] Dahan L, Sadok A, Formento JL, Seitz JF, Kovacic H. Modulation of cellular redox state underlies antagonism between oxaliplatin and cetuximab in human colorectal cancer cell lines. Br J Pharmacol. 2009, 158:610–620.

[29] Hwang IT, Chung YM, Kim JJ, et al. Drug resistance to 5-FU linked to reactive oxygen species modulator 1. Biochem Biophys Res Commun. 2007, 359:304–310.

[30] Hwang PM, Bunz F, Yu J, et al. Ferredoxin reductase affects p53-dependent, 5-fluorouracil-induced apoptosis in colorectal cancer cells. Nat Med. 2001, 7:1111–1117.

[31] Kopetz S, Lesslie DP, Dallas NA, et al. Synergistic activity of the SRC family kinase inhibitor dasatinib and oxaliplatin in colon carcinoma cells is mediated by oxidative stress. Cancer Res. 2009, 69:3842–3849.

[32] Laurent A, Nicco C, Chereau C, et al. Controlling tumor growth by modulating endogenous production of reactive oxygen species. Cancer Res. 2005, 65:948–956.

[33] Lim SC, Choi JE, Kang HS, Han SI. Ursodeoxycholic acid switches oxaliplatin-induced necrosis to apoptosis by inhibiting reactive oxygen species production and activating p53-caspase 8 pathway in HepG2 hepatocellular carcinoma. Int J Cancer. 2010, 126:1582–1595.

[34] Liu G, Chen X. The ferredoxin reductase gene is regulated by the p53 family and sensitizes cells to oxidative stress-induced apoptosis. Oncogene. 2002, 21:7195–7204.

[35] Shibata T, Kokubu A, Gotoh M, et al. Genetic alteration of Keap1 confers constitutive Nrf2 activation and resistance to chemotherapy in gallbladder cancer. Gastroenterology. 2008, 135:1358–1368.

[36] Fornaro L, Masi G, Loupakis F, Vasile E, Falcone A. Palliative treatment of unresectable metastatic colorectal cancer. Exp Opin Pharmacother 2010, 11, 63–77.

[37] Chua W, Goldstein D, Lee CK, Dhillon H, Michael M, Mitchell P, Clarke SJ and Iacopetta B. Molecular markers of response and toxicity to FOLFOX chemotherapy in metastatic colorectal cancer. Br J Cancer. 2009, 101, 998 – 1004

[38] Locker GY, Hamilton S, Harris J, Jessup JM, Kemeny N, Macdonald JS, Somerfield MR, Hayes DF and Bast RC Jr. ASCO 2006 Update of Recommendations for the Use of Tumor Markers in Gastrointestinal Cancer. J Clin Oncol, 2006, 24:5313-5327.

[39] Sargent DJ, Marsoni S, Monges G, et al. Defective mismatch repair as a predictive marker for lack of efficacy of fluorouracil based adjuvant therapy in colon cancer. J Clin Oncol. 2010, 28: 3219−26.

[40] Hutchins G, Southward K, Handley K, et al. Value of mismatch repair, KRAS, and BRAF mutations in predicting recurrence and benefits from chemotherapy in colorectal cancer. J Clin Oncol. 2011, 29:1261−70.

[41] Fink D, Nebel S, Aebi S, et al. The role of DNA mismatch repair in platinum drug resistance. Cancer Res. 1996, 56:4881-4886.

[42]. Vaisman A, Varchenko M, Umar A, et al. The role of hMLH1, hMSH3, and hMSH6 defects in cisplatin and oxaliplatin resistance: correlation with replicative bypass of platinum-DNA adducts. Cancer Res. 1998, 58:3579-3585.

[43]. Kweekel DM, Gelderblom H and Guchelaar HJ. Pharmacology of oxaliplatin and the use of pharmacogenomics to individualize therapy. Cancer Treat Rev. 2005, 31, 90–105.

[44] Stoehlmacher J, et al. A multivariate analysis of genomic polymorphisms: prediction of clinical outcome to 5-FU/oxaliplatin combination chemotherapy in refractory colorectal cancer. Br J Cancer. 2004, 91, 344–354.

[45] McLeod HL, et al. Pharmacogenetic analysis of systemic toxicity and response after 5-fluorouracil (5FU)/CPT-11, 5FU/oxaliplatin (oxal), or CPT-11/oxal therapy for advanced colorectal cancer (CRC): results from an intergroup trial. Proc Am Soc Clin Oncol. 2003, 22, Abstr. 1013.

[46] Grem JL. Intratumoral molecular or genetic markers as predictors of clinical outcome with chemotherapy in colorectal cancer. Semin Oncol. 2005, 32:120- 127.

[47] McLeod HL, Church RD. Molecular predictors of prognosis and response to therapy in colorectal cancer. Cancer Chemother Biol Response Modif. 2003, 21:791-801.

[48] Loriot Y, Mordant P, Deutsch E, Olaussen KE and Soria JC. Are RAS mutations predictive markers of resistance to standard chemotherapy? Nature Reviews Clinical Oncology. 2009, 6, 528-534.

[49] Lane DP. Cancer. p53, guardian of the genome. Nature. 1992, 358:15- 16.

[50] Liang JT, Huang KC, Cheng YM, et al. P53 overexpression predicts poor chemosensitivity to high-dose 5-fluorouracil plus leucovorin chemotherapy for stage IV colorectal cancers after palliative bowel resection. Int J Cancer. 2002, 97:451-457.

[51] Paradiso A, Simone G, Petroni S, et al. Thymidylate synthase and p53 primary tumor expression as predictive factors for advanced colorectal cancer patients. Br J Cancer. 2000, 82:560-567.

[52] Watanabe T, Wu TT, Catalano PJ, et al. Molecular predictors of survival after adjuvant chemotherapy for colon cancer. N Engl J Med. 2001, 344:1196-1206.

[53] Pinedo HM, Peters GF. Fluorouracil: Biochemistry and pharmacology. J Clin Oncol. 1988, 6:1653–1664.

[54] Santi DV, McHenry CS, Sommer H. Mechanism of interaction of thymidylate synthetase with 5-fluorodeoxyuridylate. Biochemistry. 1974,13: 471–481.

[55] Berger SH, Jenh CH, Johnson LF, et al. Thymidylate synthase overproduction and gene amplification in fluorodeoxyuridine-resistant human cells. Mol Pharmacol. 1985, 28:461– 467.

[56] Compton C. Getting to Personalized Cancer Medicine. Cancer. 2007, 110:8.

[57] Latterich M, Abramovitz M, Leyland-Jones B. Proteomics: new technologies and clinical applications. Eur J Cancer. 2008, 44 2737–2741.

[58] Wouters BG. Proteomics: methodologies and applications in oncology. Semin Radiat Oncol. 2008, 18 115–125.

[59] Steiner S, Witzmann FA. Proteomics: Applications and opportunities in preclinical drug development. Electrophoresis. 2000, 21:11, 2099–2104.

[60] Somiari RI, Sullivan A, Russell S, Somiari S, Hu H, Jordan R, George A, Katenhusen R, Buchowiecka A, Arciero C, Brzeski H, Hooke J, Shriver C. High-throughput proteomic analysis of human infiltrating ductal carcinoma of the breast. Proteomics. 2003, 3:10, 1863–1873.

[61] Tejpar S, Bertagnolli M, Bosman F, Lenz HJ, Garraway L, Waldman F, Warren R, Bild A, Brennan DC, Hahn H, Harkin P, Kennedy R,Ilyas M, Morreau H, Proutski V, Swanton C, Tomlinson I, Delorenzi M, Fiocca R, Van Cutsem E, Roth A. Prognostic and Predictive Biomarkers in Resected Colon Cancer: Current Status and Future Perspectives for Integrating Genomics into Biomarker Discovery. The Oncologist. 2010, 15, 390–404.

[62] Celisa JE, Kruhøffer M, Frederiksen C, Østergaard M, Thykjaer T, Gromova P, Yub J, Pálsdóttir H, Magnusson N, Ørntoft TF. Gene expression profiling: monitoring transcription and translation products using DNA microarrays and proteomics. FEBS Letters. 2000, 480, 2-16.

[63] Anderson L, Seilhamer JA. comparison of selected mRNA and protein abundances in human liver. Electrophoresis. 1997, 18:533–537.

[64] Chen G, Gharib TG, Huang C, Taylor JMG, Misek DE, Kardia SLR, Giordano TJ, Iannettoni MD, Orringer MB, Hanash SM, Beer DG. Discordant Protein and mRNA Expression in Lung Adenocarcinomas. Molecular & Cellular Proteomics. 2002, 1 304-313.

[65] Lage H. Proteomic approaches for investigation of therapy resistance in cancer. Proteomics Clin Appl. 2009, 3 883–911.

[66] Fan AC, Deb-Basu D, Orban MW, Gotlib JR, Natkunam Y, O'Neill R, Padua R, Xu L, Taketa D, Shirer AE, Beer S, Yee AX, Voehringer DW, Felsher DW. Nanofluidic proteomic assay for serial analysis of oncoprotein activation in clinical specimens. Nature Medicine. 2009, 15, 566-571.

[67] O'Neill RA, Bhamidipati A, Bi X, Deb-Basu D, Cahill L, Ferrante J, Gentalen E, Glazer M, Gossett J, Hacker K, Kirby C, Knittle J, Loder R, Mastroieni C, MacLaren M, Mills T, Nguyen U, Parker N, Rice A, Roach D, Suich D, Voehringer D, Voss K, Yang J, Yang T and Vander Horn PB. Isoelectric focusing technology quantifies protein signaling in 25 cells. Proc Natl Acad Sci USA. 2006, 103:44, 16153–16158.

[68] Herbst RS and Lippman SM. Molecular Signatures of Lung Cancer — Toward Personalized Therapy. N Engl J Med. 2007, 356:76-78.

[69] Wulfkuhle JD, Speer R, Pierobon M, Laird J, Espina V, Deng J, Mammano E, Yang SX, Swain SM, Nitti D, Esserman LJ, Belluco C, Liotta LA, Petricoin EF. Multiplexed Cell Signaling Analysis of Human Breast Cancer Applications for Personalized Therapy. J Proteome Res. 2008, 7:4, 1508–1517.

[70] Ginsburg GS and McCarthy JJ. Personalized medicine: revolutionizing drug discovery and patient care. TRENDS in Biotechnology. 2001, 19:12.

[71] Ross JS, Torres-Mora J, Wagle N, Jennings TA, Jones DM. Biomarker-Based Prediction of Response to Therapy for Colorectal Cancer. Am J Clin Pathol. 2010, 134:478-490.

[72] Davies SM. Pharmacogenetics, pharmacogenomics and personalized medicine: Are we there yet? Hematology. 2006, 1:111-117.

[73] Bandrés E, Zárate R, Ramirez N, Abajo A, Bitarte N, García-Foncillas J. Pharmacogenomics in colorectal cancer: The first step for individualized therapy. World J Gastroenterol. 2007, 13:5888-5901.

[74] Spruessel A, Steimann G, Jung M, Lee SA, Carr T, Fentz AK, Spangenberg J, Zornig C, Juhl H, David KA. Tissue ischemia time affects gene and protein expression patterns within minutes following surgical tumor. BioTechniques. 2004, 36, 1030-1032.

[75] Tsao MS, Aviel-Ronen S, Ding K, Lau D, Liu N, Sakurada A, Whitehead M, Zhu ZQ, Livingston R, Johnson DH, Rigas J, Seymour L, Winton T and Shepherd FA. Prognostic and Predictive Importance of p53 and RAS for Adjuvant Chemotherapy in Non–Small-Cell Lung Cancer. J Clin Oncol. 2007, 25:5240-5247.

[76] Russo A, Bazan V, Lacopetta B, Soussi T, Gebbia N and for the TP53-CRC Collaborative Study Group. The TP53 Colorectal Cancer International Collaborative Study on the Prognostic and Predictive Significance of p53 Mutation: Influence of Tumor Site, Type of Mutation, and Adjuvant Treatment. J Clin Oncol. 2005, 20:7518-7528.

[77] Maehara Y, Anai H, Tamada R, Sugimachi K. The ATP assay is more sensitive than the succinate dehydrogenase inhibition test for predicting cell viability. European Journal of Cancer and Clinical Oncology.1987, 23:3, 273-276.

[78] Kurbacher CM, Cree IA, Bruckner HW, Brenne U, Kurbacher JA, Müller K, Ackermann T, Gilster TJ, Wilhelm LM, Engel H, Mallmann PK, Andreotti PE. Use of an ex vivo ATP luminescence assay to direct chemotherapy for recurrent ovarian cancer. Anti-cancer Drugs. 1998, 9:1, 51-57.

[79] Konecny G, Crohns C, Pegram M, FelberM, Lude S, Kurbacher CM, Cree IA, Hepp H, Untch M. Correlation of drug response with ATP Tumorchemosensitivity Assay in primary FIGO Stage III ovarian cancer. Gynecol Oncol. 2000, 77, 258-263.

[80] Kurbacher CM, Grecu OM, Stier U, Gilster TJ, Janat MM, Untch M, Konecny G, Bruckner HW, Cree IA. ATP chemosensitivity testing in ovarian and breast cancer: early clinical trials. Recent Results Cancer Res. 2003, 161, 221-230.

[81] Yanagawa E, Nishiyama M, Saeki T, Kim R, Jinushi K, Kirihara Y, Takagami S, Niimoto M, Hattori T. Chemosensitivity tests in colorectal cancer patients. Jpn J Surg. 1989, 19, 432-438.

[82] Moon YW, Choi SH, Kim YT, Sohn JH, Chang J, Kim SK, Park MS, Chung KY, Lee HJ, Kim JH. Adenosine triphosphate-based chemotherapy response assay (ATP-CRA)-guided platinum-based 2-drug chemotherapy for unresectable nonsmall-cell lung cancer. Cancer. 2007, 109:1829-1835.

[83] Raymond E, Buquet-Fagot C, Djelloul S. Antitumor activity of oxaliplatin in combination with 5-fluorouracil and the thymidylate synthase inhibitor AG337 in human colon, breast and ovarian cancers. Anticancer Drugs. 1997, 8:876–85.

[84] Crimin KS, McKean J, Vidmar TJ. Rank-based estimate of four-parameter logistic model. Pharmaceutical statistics. 2012, 11(3):214-221.

[85] Cree IA. Chemosensitivity and chemoresistance testing in ovarian cancer. Curr Opin Obstet Gynecol. 2009, 21:39-43.

[86] Wiener MC, Sachs JR, Deyanova EG and Yates NA. Differential Mass Spectrometry: A Label-Free LC−MS Method for Finding Significant Differences in Complex Peptide and Protein Mixtures. Anal Chem. 2004, 76:20, 6085–6096.

[87] Wang G, Wu WW, Zeng W, Chou CL and Shen RF. Label-Free Protein Quantification Using LC-Coupled Ion Trap or FT Mass Spectrometry: Reproducibility, Linearity, and Application with Complex Proteomes. J Proteome Res. 2006, 5:5, 1214–1223.

[88] Neubert H, Bonnert TP, Rumpel K, Hunt BT, Henle ES and James IT. Label-Free Detection of Differential Protein Expression by LC/MALDI Mass Spectrometry. J Proteome Res. 2008, 7(6)2270–2279.

[89] Zhu W, Smith JW and Huang CM. Mass Spectrometry-Based Label-Free Quantitative Proteomics. Journal of Biomedicine and Biotechnology. 2010, Article ID 840518.

[90] Noor R, Mittal S, Iqbal J. Superoxide dismutase--applications and relevance to human diseases. Med Sci Monit. 2002,(9):RA210-5.

[91] Brown DPG, Chin-Sinex H, Nie B, Mendonca MS and Wang M. Targeting superoxide dismutase 1 to overcome cisplatin resistance in human ovarian cancer. Cancer Chemotherapy and Pharmacology. 2009, 63:4, 723-730.

[92] Fitzpatrick DPG, You JS, Bemis KG, Wery JP, Ludwig JR and Wang M. Searching for potential biomarkers of cisplatin resistance in human ovarian cancer using a label-free LC/MS-based protein quantification method. Proteomics Clin Appl. 2007, 1, 246–263.

[P93] Kuo MT, Chen HWH, Song IS, Savaraj N and Ishikawa T. The roles of copper transporters in cisplatin resistance. Cancer and Metastasis Reviews. 2007, 26:1, 71-83.

[94] Kim JW, Nie B, Sahm H, Brown DP, Tegeler T, You JS, Wang M. Targeted quantitative analysis of superoxide dismutase 1 in cisplatin-sensitive and cisplatin-resistant human ovarian cancer cells. J Chromatogr B Analyt Technol Biomed Life Sci. 2010, 1; 878(7-8):700-4.

[95] Fujimura M, Morita-Fujimura Y, Narasimhan P, Copin JC, et al. Copper-Zinc Superoxide Dismutase Prevents the Early Decrease of Apurinic/Apyrimidinic Endonuclease and Subsequent DNA Fragmentation After Transient Focal Cerebral Ischemia in Mice. Stroke. 1999, 30, 2408–2415.

[96] Bukau B, Weissman J and Horwich A. Molecular chaperones and protein quality control. Cell. 2006, 125:443–451.

[97] Lindquist S and Craig EA. The heat-shock proteins. Annu Rev Genet. 1988, 22:631–677.

[98] Rohde M, Daugaard M, Jensen MH, Helin K, Nylandsted J and Jaattela M. Members of the heat-shock protein 70 family promote cancer cell growth by distinct mechanisms. Genes Dev. 2005, 19:570–582.

[99] Gething MJ and Sambrook J. Protein folding in the cell. Nature. 1992, 355:33–45.

[100] Tsukahara F and Maru Y. Identification of novel nuclear export and nuclear localization-related signals in human heat shock cognate protein 70. J Biol Chem. 2004, 279:8867–72.

[101] Kodiha M, Chu A, Lazrak O, Stochaj U. Stress inhibits nucleocytoplasmic shuttling of heat shock protein hsc70. Am J Physiol Cell Physiol. 2005, 289:C1034–41.

[102] Matsui H, Asou H and Inaba T. Cytokines direct the regulation of Bim mRNA stability by heat-shock cognate protein 70. Mol Cell. 2007, 25:99–112.

[103] Ciocca DR, Fuqua SA, Lock-Lim S, Toft DO, Welch WJ, McGuire WL. Response of human breast cancer cells to heat shock and chemotherapeutic drugs. Cancer Res. 1992, 52: 648–3654.

[104] Vargas-Roig LM, Fanelli MA, Lopez LA, Gago FE, Tello O, Aznar JC, et al. Heat shock proteins and cell proliferation in human breast cancer biopsy samples. Cancer Detect Prev. 1997, 21:441–451.

[105] Vargas-Roig LM, Gago FE, Tello O, Aznar JC, Ciocca DR. Heat shock protein expression and drug resistance in breast cancer patients treated with induction chemotherapy. Int J Cancer. 1998, 79: 468–475.

[106] Castagna A, Antonioli P, Astner H, Hamdan M, Righetti SC, Perego P, Zunino F and Righetti PG. A proteomic approach to cisplatin resistance in the cervix squamous cell carcinoma cell line A431. Proteomics. 2004, 4, 3246–3267.

[107] Duncan M, Short ID, Heron JLA, Birse-Archbold LEK, Sharkey J and McCulloch J. Apoptosis induced by staurosporine alters chaperone and endoplasmic reticulum proteins: Identification by quantitative proteomics. Proteomics. 2007, 7, 3085–3096.

[108] Faehnle CR, Joshua-Tor L. Argonautes confront new small RNAs. Curr Opin Chem Biol. 2007, 11:569-577.

[109] Li L, Yu C, Gao H, Li Y. Argonaute proteins: potential biomarkers for human colon cancer. BMC Cancer. 2010, 10:38.

[110] Höck J, Weinmann L, Ender C, Rüdel S, Kremmer E, Raabe M, Urlaub H and Meister G. Proteomic and functional analysis of Argonautecontaining mRNA–protein complexes in human cells. EMBO reports. 2007, 8, 1052–1060.

[111] Buchberger A, Howard MJ, Proctor M, Bycroft M. The UBX domain: a widespread ubiquitin-like module. J Mol Biol. 2001, 307, 17–24.

[112] Nagahama M, Ohnishi M, Kawate Y, Matsui T, Miyake H, Yuasa K, Tani K, Tagaya M, Tsuji A. UBXD1 is a VCP-interacting protein that is involved in ER-associated degradation. Biochemical and Biophysical Research Communications. 2009, 382, 303–308.

[113] Meussr B, Hirsch C, Jarosch E, Sommer T. ERAD: the long road to destruction, Nat Cell Biol , 2005, 7, 766–772.

[114] Römisch K. Endoplasmic reticulum associated degradation. Annu Rev Cell Dev Biol. 2005, 21, 435–456.

[115] Oyadomari S, Araki E, Mori M. Endoplasmic reticulum stress-mediated apoptosis in pancreatic β-cells. Apoptosis. 2002, 7: 335–345.

[116] Burwick NR, Wahl ML, Fang J, Zhong Z, Moser TL, Li B, Capaldi RA, Kenan DJ, Pizzo SV. An Inhibitor of the F1 subunit of ATP synthase (IF1) modulates the activity of angiostatin on the endothelial cell surface. J Biol Chem. 2005, 280:1740-1745.

[117] Aggeler R, Coons J, Taylor SW, Ghosh SS, Garcia JJ, Capaldi RA, Marusich MF. A functionally active human F1F0 ATPase can be purified by immunocapture from heart tissue and fibroblast cell lines. Subunit structure and activity studies. J Biol Chem. 2002, 277:33906-33912.

[118] Campanella M, Parker N, Tan CH, Hall AM, Duchen MR. IF(1): setting the pace of the F(1)F(o)-ATP synthase. Trends Biochem Sci. 2009, 34(7):343-50.

[119] Shah VP. The history of bioanalytical method validation and regulation: evolution of a guidance document on bioanalytical methods validation. AAPS Journal. 2007, 9(1).

[120] Fontaine N, Rosengren B. Directive 2001/20/EC of the european parliament and of the council: on the approximation of the laws, regulations and administrative provisions of the members states relating to the implementation of good clinical practice in the conduct of clinical trails on medicinal products for human use. OJEC, 2001, 4-4.

[121] FDA. Guidance for industry: bioanalytical method validation. 2001.

[122] Martinkova J, Gadher SJ, Hajduch M, et al. Challenges in cancer research and multifaceted approaches for cancer biomarker quest. FEBS Letters. 2009, 583(11):1772–84.

[123] Alymani NA, Smith MD, Williams DJ, Petty RD. Predictive biomarkers for personalised anti-cancer drug use: Discovery to clinical implementation. European Journal of cancer. 2010, 4:6, 869–879.

[124] Chau CH, Rixe O, McLeod H, et al. Validation of analytic methods for biomarkers used in drug development. Clin Cancer Res. 2008, 14(19):5967–76.

[125] Bose R, Molina H, Patterson AS, Bitok JK, Periaswamy B, Bader JS, Pandey A, Cole PA. Phosphoproteomic analysis of Her2 neu signaling and inhibition. Proc Natl Acad Sci USA. 2006, 103(26) 9773–9778.

[126] Ahmed N, Oliva KT, Barker G, Hoffmann P, Reeve S, Smith IA, Quinn MA, Rice GE. Proteomic tracking of serum protein isoforms as screening biomarkers of ovarian cancer. Proteomics. 2005, 5, 4625-4636.

[127] Ricolleau G, Charbonnel C, Lode L, Loussouarn D, Joalland MP, Bogumil R, Jourdain S, Minvielle S, Campone M, Deporte-Fety R, Campion L, Jezequel P. Surface-enhanced laser desorption/ionization time of flight mass spectrometry protein profiling identifies ubiquitin and ferritin light chain as prognostic biomarkers in node-negative breast cancer tumors. Proteomics. 2006, 6, 1963-1975.

[128] Simon R. When is a genomic classifi er ready for prime time? Natl Clin Practice Oncol. 2004, 1, 4–5.

[129] Kattan MW. Evaluating a new marker's predictive contribution. Clin Cancer Res. 2004, 10, 822–4.

[130] Lee JW, Devanarayan V, Barrett YC, et al. Fit-for-purpose method development and validation for successful biomarker measurement. Pharm Res. 2006, 23(2):312–28.

[131] Wulfkuhle JD, Speer R, Pierobon M, Laird J, Espina V, Deng J, Mammano E, Yang SX, Swain SM, Nitti D, Esserman LJ, Belluco C, Liotta LA, Petricoin EF. Multiplexed Cell Signaling Analysis of Human Breast Cancer Applications for Personalized Therapy. Journal of Proteome Research. 2008, 7, 1508–1517.

[132] Haab BB, Dunham MJ, O´Brown P. Protein microarrays for highly parallel detection and quantification of specific proteins and antibodies in complex solutions. Genome biology. 2001, 2:2, research00041-000413.

[133] Amur S, Frueh F, Lesko LJ, et al. Integration and use of biomarkers in drug development, regulations and clinical practice: a US regulatory perspective. Biomarkers Med. 2008, 2(3):305–11.

[134] Søreide K. Receiver-operating characteristic curve analysis in diagnostic, prognostic and predictive biomarker research. J Clin Pathol. 2009, 62:1.

[135] Ma S and Huang J. Regularized ROC method for disease classification and biomarker selection with microarray data. Bioinformatics. 2005, 21:24, 4356–4362.

[136] Sargent DJ, Conley BA, Allegra C, et al. Clinical trial designs for predictive marker validation in cancer treatment trials. J Clin Oncol. 2005, 23(9):2020–7.

[137] Buyse M, Sargent DJ, Grothey A, Matheson A and de Gramont A. Biomarkers and surrogate end points the challenge of statistical validation. Nat Rev Clin Oncol. 2010, 7, 309–317.

[138] Brunner N, Vang Nielsen K, Offenberg H, et al. Biomarkers for therapeutic efficacy. Eur J Cancer. 2007, 5(5 Suppl.):129–42.

[139] Simon R. Clinical trial designs for evaluating the medical utility of prognostic and predictive biomarkers in oncology. Per Med. 2010, 7(1): 33–47.

[140] Simon R. Development and Validation of Therapeutically Relevant Multi-Gene Biomarker Classifiers. Journal of the National Cancer Institute. 2005, 97:12.

[141] Mandrekar SJ and Sargent DJ. Clinical Trial Designs for Predictive Biomarker Validation: Theoretical Considerations and Practical Challenges. J Clin Oncol. 2009, 27:4027-4034.

[142] NIH, Biomarkers Definitions Working Group. Biomarkers and surrogate endpoints: preferred definitions and conceptual framework. Clin Pharmacol Toxicol. 2001, 69(3):2020–27.

[143] Mandrekar SJ and Sargent DJ. Clinical Trial Designs for Predictive Biomarker Validation: One Size Does Not Fit All. J Biopharm Stat. 2009, 19(3): 530–542.

[144] Jenkins M, Flynn A, Smart T, Harbron C, Sabin T, Ratnayake J, Delmar P, Herath A, Jarvis P, Matcham J and on behalf of the PSI Biomarker Special Interest Group. A

statistician's perspective on biomarkers in drug development. Pharmaceut Statist. 2011, 10 494–507.

[145] Goodsaid F, Frueh F. Biomarker qualification pilot process at the US Food and Drug Administration. AAPS J. 2007, 9(1):E105–8.

[146] McShane LM, Altman DG, Sauerbrei W, et al. Reporting recommendations for tumour MARKer prognostic studies (REMARK). Eur J Cancer. 2005, 41(12):1690–6.

[147] Smith V, Dai F, Spitz M, Peters GJ, Fiebig HH, Hussain A, Burger AM. Telomerase activity and telomere length in human tumor cells with acquired resistance to anticancer agents. J Chemother. 2009, 21(5), 542-9.

[148] Galli-Taliadoros LA, Sedgwick JD, Wood SA, Kijrner H. Gene knock-out technology: a methodological overview for the interested novice. Journal of Immunological Methods. 1995, 181, 1-15.

[149] Huang P, Feng L, Oldham EA, Keating MJ, Plunkett W. Superoxide dismutase as a target for the selective killing of cancer cells. Nature. 2000, 407, 390-395.

[150] Somwar R, Erdjument-Bromage H, Larsson E, Shum D, Lockwood WW, Yang G, Sander, Ouerfelli O, Tempst PJ, Djaballah H and Varmus HE. Superoxide dismutase 1 (SOD1) is a target for a small molecule identified in a screen for inhibitors of the growth of lung adenocarcinoma cell lines. Proc Natl Acad Sci USA. 2011, 108:39, 16375–16380.

[151] Lowndes SA, Sheldon HV, Cai S, Taylor JM, Harris AL. Copper chelator ATN-224 inhibits endothelial function by multiple mechanisms. Microvascular Research. 2009, 77, 14–326.

[152] Juarez JC, Betancourt O, Pirie-Shepherd SR, Guan X, Price ML, Shaw DE, Mazar AP and Doate F. Copper Binding by TetrathiomolybdateAttenuates Angiogenesis and Tumor Cell Proliferation through the Inhibition of Superoxide Dismutase . Clin Cancer Res. 2006, 12:4974-4982.

[153] Donate F, Juarez JC, Burnett ME, Manuia MM, Guan X, Shaw DE, Smith ELP, Timucin C, Braunstein MJ, Batuman OA and Mazar AP. Identification of biomarkers for the antiangiogenic and antitumour activity of the superoxide dismutase 1 (SOD1) inhibitor tetrathiomolybdate (ATN-224). British Journal of Cancer. 2008, 98, 76–783.

8 Publications

Poster and Abstracts

1. Florian T. Unger, Birgit Rabe, Agnieszka Harasym, Katja Pursche, Cordula Rosenbrock, Hartmut Juhl and Kerstin A. David. Top Down LC-MALDI Discovery of Cu/Zn SOD as potential biomarker for intrinsic chemoresistance. EACR-22 - from Basic Research to Personalised Cancer Treatment. July 7-10. 2012. Barcelona, Spain.

2. Florian T. Unger, Cordula Rosenbrock, Jana Krueger, Janina Schaller, Birgit Rabe, Hartmut Juhl and Kerstin A. David. Effects of antibody-mediated EGF-receptor inhibition on ERK 1/2 isoform phosphorylation in organoid cultures. AACR Annual Meeting; March 31-April 4, 2012; Chicago,IL

3. Florian T. Unger, Markus Meyer, Monika Spörl, Agnieszka Harasym, Katja Pursche, Hartmut Juhl, and Kerstin A. David. Early detection biomarker for colorectal malignancies identified by a novel comparative proteomic workflow**.** *Cancer Res.*, Apr 2011; 71: 3177. AACR Annual Meeting; April 2-6, 2011; Orlando, FL

3. Florian T. Unger, Birgit Rabe, Cordula Rosenbrock, Jana Krueger, Janina Schaller, Jasmin Oehlmann, Christine Hein, Hartmut Juhl, and Kerstin A. David. Preclinical analysis of therapeutic antibody efficacy using an organoid model-based drug testing platform. *Mol. Cancer Ther.*, Nov 2011; 10: 228 AACR-NCI-EORTC International Conference: Molecular Targets and Cancer Therapeutics; November 12-16, 2011; San Francisco, CA.

4. Florian T. Unger, Markus Meyer, Monika Spörl, Agnieszka Harasym, Katja Pursche, Hartmut Juhl, and Kerstin A. David. Identification of biomarkers associated with tumor progression using laser microdissected tissues from colon adenoma and cancer. *Ejc Supplements*, ISSN: 1359-6349, Volume: 8, Issue: 7, Date: 2010-11-01, Page: 202 EORTC-NCI-AACR Symposium on "Molecular Targets and Cancer Therapeutics"; November 16-19, 2010; Berlin, Germany.

5. Florian T. Unger, Agnieszka Harasym, Jana Krüger, Cordula Rosenbrock, Hartmut Juhl, Kerstin A. David. Evaluation of drug response and comparative proteomic analysis of cultivated colorectal cancer tissue slices. In: Proceedings of the AACR Special Conferences – Colorectal Cancer: Biology To The Therapy; Oct 27-30, 2010; Philadelphia, PA.

6. Florian T. Unger, Markus Meyer, Monika Spörl, Agnieszka Harasym, Kevin Sullivan, Hartmut Juhl, and Kerstin A. David. Comparative proteomic analysis of colorectal cell lines to identify biomarkers for the prediction of intrinsic resistance to FOLFOX chemotherapy. *Clin. Cancer Research*: July 15, 2010; Volume 16, Issue 14, Supplement 2 AACR International Conference: Translational Cancer Medicine; Jul 11-14, 2010; San Francisco, CA

7. Florian Unger, Markus Meyer, Monika Spörl, Agnieszka Harasym, Kevin Sullivan, Hartmut Juhl and Kerstin A. David. Discovery of predictive biomarkers based on differential chemosensitivity of colorectal cell lines. AACR 101st Annual Meeting ; Washington, D.C., April 17-21, 2010.

8. Unger F., Meyer M., Spörl M., Juhl H., David K. Discovery of predictive biomarkers based on differential chemosensitivity of colorectal cell lines. 1st International Meeting on Molecular-Based Treatment of GI-Cancer. September 23–24, 2009, Göttingen.

Research articles and reviews

1. Unger FT, Klasen HA, Tchartchian G, de Wilde RL, Witte I (2009) DNA damage induced by cis- and carboplatin as indicator for in vitro sensitivity of ovarian carcinoma cells. *BMC Cancer* 9 359-368. (Research article)

2. Florian T. Unger, Irene Witte and Kerstin A. David (2012) Prediction of Individual Response to Anticancer Therapy – State of Art and Future Perspectives. *Cellular and Molecular Life Sciences*. (Review article) accepted

3. Florian T. Unger, Markus Meyer, Hartmut Juhl and Kerstin David. Discovery of predictive biomarker for intrinsic resistance to FOLFOX chemotherapy in colon cancer using a Top Down LC-MALDI approach to analyze the low molecular weight proteome. *BMC Cancer.* (Research article)
submitted

Acknowledgements

First and foremost I would like to thank PD Dr. Kerstin A. David for her supervision, the freedom and support she granted me in my research activities. Furthermore, I would like to thank her for all the discussions we had, her advice while preparing this thesis and the opportunity to attend numerous scientific meetings.

I would also like to thank Prof. Dr. Juhl for funding and support of this thesis. Prof. Dr. Bredehorst is thanked for the academical supervision of this thesis.

Thanks to the members of the Indivumed GmbH for the pleasant working environment and all employees of the Indivumed research facility for their support and discussions during my thesis. In particular, I would like to thank Jana Krüger, Janina Schaller, Cordula Rosenbrock, as well as Katja Pursche, Monika Schöppler for their humor and patience. Special thanks to Agnieszka Harasym for her support in the proteomic studies.

Furthermore, I would like to thank Dr. Markus Meyer, Dr. Ilona Schonn, Dr. Heinz Joachim List and Dr. Jörg Spangenberg for their support.

I would like to thank my parents for always supporting and believing in me. Furthermore, thanks belong to Jasmin Oehlmann for always being there and supporting me.

Acknowledgements

First and foremost I would like to thank PD Dr. Kerstin A. David for her supervision, the freedom and support she granted me in my research activities. Furthermore, I would like to thank her for all the discussions we had, her advice while preparing this thesis and the opportunity to attend numerous scientific meetings.

I would also like to thank Prof. Dr. Juhl for funding and support of this thesis. Prof. Dr. Bredehorst is thanked for the academical supervision of this thesis.

Thanks to the members of the Indivumed GmbH for the pleasant working environment and all employees of the Indivumed research facility for their support and discussions during my thesis. In particular, I would like to thank Jana Krüger, Janina Schaller, Cordula Rosenbrock, as well as Katja Pursche, Monika Schöppler for their humor and patience. Special thanks to Agnieszka Harasym for her support in the proteomic studies.

Furthermore, I would like to thank Dr. Markus Meyer, Dr. Ilona Schonn, Dr. Heinz Joachim List and Dr. Jörg Spangenberg for their support.

I would like to thank my parents for always supporting and believing in me. Furthermore, thanks belong to Jasmin Oehlmann for always being there and supporting me.

Curriculum Vitae

Personal data

Name:	Florian T. Unger
Date of Birth:	01. March1982
Brthplace:	Rotenburg (Wümme)
Nationality:	German

Education

1988-2001	Elementary school and Gymnasium, Rotenburg (Wümme)
2001-2002	Alternative service (Zivildienst), Rotenburg (Wümme)
2002-2007	Studies of Biology, University of Oldenburg
Diploma thesis:	“Korrelation der zyto- und gentoxischen Wirkung von Zytostatika und Zytostatikagemischen auf Zellen des ovarialen Karzinoms.” (DNA damage induced by cis- and carboplatin as indicator for *in vitro* sensitivity of ovarian carcinoma cells.)
2008-2012	Doctoral thesis

Affidavit

I hereby declare, that I have done the present work by myself, not used other than the stated sources and aids. Any used statements from literature are notes as so.
I further confirm, that this dissertation is not submitted to any other institution to open the dissertation procedure.

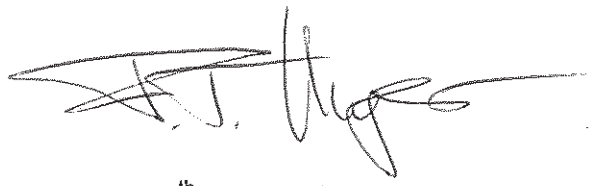

Hamburg, 13th June 2012